CITATION REPORT List of articles citing

Probabilistic diffusion tractography with multiple fibre orientations: What can we gain?

DOI: 10.1016/j.neuroimage.2006.09.018 NeuroImage, 2007, 34, 144-55.

Source: https://exaly.com/paper-pdf/42088846/citation-report.pdf

Version: 2024-04-28

This report has been generated based on the citations recorded by exaly.com for the above article. For the latest version of this publication list, visit the link given above.

The third column is the impact factor (IF) of the journal, and the fourth column is the number of citations of the article.

#	Paper	IF	Citations
2316	High Angular Resolution Diffusion Imaging (HARDI). 1-25		12
2315	Reversible posterior leukencephalopathy syndrome induced by granulocyte stimulating factor filgrastim. 2000 , 69, 280-1		15
2314	White Matter Tractography and Diffusion-Weighted Imaging. 1-9		1
2313	Exploiting peak anisotropy for tracking through complex structures. 2007,		23
2312	SPLITTING TRACKING THROUGH CROSSING FIBERS: MULTIDIRECTIONAL Q-BALL TRACKING. 2007,		10
2311	Multimodal Imaging in Neurology: Special Focus on MRI Applications and MEG. 2007 , 2, 1-75		2
2310	Probabilistic Anatomical Connection Derived from QBI with MFACT Approach. 2007,		3
2309	Probabilistic inference on Q-ball imaging data. 2007 , 26, 1515-24		11
2308	A probabilistic model-based approach to consistent white matter tract segmentation. 2007 , 26, 1555-61		71
2307	TWO-TENSOR FIBER TRACTOGRAPHY. 2007,		10
2306	The development of brain connectivity browser by tractography of QBI. 2007, 2007, 2094-7		O
2305	Human motor corpus callosum: topography, somatotopy, and link between microstructure and function. 2007 , 27, 12132-8		336
2304	From hodology to function. 2007 , 130, 602-5		138
2303	Robust determination of the fibre orientation distribution in diffusion MRI: non-negativity constrained super-resolved spherical deconvolution. <i>NeuroImage</i> , 2007 , 35, 1459-72	7.9	1354
2302	Effects of diffusion weighting schemes on the reproducibility of DTI-derived fractional anisotropy, mean diffusivity, and principal eigenvector measurements at 1.5T. <i>NeuroImage</i> , 2007 , 36, 1123-38	7.9	236
2301	Integrity of white matter in the corpus callosum correlates with bimanual co-ordination skills. <i>NeuroImage</i> , 2007 , 36 Suppl 2, T16-21	7.9	187
2300	A novel tensor distribution model for the diffusion-weighted MR signal. <i>NeuroImage</i> , 2007 , 37, 164-76	7.9	166

(2008-2007)

2299	A Bayesian framework for global tractography. <i>NeuroImage</i> , 2007 , 37, 116-29	7.9	215
2298	Topography of cortical and subcortical connections of the human pedunculopontine and subthalamic nuclei. <i>Neurolmage</i> , 2007 , 37, 694-705	7.9	164
2297	Validation of in vitro probabilistic tractography. <i>NeuroImage</i> , 2007 , 37, 1267-77	7.9	194
2296	Topological visualization of brain diffusion MRI data. 2007 , 13, 1496-503		38
2295	Diffusion-weighted imaging tractography-based parcellation of the human lateral premotor cortex identifies dorsal and ventral subregions with anatomical and functional specializations. 2007 , 27, 1025	9-69	275
2294	A unified computational framework for deconvolution to reconstruct multiple fibers from diffusion weighted MRI. 2007 , 26, 1464-71		149
2293	Interfrontal commissural abnormality in schizophrenia: tractography-assisted callosal parcellation. 2007 , 97, 236-41		21
2292	Diffusion tensor imaging and tractwise fractional anisotropy statistics: quantitative analysis in white matter pathology. 2007 , 6, 42		46
2291	Triangulating a cognitive control network using diffusion-weighted magnetic resonance imaging (MRI) and functional MRI. 2007 , 27, 3743-52		738
2290	Diffusion tensor imaging of the brain. 2007 , 4, 316-29		1673
2290 2289	Diffusion tensor imaging of the brain. 2007, 4, 316-29 Individual differences in white-matter microstructure reflect variation in functional connectivity during choice. 2007, 17, 1426-31		1673 115
	Individual differences in white-matter microstructure reflect variation in functional connectivity		
2289	Individual differences in white-matter microstructure reflect variation in functional connectivity during choice. 2007 , 17, 1426-31 Cortical projection to the human red nucleus: complementary results with probabilistic		115
2289	Individual differences in white-matter microstructure reflect variation in functional connectivity during choice. 2007 , 17, 1426-31 Cortical projection to the human red nucleus: complementary results with probabilistic tractography at 3 T. 2007 , 49, 777-84 Anatomical parcellation of the brainstem and cerebellar white matter: a preliminary probabilistic		115
2289 2288 2287	Individual differences in white-matter microstructure reflect variation in functional connectivity during choice. 2007 , 17, 1426-31 Cortical projection to the human red nucleus: complementary results with probabilistic tractography at 3 T. 2007 , 49, 777-84 Anatomical parcellation of the brainstem and cerebellar white matter: a preliminary probabilistic tractography study at 3 T. 2007 , 49, 849-63		11566113
2289 2288 2287 2286	Individual differences in white-matter microstructure reflect variation in functional connectivity during choice. 2007, 17, 1426-31 Cortical projection to the human red nucleus: complementary results with probabilistic tractography at 3 T. 2007, 49, 777-84 Anatomical parcellation of the brainstem and cerebellar white matter: a preliminary probabilistic tractography study at 3 T. 2007, 49, 849-63 Principles and implementation of diffusion-weighted and diffusion tensor imaging. 2007, 37, 739-48 Application of a probabilistic double-fibre structure model to diffusion-weighted MR images of the		1156611326
2289 2288 2287 2286	Individual differences in white-matter microstructure reflect variation in functional connectivity during choice. 2007, 17, 1426-31 Cortical projection to the human red nucleus: complementary results with probabilistic tractography at 3 T. 2007, 49, 777-84 Anatomical parcellation of the brainstem and cerebellar white matter: a preliminary probabilistic tractography study at 3 T. 2007, 49, 849-63 Principles and implementation of diffusion-weighted and diffusion tensor imaging. 2007, 37, 739-48 Application of a probabilistic double-fibre structure model to diffusion-weighted MR images of the human brain. 2008, 26, 236-45 A regularized two-tensor model fit to low angular resolution diffusion images using basis		115 66 113 26

2281	Fiber tracking of human brain using fourth-order tensor and high angular resolution diffusion imaging. 2008 , 60, 1207-17		13
2280	A multiple streamline approach to high angular resolution diffusion tractography. 2008 , 30, 989-96		21
2279	The evolution of the arcuate fasciculus revealed with comparative DTI. 2008, 11, 426-8		652
2278	Language lateralization in temporal lobe epilepsy using functional MRI and probabilistic tractography. 2008 , 49, 1367-76		36
2277	Connecting the developing preterm brain. 2008 , 84, 777-82		48
2276	Diffusion-based tractography in neurological disorders: concepts, applications, and future developments. 2008 , 7, 715-27		300
2275	The brain in chronic CRPS pain: abnormal gray-white matter interactions in emotional and autonomic regions. 2008 , 60, 570-81		372
2274	DTI tractography of the human brain's language pathways. 2008 , 18, 2471-82		458
2273	Studying connections in the living human brain with diffusion MRI. 2008, 44, 936-52		373
2272	Diffusion spectrum magnetic resonance imaging (DSI) tractography of crossing fibers. <i>NeuroImage</i> , 2008 , 41, 1267-77	7.9	730
2271	Estimating crossing fibers: a tensor decomposition approach. 2008, 14, 1635-42		88
2270	Probabilistic streamline q-ball tractography using the residual bootstrap. <i>NeuroImage</i> , 2008 , 39, 215-22	7.9	133
2269	Structural damage to the corticospinal tract correlates with bilateral sensorimotor cortex reorganization in stroke patients. <i>NeuroImage</i> , 2008 , 39, 1370-82	7.9	98
2268	Recent advances in recording electrophysiological data simultaneously with magnetic resonance imaging. <i>Neurolmage</i> , 2008 , 40, 515-528	7.9	152
2267	Labeling of ambiguous subvoxel fibre bundle configurations in high angular resolution diffusion MRI. <i>NeuroImage</i> , 2008 , 41, 58-68	7.9	65
2266	A Bayesian framework to identify principal intravoxel diffusion profiles based on diffusion-weighted MR imaging. <i>NeuroImage</i> , 2008 , 42, 750-70	7.9	15
2265	Resolving crossing fibres using constrained spherical deconvolution: validation using diffusion-weighted imaging phantom data. <i>NeuroImage</i> , 2008 , 42, 617-25	7.9	410
2264	Connecting and merging fibres: pathway extraction by combining probability maps. <i>NeuroImage</i> , 2008 , 43, 81-9	7.9	60

(2008-2008)

2263	The multiple synaesthete E.S.: neuroanatomical basis of interval-taste and tone-colour synaesthesia. <i>NeuroImage</i> , 2008 , 43, 192-203	7.9	72
2262	Two-tensor streamline tractography through white matter intra-voxel fiber crossings: Assessed by fMRI. 2008 ,		
2261	Multi-fiber reconstruction from DW-MRI using a continuous mixture of von Mises-Fisher distributions. 2008 ,		10
2260	DT-MRI fiber tracking: a shortest paths approach. 2008 , 27, 1458-71		59
2259	The human motor corpus callosum. 2008 , 19, 451-66		25
2258	Changes in connectivity after visual cortical brain damage underlie altered visual function. 2008 , 131, 1433-44		185
2257	Anatomical connectivity of the subgenual cingulate region targeted with deep brain stimulation for treatment-resistant depression. 2008 , 18, 1374-83		450
2256	Diffusion tensor MR imaging and fiber tractography: theoretic underpinnings. 2008, 29, 632-41		339
2255	Diffusion tensor MR imaging and fiber tractography: technical considerations. 2008 , 29, 843-52		299
2254	Regularized super-resolution for diffusion MRI. 2008,		8
2254	Regularized super-resolution for diffusion MRI. 2008, Voxelwise regularisation of high angular resolution diffusion imaging data. 2008, 2008, 90-3		8
			8
2253	Voxelwise regularisation of high angular resolution diffusion imaging data. 2008, 2008, 90-3 Prediction correction tractography through statistical tracking. 2008,		3
2253	Voxelwise regularisation of high angular resolution diffusion imaging data. 2008, 2008, 90-3 Prediction correction tractography through statistical tracking. 2008,		
2253	Voxelwise regularisation of high angular resolution diffusion imaging data. 2008, 2008, 90-3 Prediction correction tractography through statistical tracking. 2008, A Brief Introduction to Common Neuroimaging Techniques. 2008, 57-67 ConTrack: finding the most likely pathways between brain regions using diffusion tractography.	06	3
2253 2252 2251 2250	Voxelwise regularisation of high angular resolution diffusion imaging data. 2008, 2008, 90-3 Prediction correction tractography through statistical tracking. 2008, A Brief Introduction to Common Neuroimaging Techniques. 2008, 57-67 ConTrack: finding the most likely pathways between brain regions using diffusion tractography. 2008, 8, 15.1-16 Connectivity-based parcellation of the cortical mantle using q-ball diffusion imaging. 2008, 2008, 3684	06	3 70
2253 2252 2251 2250 2249	Voxelwise regularisation of high angular resolution diffusion imaging data. 2008, 2008, 90-3 Prediction correction tractography through statistical tracking. 2008, A Brief Introduction to Common Neuroimaging Techniques. 2008, 57-67 ConTrack: finding the most likely pathways between brain regions using diffusion tractography. 2008, 8, 15.1-16 Connectivity-based parcellation of the cortical mantle using q-ball diffusion imaging. 2008, 2008, 3684		3 70 26

2245 Diffusion and the MR signal. 173-202

2244	Age- and gender-related differences in the cortical anatomical network. 2009 , 29, 15684-93	500
	Mesh-based spherical deconvolution for physically valid fiber orientation reconstruction from	
2243	diffusion-weighted MRI. 2009 ,	2
2242	Modelling, Fitting and Sampling in Diffusion MRI. 2009 , 3-20	8
2241	Anatomical priors for global probabilistic diffusion tractography. 2009,	0
2240	Functional but not structural networks of the human laryngeal motor cortex show left hemispheric lateralization during syllable but not breathing production. 2009 , 29, 14912-23	84
2239	Frontal-limbic white matter pathway associations with the serotonin transporter gene promoter region (5-HTTLPR) polymorphism. 2009 , 29, 6229-33	115
2238	Cerebellothalamocortical connectivity regulates penetrance in dystonia. 2009 , 29, 9740-7	230
2237	Maturation of thalamic radiations between 34 and 41 weeks' gestation: a combined voxel-based study and probabilistic tractography with diffusion tensor imaging. 2009 , 30, 1780-6	46
2236	Regional white matter integrity differentiates between vascular dementia and Alzheimer disease. 2009 , 40, 773-9	69
2235	Real-time magnetic resonance Q-Ball imaging using Kalman filtering with Laplace-Beltrami regularization. 2009 ,	
2234	Reduced limbic connections may contraindicate subgenual cingulate deep brain stimulation for intractable depression. 2009 , 111, 780-4	22
2233	Semiautomatic tractography: motor pathway segmentation in patients with intracranial vascular malformations. Clinical article. 2009 , 111, 132-40	11
2232	A voxel-based diffusion tensor imaging study of white matter in bipolar disorder. 2009 , 34, 1590-600	86
2231	Integrated imaging approach with MEG and DTI to detect mild traumatic brain injury in military and civilian patients. 2009 , 26, 1213-26	165
2230	Brain anatomical network and intelligence. 2009 , 5, e1000395	452
2229	Imaging studies in congenital anophthalmia reveal preservation of brain architecture in 'visual' cortex. 2009 , 132, 3467-80	105
2228	Functional relevance of interindividual differences in temporal lobe callosal pathways: a DTI tractography study. 2009 , 19, 1322-9	89

(2009-2009)

2227	Extraction of prefronto-amygdalar pathways by combining probability maps. 2009 , 174, 217-22	44
2226	Deterministic and probabilistic tractography based on complex fibre orientation distributions. 2009 , 28, 269-86	493
2225	Using the model-based residual bootstrap to quantify uncertainty in fiber orientations from Q-ball analysis. 2009 , 28, 535-50	37
2224	A DTI-derived measure of cortico-cortical connectivity. 2009 , 28, 1023-36	112
2223	K-space and image-space combination for motion-induced phase-error correction in self-navigated multicoil multishot DWI. 2009 , 28, 1770-80	15
2222	Frontoparietal activity and its structural connectivity in binocular rivalry. 2009 , 1305, 96-107	34
2221	Automated white-matter tractography using a probabilistic diffusion tensor atlas: Application to temporal lobe epilepsy. 2009 , 30, 1535-47	144
2220	Assessing and minimizing the effects of noise and motion in clinical DTI at 3 T. 2009 , 30, 2641-55	36
2219	Probabilistic topography of human corpus callosum using cytoarchitectural parcellation and high angular resolution diffusion imaging tractography. 2009 , 30, 3172-87	135
2218	Thalamo-frontal white matter alterations in chronic schizophrenia: a quantitative diffusion tractography study. 2009 , 30, 3812-25	75
2217	Functional and structural changes in the memory network associated with left temporal lobe epilepsy. 2009 , 30, 4070-81	62
2216	Whole-brain single-shot STEAM DTI at 4 Tesla utilizing transverse coherences for enhanced SNR. 2009 , 61, 372-80	7
2215	High-field diffusion MR histology: image-based correction of eddy-current ghosts in diffusion-weighted rapid acquisition with relaxation enhancement (DW-RARE). 2009 , 61, 728-33	7
2214	Mathematical description of q-space in spherical coordinates: exact q-ball imaging. 2009 , 61, 1350-67	64
2213	Reproducibility and consistency of evaluation techniques for HARDI data. 2009 , 22, 63-70	34
2212	Intersubject variability in the analysis of diffusion tensor images at the group level: fractional anisotropy mapping and fiber tracking techniques. 2009 , 27, 324-34	34
2211	An anatomical signature for literacy. 2009 , 461, 983-6	311
2210	Probabilistic white matter fiber tracking using particle filtering and von Mises-Fisher sampling. 2009 , 13, 5-18	46

2209	Optimal real-time Q-ball imaging using regularized Kalman filtering with incremental orientation sets. 2009 , 13, 564-79	33
2208	Essentials of Functional Neuroimaging. 2009,	2
2207	Error-related negativity is mediated by fractional anisotropy in the posterior cingulate gyrusa study combining diffusion tensor imaging and electrophysiology in healthy adults. 2009 , 19, 293-304	64
2206	A tractography analysis of two deep brain stimulation white matter targets for depression. 2009 , 65, 276-82	172
2205	Reduced white matter integrity correlated with cortico-subcortical gray matter deficits in schizophrenia. 2009 , 111, 78-85	33
2204	Adaptive kernels for multi-fiber reconstruction. 2009 , 21, 338-49	14
2203	Mapping anatomical connectivity patterns of human cerebral cortex using in vivo diffusion tensor imaging tractography. 2009 , 19, 524-36	814
2202	Variational Bayesian Inference for a Nonlinear Forward Model. 2009 , 57, 223-236	2 00
2201	Quantifying brain connectivity: a comparative tractography study. 2009 , 12, 886-93	18
2200	Tensors in Image Processing and Computer Vision. 2009,	25
2199	fMRI Techniques and Protocols. 2009 ,	11
2198	Multiple Fibers. 2009 , 55-72	21
2197	MR Diffusion Tractography. 2009 , 333-351	20
2196	Validation of Tractography. 2009 , 353-375	10
2195	Connectivity Fingerprinting of Gray Matter. 2009 , 377-402	2
2194	Tractography for Surgical Targeting. 2009 , 415-444	2
2193	[Magnetic resonance tractography in neuroradiological diagnostic aspects]. 2009, 63, 403-6	1
2192	3D stochastic completion fields for fiber tractography. 2009 ,	4

(2010-2009)

2191	Resolving crossings in the corticospinal tract by two-tensor streamline tractography: Method and clinical assessment using fMRI. <i>NeuroImage</i> , 2009 , 47 Suppl 2, T98-106	7.9	90
2190	Determination of the human brainstem respiratory control network and its cortical connections in vivo using functional and structural imaging. <i>NeuroImage</i> , 2009 , 44, 295-305	7.9	116
2189	A random effects modelling approach to the crossing-fibre problem in tractography. <i>NeuroImage</i> , 2009 , 44, 753-68	7.9	18
2188	Reproducibility of tract segmentation between sessions using an unsupervised modelling-based approach. <i>NeuroImage</i> , 2009 , 45, 377-85	7.9	33
2187	High resolution diffusion-weighted imaging in fixed human brain using diffusion-weighted steady state free precession. <i>NeuroImage</i> , 2009 , 46, 775-85	7.9	142
2186	Fully automated classification of HARDI in vivo data using a support vector machine. <i>NeuroImage</i> , 2009 , 46, 642-51	7.9	16
2185	A software tool to generate simulated white matter structures for the assessment of fibre-tracking algorithms. <i>NeuroImage</i> , 2009 , 47, 1288-300	7.9	63
2184	White matter integrity in the vicinity of Broca's area predicts grammar learning success. <i>NeuroImage</i> , 2009 , 47, 1974-81	7.9	101
2183	Mathematical methods for diffusion MRI processing. <i>NeuroImage</i> , 2009 , 45, S111-22	7.9	60
2182	Connectivity-based parcellation of human cingulate cortex and its relation to functional specialization. 2009 , 29, 1175-90		635
2181	Bayesian analysis of neuroimaging data in FSL. <i>NeuroImage</i> , 2009 , 45, S173-86	7.9	1553
2180	Using diffusion imaging to study human connectional anatomy. 2009 , 32, 75-94		248
2179	MR tractography: a review of its clinical applications. 2009 , 8, 165-74		223
2178	Diffusion-tensor imaging in brain tumors. 2009 , 1, 155-171		3
2177	An improved Bayesian tensor regularization and sampling algorithm to track neuronal fiber pathways in the language circuit. 2010 , 37, 4274-87		9
2176	Tract-specific analysis for investigation of Alzheimer disease: a brief review. 2010 , 28, 494-501		6
2175	Disease and the brain's dark energy. 2010 , 6, 15-28		673
2174	Optimum b value for resolving crossing fibers: a study with standard clinical b value using 1.5-T MR. 2010 , 52, 723-8		5

2173	Mapping of the cortical spinal tracts using magnetoencephalography and diffusion tensor tractography in pediatric brain tumor patients. 2010 , 26, 1639-45	22
2172	White matter integrity in the splenium of the corpus callosum is related to successful cognitive aging and partly mediates the protective effect of an ancestral polymorphism in ADRB2. 2010 , 40, 146-56	31
2171	Filtered multitensor tractography. 2010 , 29, 1664-75	133
2170	Estimation of diffusion properties in crossing fiber bundles. 2010 , 29, 1504-15	30
2169	Visual activation of extra-striate cortex in the absence of V1 activation. 2010 , 48, 4148-54	49
2168	Fronto-cerebellar circuits and eye movement control: a diffusion imaging tractography study of human cortico-pontine projections. 2010 , 1307, 63-71	39
2167	Location of the corticospinal tract at the corona radiata in human brain. 2010 , 1326, 75-80	41
2166	Neural pathway from nucleus basalis of Meynert passing through the cingulum in the human brain. 2010 , 1346, 190-4	29
2165	Traumatic brain injury, major depression, and diffusion tensor imaging: making connections. 2010 , 64, 213-40	75
2164	Mapping brain anatomical connectivity using white matter tractography. 2010 , 23, 821-35	86
2163	Abnormal water diffusivity in corticostriatal projections in children with Tourette syndrome. 2010 , 31, 1665-74	27
2162	Tensor kernels for simultaneous fiber model estimation and tractography. 2010 , 64, 138-48	7
2161	Separation of macrovascular signal in multi-inversion time arterial spin labelling MRI. 2010, 63, 1357-65	79
2160	A filtered approach to neural tractography using the Watson directional function. 2010 , 14, 58-69	38
2159	MR connectomics: Principles and challenges. 2010 , 194, 34-45	218
2158	Fuzzy anatomical connectedness of the brain using single and multiple fibre orientations estimated from diffusion MRI. 2010 , 34, 504-13	4
2157	New anatomic MRI techniques. 2010 , 51 Suppl 1, 80-2	4
2156	Altered white matter integrity in temporal lobe epilepsy: association with cognitive and clinical profiles. 2010 , 51, 536-45	120

2155 Neuroimaging of mood disorders: commentary. 197-204

2154 Neuroplasticity associated with tactile language communication in a deaf-blind subject. 2010 , 3, 60	10
2153 Influences of Neural Pathway Integrity on Children's Response to Reading Instruction. 2010 , 4, 150	13
Cerebellum abnormalities in idiopathic generalized epilepsy with generalized tonic-clonic seizures revealed by diffusion tensor imaging. 2010 , 5, e15219	39
2151 A diffusion tensor imaging study on the auditory system and tinnitus. 2010 , 4, 16-25	76
Greater default-mode network abnormalities compared to high order visual processing systems in amnestic mild cognitive impairment: an integrated multi-modal MRI study. 2010 , 22, 523-39	19
2149 An introduction to model-independent diffusion magnetic resonance imaging. 2010 , 21, 339-54	18
2148 Injury of the spino-thalamo-cortical pathway is necessary for central post-stroke pain. 2010 , 64, 163-8	65
A general factor of brain white matter integrity predicts information processing speed in healthy older people. 2010 , 30, 7569-74	236
Ultrahigh-resolution microstructural diffusion tensor imaging reveals perforant path degradation in aged humans in vivo. 2010 , 107, 12687-91	176
Cortico-striatal connections predict control over speed and accuracy in perceptual decision making. 2010 , 107, 15916-20	268
Scalar connectivity measures from fast-marching tractography reveal heritability of white matter architecture. 2010 ,	4
2143 Theory and applications of diffusion MRI. 2010 ,	O
Cortical and subcortical interactions during action reprogramming and their related white matter pathways. 2010 , 107, 13240-5	193
Dynamic properties of human brain structure: learning-related changes in cortical areas and associated fiber connections. 2010 , 30, 11670-7	355
2140 Medical Imaging and Augmented Reality. 2010 ,	8
Gesture discrimination in primary progressive aphasia: the intersection between gesture and language processing pathways. 2010 , 30, 6334-41	65
2138 Tractographic analysis of historical lesion surgery for depression. 2010 , 35, 2553-63	67

2137	Noninvasive functional and structural connectivity mapping of the human thalamocortical system. 2010 , 20, 1187-94		275
2136	Evaluating a visualization of uncertainty in probabilistic tractography. 2010 ,		5
2135	The structural plasticity of white matter networks following anterior temporal lobe resection. 2010 , 133, 2348-64		97
2134	White matter abnormalities in methcathinone abusers with an extrapyramidal syndrome. 2010 , 133, 3676-84		36
2133	Lesion load of the corticospinal tract predicts motor impairment in chronic stroke. 2010 , 41, 910-5		220
2132	DTI white matter fiber tractography using bayesian framework. 2010 ,		
2131	Anatomical and functional connectivity of cytoarchitectonic areas within the human parietal operculum. 2010 , 30, 6409-21		283
2130	Quantifying the effects of normal ageing on white matter structure using unsupervised tract shape modelling. <i>NeuroImage</i> , 2010 , 51, 1-10	7.9	47
2129	[Value of the functional neural tractography in the reconstruction of the visual pathways in DTMRI]. 2010 , 33, 670-9		1
2128	Opportunities and pitfalls in the quantification of fiber integrity: what can we gain from Q-ball imaging?. <i>NeuroImage</i> , 2010 , 51, 242-51	7.9	67
2127	The effect of finite diffusion gradient pulse duration on fibre orientation estimation in diffusion MRI. <i>NeuroImage</i> , 2010 , 51, 743-51	7.9	20
2126	Mesh-based spherical deconvolution: a flexible approach to reconstruction of non-negative fiber orientation distributions. <i>NeuroImage</i> , 2010 , 51, 1071-81	7.9	18
2125	Topography of connections between human prefrontal cortex and mediodorsal thalamus studied with diffusion tractography. <i>NeuroImage</i> , 2010 , 51, 555-64	7.9	144
2124	Somatotopic location of corticospinal tract at pons in human brain: a diffusion tensor tractography study. <i>NeuroImage</i> , 2010 , 51, 952-5	7.9	54
2123	The effect and reproducibility of different clinical DTI gradient sets on small world brain connectivity measures. <i>NeuroImage</i> , 2010 , 51, 1106-16	7.9	98
2122	Comparative mouse brain tractography of diffusion magnetic resonance imaging. <i>NeuroImage</i> , 2010 , 51, 1027-36	7.9	59
2121	Development of functional and structural connectivity within the default mode network in young children. <i>NeuroImage</i> , 2010 , 52, 290-301	7.9	381
2120	Reproducibility of thalamic segmentation based on probabilistic tractography. <i>NeuroImage</i> , 2010 , 52, 69-85	7.9	62

(2010-2010)

2119	Horizontal portion of arcuate fasciculus fibers track to pars opercularis, not pars triangularis, in right and left hemispheres: a DTI study. <i>NeuroImage</i> , 2010 , 52, 436-44	7.9	49	
2118	Structural connectivity of Broca's area and medial frontal cortex. <i>NeuroImage</i> , 2010 , 52, 1230-7	7.9	97	
2117	Topographic organization of V1 projections through the corpus callosum in humans. <i>NeuroImage</i> , 2010 , 52, 1224-9	7.9	51	
2116	Connectivity-based segmentation of the substantia nigra in human and its implications in Parkinson's disease. <i>NeuroImage</i> , 2010 , 52, 1175-80	7.9	102	
2115	Track-density imaging (TDI): super-resolution white matter imaging using whole-brain track-density mapping. <i>NeuroImage</i> , 2010 , 53, 1233-43	7.9	271	
2114	Identification of spinothalamic tract and its related thalamocortical fibers in human brain. 2010 , 468, 102-5		48	
2113	Mammillothalamic tract in human brain: diffusion tensor tractography study. 2010 , 481, 51-3		30	
2112	Crossing fibres in tract-based spatial statistics. <i>NeuroImage</i> , 2010 , 49, 249-56	7.9	145	
2111	Combining shape and connectivity analysis: an MRI study of thalamic degeneration in Alzheimer's disease. <i>NeuroImage</i> , 2010 , 49, 1-8	7.9	138	
2 110	A modified damped Richardson-Lucy algorithm to reduce isotropic background effects in spherical deconvolution. <i>NeuroImage</i> , 2010 , 49, 1446-58	7.9	235	
2109	Diffusion orientation transform revisited. <i>NeuroImage</i> , 2010 , 49, 1326-39	7.9	28	
2108	Brain tractography using Q-ball imaging and graph theory: Improved connectivities through fibre crossings via a model-based approach. <i>NeuroImage</i> , 2010 , 49, 2444-56	7.9	52	
2107	Probabilistic tractography of the optic radiationsan automated method and anatomical validation. <i>NeuroImage</i> , 2010 , 49, 2001-12	7.9	29	
2106	Deconvolution in diffusion spectrum imaging. <i>NeuroImage</i> , 2010 , 50, 136-49	7.9	29	
2105	Whole-brain anatomical networks: does the choice of nodes matter?. <i>NeuroImage</i> , 2010 , 50, 970-83	7.9	877	
2104	Identifying population differences in whole-brain structural networks: a machine learning approach. <i>NeuroImage</i> , 2010 , 50, 910-9	7.9	76	
2103	An automated strategy for the delineation and parcellation of commissural pathways suitable for clinical populations utilising high angular resolution diffusion imaging tractography. <i>NeuroImage</i> , 2010 , 50, 1044-53	7.9	34	
2102	On approximation of orientation distributions by means of spherical ridgelets. 2010 , 19, 461-77		53	

2101	Fast and accurate reconstruction of HARDI data using compressed sensing. 2010 , 13, 607-14		14
2100	Motor recovery mechanism in a quadriplegic patient with locked-in syndrome. 2012 , 30, 113-7		5
2099	A translational bridge between mouse and human models of learned safety. 2010 , 42, 115-22		40
2098	Estimation of Anisotropic Water Diffusion Indexes on Axon Bundle Crossings. 2011 ,		
2097	Increased regional fractional anisotropy in highly screened attention-deficit hyperactivity disorder (ADHD). 2011 , 26, 1296-302		61
2096	Disrupted axonal fiber connectivity in schizophrenia. 2011 , 69, 80-9		363
2095	Resolving axon fiber crossings at clinical b-values: an evaluation study. 2011 , 38, 5239-53		15
2094	Digital Processing of Diffusion-Tensor Images of Avascular Tissues. 2011 , 341-371		1
2093	Probabilistic somatotopy of the spinothalamic pathway at the ventroposterolateral nucleus of the thalamus in the human brain. 2011 , 32, 1358-62		14
2092	BDNF gene effects on brain circuitry replicated in 455 twins. <i>NeuroImage</i> , 2011 , 55, 448-54	7.9	94
2091	Error-related medial frontal theta activity predicts cingulate-related structural connectivity. <i>NeuroImage</i> , 2011 , 55, 1373-83	7.9	142
2090	Connectivity constraints on cortical reorganization of neural circuits involved in object naming. <i>NeuroImage</i> , 2011 , 55, 1306-13	7.9	48
2089	Quantitative evaluation of 10 tractography algorithms on a realistic diffusion MR phantom. <i>NeuroImage</i> , 2011 , 56, 220-34	7.9	312
2088	Symmetric diffeomorphic registration of fibre orientation distributions. <i>NeuroImage</i> , 2011 , 56, 1171-80	7.9	145
2087	Connectivity-based segmentation of human amygdala nuclei using probabilistic tractography. <i>NeuroImage</i> , 2011 , 56, 1353-61	7.9	89
2086	A critical re-examination of sexual dimorphism in the corpus callosum microstructure. <i>NeuroImage</i> , 2011 , 56, 874-80	7.9	37
2085	Cerebello-thalamo-cerebral connections in pediatric brain tumor patients: impact on working memory. <i>NeuroImage</i> , 2011 , 56, 2238-48	7.9	83
2084	Diffusion imaging of whole, post-mortem human brains on a clinical MRI scanner. <i>NeuroImage</i> , 2011 , 57, 167-181	7.9	193

2083	MEG beamforming using Bayesian PCA for adaptive data covariance matrix regularization. <i>Neurolmage</i> , 2011 , 57, 1466-79	7.9	88
2082	Robust subdivision of the thalamus in children based on probability distribution functions calculated from probabilistic tractography. <i>NeuroImage</i> , 2011 , 57, 403-15	7.9	20
2081	Discriminating schizophrenia and bipolar disorder by fusing fMRI and DTI in a multimodal CCA+ joint ICA model. <i>NeuroImage</i> , 2011 , 57, 839-55	7.9	179
2080	Direct segmentation of the major white matter tracts in diffusion tensor images. <i>NeuroImage</i> , 2011 , 58, 458-68	7.9	50
2079	Probabilistic fibre tract analysis of cytoarchitectonically defined human inferior parietal lobule areas reveals similarities to macaques. <i>NeuroImage</i> , 2011 , 58, 362-80	7.9	181
2078	Multivariate models of inter-subject anatomical variability. <i>NeuroImage</i> , 2011 , 56, 422-39	7.9	34
2077	Partition-based mass clustering of tractography streamlines. <i>NeuroImage</i> , 2011 , 54, 303-12	7.9	35
2076	Conserved and variable architecture of human white matter connectivity. <i>NeuroImage</i> , 2011 , 54, 1262-	79 7.9	284
2075	Atlas-based fiber bundle segmentation using principal diffusion directions and spherical harmonic coefficients. <i>NeuroImage</i> , 2011 , 54 Suppl 1, S146-64	7.9	18
2074	Corpus callosal diffusivity predicts motor impairment in relapsing-remitting multiple sclerosis: a TBSS and tractography study. <i>NeuroImage</i> , 2011 , 55, 1169-77	7.9	52
2073	Processing social aspects of human gaze: a combined fMRI-DTI study. <i>NeuroImage</i> , 2011 , 55, 411-9	7.9	98
2072	DTI measures in crossing-fibre areas: increased diffusion anisotropy reveals early white matter alteration in MCI and mild Alzheimer's disease. <i>NeuroImage</i> , 2011 , 55, 880-90	7.9	381
2071	SPHERE: SPherical Harmonic Elastic REgistration of HARDI data. <i>NeuroImage</i> , 2011 , 55, 545-56	7.9	28
2070	White matter integrity in right hemisphere predicts pitch-related grammar learning. <i>NeuroImage</i> , 2011 , 55, 500-7	7.9	52
2069	Animal Models of Behavioral Analysis. 2011 ,		3
2068	Neuroanatomical prerequisites for language functions in the maturing brain. 2011 , 21, 459-66		202
2067	Brain Imaging in Behavioral Medicine and Clinical Neuroscience. 2011,		5
2066	An introduction to diffusion tensor image analysis. 2011 , 22, 185-96, viii		205

2065	Structural and Functional Neuroimaging Methods: Applications to Substance Abuse and Addiction. 2011 , 37-82	1
2064	Medical Image Processing. 2011 ,	31
2063	Advanced MRI in multiple sclerosis: current status and future challenges. 2011 , 29, 357-80	25
2062	Anatomic and electro-physiologic connectivity of the language system: a combined DTI-CCEP study. 2011 , 41, 1100-9	62
2061	Quantitative diffusion tensor deterministic and probabilistic fiber tractography in relapsing-remitting multiple sclerosis. 2011 , 79, 101-7	17
2060	Effects of practice and experience on the arcuate fasciculus: comparing singers, instrumentalists, and non-musicians. 2011 , 2, 156	182
2059	The anatomical characteristics of the stria terminalis in the human brain: a diffusion tensor tractography study. 2011 , 500, 99-102	16
2058	The rubrospinal tract in the human brain: diffusion tensor imaging study. 2011 , 504, 45-8	32
2057	Current challenges in the practice of epilepsy surgery. 2011 , 22, 23-31	20
2056	Caudate atrophy and impaired frontostriatal connections are linked to executive dysfunction in temporal lobe epilepsy. 2011 , 21, 80-7	49
2055	Syntactic processing depends on dorsal language tracts. 2011 , 72, 397-403	206
2054	Brain connectivity: gender makes a difference. 2011 , 17, 575-91	204
2053	Integrating temporal and spatial scales: human structural network motifs across age and region of interest size. 2011 , 5, 10	19
2052	White matter damage in primary progressive aphasias: a diffusion tensor tractography study. 2011 , 134, 3011-29	235
2051	Recovery of the corticospinal tract after injury by transtentorial herniation: a case report. 2011 , 29, 243-6	4
2050	Searching for novel biomarkers using high resolution diffusion tensor imaging. 2011 , 26 Suppl 3, 297-305	5
2049	Diffusion tensor imaging: exploring the motor networks and clinical applications. 2011 , 12, 651-61	24
2048	Callosal connections of primary visual cortex predict the spatial spreading of binocular rivalry across the visual hemifields. 2011 , 5, 161	32

(2011-2011)

2047	Automated probabilistic reconstruction of white-matter pathways in health and disease using an atlas of the underlying anatomy. 2011 , 5, 23	361
2046	The role of long-range connectivity for the characterization of the functional-anatomical organization of the cortex. 2011 , 5, 58	37
2045	Differential development of human brain white matter tracts. 2011 , 6, e23437	55
2044	Nonparametric tests of structure for high angular resolution diffusion imaging in Q-space. 2011 , 5,	
2043	Neural Network Related to Hand Movement: A Combined Study of Diffusion Tensor Tractography and Functional MRI. 2011 , 23, 97-101	5
2042	Brain aging, cognition in youth and old age and vascular disease in the Lothian Birth Cohort 1936: rationale, design and methodology of the imaging protocol. 2011 , 6, 547-59	150
2041	Complementary image analysis of diffusion tensor imaging and 3-dimensional t1-weighted imaging: white matter analysis in amyotrophic lateral sclerosis. 2011 , 21, 24-33	10
2040	Regularization of bending and crossing white matter fibers in MRI Q-ball fields. 2011 , 29, 916-26	10
2039	Connectivity-based segmentation of the striatum in Huntington's disease: vulnerability of motor pathways. 2011 , 42, 475-81	72
2038	PopTract: population-based tractography. 2011 , 30, 1829-40	18
2037	Hippocampal-prefrontal connectivity predicts midfrontal oscillations and long-term memory performance. 2011 , 21, 1900-5	57
2036	ESMRMB 2011, 28th Annual Scientific Meeting, Leipzig, Germany, 6-8 October: Abstracts, Saturday. 2011 , 24, 183-270	2
2035	Distance-based tractography in high angular resolution diffusion MRI. 2011 , 27, 729-738	6
2034	Diffusion tensor imaging shows white matter tracts between human auditory and visual cortex. 2011 , 213, 299-308	96
2033	Mammillotegmental tract in the human brain: diffusion tensor tractography study. 2011 , 53, 623-6	7
2032	Dentatorubrothalamic tract in human brain: diffusion tensor tractography study. 2011 , 53, 787-91	83
2031	A Hough transform global probabilistic approach to multiple-subject diffusion MRI tractography. 2011 , 15, 414-25	105
2030	Recent advances in diffusion MRI modeling: Angular and radial reconstruction. 2011 , 15, 369-96	77

2029	Developmental malformation of the corpus callosum: a review of typical callosal development and examples of developmental disorders with callosal involvement. 2011 , 3, 3-27	147
2028	A full bi-tensor neural tractography algorithm using the unscented Kalman filter. 2011 , 2011,	6
2027	Ex vivo water diffusion tensor properties of the fibroid uterus at 7 T and their relation to tissue morphology. 2011 , 34, 1445-51	5
2026	Diffusion tensor imaging and beyond. 2011 , 65, 1532-56	618
2025	Probabilistic fiber tracking using the residual bootstrap with constrained spherical deconvolution. 2011 , 32, 461-79	279
2024	An ex vivo imaging pipeline for producing high-quality and high-resolution diffusion-weighted imaging datasets. 2011 , 32, 544-63	166
2023	Topographical relationships between arcuate fasciculus connectivity and cortical thickness. 2011 , 32, 1788-801	19
2022	Diffusion tensor-based fast marching for modeling human brain connectivity network. 2011 , 35, 167-78	9
2021	A framework on surface-based connectivity quantification for the human brain. 2011 , 197, 324-32	6
2020	Multiple q-shell diffusion propagator imaging. 2011 , 15, 603-21	127
2020	Multiple q-shell diffusion propagator imaging. 2011 , 15, 603-21 Diffusion-Tensor MRI Based Skeletal Muscle Fiber Tracking. 2011 , 3, 675-687	127 25
2019	Diffusion-Tensor MRI Based Skeletal Muscle Fiber Tracking. 2011 , 3, 675-687 Principles and limitations of computational algorithms in clinical diffusion tensor MR tractography.	25
2019	Diffusion-Tensor MRI Based Skeletal Muscle Fiber Tracking. 2011 , 3, 675-687 Principles and limitations of computational algorithms in clinical diffusion tensor MR tractography. 2011 , 32, 3-13 Anatomic location and somatotopic arrangement of the corticospinal tract at the cerebral peduncle	25
2019 2018 2017	Diffusion-Tensor MRI Based Skeletal Muscle Fiber Tracking. 2011, 3, 675-687 Principles and limitations of computational algorithms in clinical diffusion tensor MR tractography. 2011, 32, 3-13 Anatomic location and somatotopic arrangement of the corticospinal tract at the cerebral peduncle in the human brain. 2011, 32, 2116-9 Modeling diffusion-weighted MRI as a spatially variant gaussian mixture: application to image	25 86 27
2019 2018 2017 2016	Diffusion-Tensor MRI Based Skeletal Muscle Fiber Tracking. 2011, 3, 675-687 Principles and limitations of computational algorithms in clinical diffusion tensor MR tractography. 2011, 32, 3-13 Anatomic location and somatotopic arrangement of the corticospinal tract at the cerebral peduncle in the human brain. 2011, 32, 2116-9 Modeling diffusion-weighted MRI as a spatially variant gaussian mixture: application to image denoising. 2011, 38, 4350-64	25 86 27
2019 2018 2017 2016 2015	Diffusion-Tensor MRI Based Skeletal Muscle Fiber Tracking. 2011, 3, 675-687 Principles and limitations of computational algorithms in clinical diffusion tensor MR tractography. 2011, 32, 3-13 Anatomic location and somatotopic arrangement of the corticospinal tract at the cerebral peduncle in the human brain. 2011, 32, 2116-9 Modeling diffusion-weighted MRI as a spatially variant gaussian mixture: application to image denoising. 2011, 38, 4350-64 Exploring workflow interoperability tools for neuroimaging data analysis. 2011, Multi-institutional evaluation of deep brain stimulation targeting using probabilistic	25 86 27 7

2011	Source-based morphometry analysis of group differences in fractional anisotropy in schizophrenia. 2011 , 1, 133-45	37
2010	Effect of white matter anisotropy in modeling electroconvulsive therapy. 2011 , 2011, 5492-5	
2009	Assessment of functional and structural connectivity between motor cortex and thalamus using fMRI and DWI. 2011 , 2011, 5056-9	10
2008	The speed-accuracy tradeoff in the elderly brain: a structural model-based approach. 2011 , 31, 17242-9	144
2007	Direct structural connections between voice- and face-recognition areas. 2011 , 31, 12906-15	117
2006	Ventral premotor cortex may be required for dynamic changes in the feeling of limb ownership: a lesion study. 2011 , 31, 4852-7	85
2005	Somatotopic arrangement of the corticospinal tract at the medullary pyramid in the human brain. 2011 , 65, 46-9	11
2004	White matter anisotropy in the ventral language pathway predicts sound-to-word learning success. 2011 , 31, 8780-5	86
2003	A stable sparse fear memory trace in human amygdala. 2011 , 31, 9383-9	56
2002	One week of motor adaptation induces structural changes in primary motor cortex that predict long-term memory one year later. 2011 , 31, 11808-13	104
2001	Segmenting thalamic nuclei: what can we gain from HARdI?. 2011 , 14, 141-8	3
2 000	Resolving complex fibre configurations using two-tensor random-walk stochastic algorithms. 2011,	
1999	Atrophy, hypometabolism and white matter abnormalities in semantic dementia tell a coherent story. 2011 , 134, 2025-35	152
1998	Posterior medial frontal cortex activity predicts post-error adaptations in task-related visual and motor areas. 2011 , 31, 1780-9	186
1997	Deep and superficial amygdala nuclei projections revealed in vivo by probabilistic tractography. 2011 , 31, 618-23	115
1996	Rules ventral prefrontal cortical axons use to reach their targets: implications for diffusion tensor imaging tractography and deep brain stimulation for psychiatric illness. 2011 , 31, 10392-402	151
1995	High connectivity between reduced cortical thickness and disrupted white matter tracts in long-standing type 1 diabetes. 2011 , 60, 315-9	51
1994	Diffusion-weighted imaging tractography-based parcellation of the human parietal cortex and comparison with human and macaque resting-state functional connectivity. 2011 , 31, 4087-100	394

Global estimation of anatomical connection strength in diffusion MRI tractography by message-passing. **2011**,

Motor practice promotes increased activity in brain regions structurally disconnected after subcortical stroke. 2011 , 25, 607-16	42
The brain structural hub of interhemispheric information integration for visual motion perception 2012 , 22, 337-44	on. 16
DTI and MR Volumetry of Hippocampus-PC/PCC Circuit: In Search of Early Micro- and Macrostructural Signs of Alzheimers's Disease. 2012 , 2012, 517876	26
Normative development of white matter tracts: similarities and differences in relation to age, gender, and intelligence. 2012 , 22, 1738-47	123
Medial temporal lobe epilepsy is associated with neuronal fibre loss and paradoxical increase in structural connectivity of limbic structures. 2012 , 83, 903-9	152
Investigation of anatomical thalamo-cortical connectivity and FMRI activation in schizophrenia. 2012 , 37, 499-507	115
Homonymous hemimacular thinning: a unique presentation of optic tract injury in neuromyelities optica. 2012 , 32, 150-3	s 14
1985 White-matter connectivity between face-responsive regions in the human brain. 2012 , 22, 1564	-76 200
Generation of individualized thalamus target maps by using statistical shape models and thalamocortical tractography. 2012 , 33, 2110-6	52
Accelerating Fibre Orientation Estimation from Diffusion Weighted Magnetic Resonance Imagin Using GPUs. 2012 ,	ng 3
Langevin dynamics modeling of the water diffusion tensor in partially aligned collagen network 2012 , 86, 031917	S. 12
Effects of electroconvulsive therapy stimulus pulsewidth and amplitude computed with an anatomically-realistic head model. 2012 , 2012, 2559-62	3
1980 Neural systems for speech and song in autism. 2012 , 135, 961-75	108
Diffusion tensor imaging correlates of visual impairment in multiple sclerosis and chronic optic neuritis. 2012 , 53, 825-32	34
Emotional voice areas: anatomic location, functional properties, and structural connections revealed by combined fMRI/DTI. 2012 , 22, 191-200	130
1977 Continuity, divergence, and the evolution of brain language pathways. 2011 , 3, 11	111
Somatotopic organization of motor pathways in the internal capsule: a probabilistic diffusion tractography study. 2012 , 33, 1274-80	48

(2012-2012)

1975	Spatiotemporal dynamics of bimanual integration in human somatosensory cortex and their relevance to bimanual object manipulation. 2012 , 32, 5667-77	23
1974	Aging and inhibitory control of action: cortico-subthalamic connection strength predicts stopping performance. 2012 , 32, 8401-12	115
1973	The prevalence of central poststroke pain according to the integrity of the spino-thalamo-cortical pathway. 2012 , 67, 12-7	35
1972	Functional graph alterations in schizophrenia: a result from a global anatomic decoupling?. 2012 , 45 Suppl 1, S57-64	23
1971	A combined post-mortem magnetic resonance imaging and quantitative histological study of multiple sclerosis pathology. 2012 , 135, 2938-51	111
1970	Clinical and neuroanatomical predictors of cerebellar mutism syndrome. 2012 , 14, 1294-303	87
1969	Neuronal loss in the medial cholinergic pathway from the nucleus basalis of Meynert in patients with traumatic axonal injury: a preliminary diffusion tensor imaging study. 2012 , 27, 172-6	8
1968	Structural human brain networks: hot topics in diffusion tractography. 2012 , 25, 375-83	99
1967	Limb apraxia in a patient with cerebral infarct: diffusion tensor tractography study. 2012, 30, 255-9	20
1966	Abnormalities of the fornix in mild cognitive impairment are related to episodic memory loss. 2012 , 29, 629-39	32
1965	Differences between the somatotopic corticospinal tract for the fingers and toes in the human brain. 2012 , 31, 395-9	6
1964	Mapping inter-regional connectivity of the entire cortex to characterize major depressive disorder: a whole-brain diffusion tensor imaging tractography study. 2012 , 23, 566-71	46
1963	A Monte Carlo based formalism to identify potential locations at high risk of tumor recurrence with a numerical model for glioblastoma multiforme. 2012 , 39, 6682-91	5
1962	Connectivity-based structural and functional parcellation of the human cortex using diffusion imaging and tractography. 2012 , 6, 34	51
1961	Enhanced DTI Tracking with Adaptive Tensor Interpolation. 2012 , 173-190	2
1960	Probabilistic Brain Fiber Tractography on GPUs. 2012 ,	2
1959	The Structural Connectivity Underpinning Language Aptitude, Working Memory, and IQ in the Perisylvian Language Network. 2012 , 62, 110-130	37
1958	Beyond the arcuate fasciculus: consensus and controversy in the connectional anatomy of language. 2012 , 135, 3529-50	293

1957	SMT: a reliability based interactive DTI tractography algorithm. 2012 , 31, 1929-40		6
1956	The Human Connectome Project: a data acquisition perspective. <i>NeuroImage</i> , 2012 , 62, 2222-31	7.9	1284
1955	Toward whole-brain maps of neural connections: Logical framework and fast implementation. 2012		
1954	The pulvinar regulates information transmission between cortical areas based on attention demands. 2012 , 337, 753-6		613
1953	Structural changes after videogame practice related to a brain network associated with intelligence. 2012 , 40, 479-489		31
1952	Difference of neural connectivity for motor function in chronic hemiparetic stroke patients with intracerebral hemorrhage. 2012 , 531, 80-5		7
1951	Thalamic shape and connectivity abnormalities in children with attention-deficit/hyperactivity disorder. 2012 , 204, 161-7		58
1950	Fronto-limbic microstructure and structural connectivity in remission from major depression. 2012 , 204, 40-8		35
1949	Brain connectivity and postural control in young traumatic brain injury patients: A diffusion MRI based network analysis. 2012 , 1, 106-15		60
1948	Simultaneous ODF estimation and tractography in HARDI. 2012 , 2012, 86-9		4
1947	Multivalued Geodesic Ray-Tracing for Computing Brain Connections Using Diffusion Tensor Imaging. 2012 , 5, 483-504		13
1946	A NOVEL INTRINSIC UNSCENTED KALMAN FILTER FOR TRACTOGRAPHY FROM HARDI*. 2012 , 2012, 534-537		3
1945	Frontal-occipital connectivity during visual search. 2012 , 2, 164-75		19
1944	Differences between chimpanzees and bonobos in neural systems supporting social cognition. 2012 , 7, 369-79		103
1943	Interpolating multi-fiber models by Gaussian mixture simplification. 2012,		5
1942	Peak Geodesic Concentration: A measure of WM complexity in HARDI. 2012 ,		
1941	Connectivity-based subdivisions of the human right "temporoparietal junction area": evidence for different areas participating in different cortical networks. 2012 , 22, 1894-903		383
1940	A genome-wide search for genetic influences and biological pathways related to the brain's white matter integrity. 2012 , 33, 1847.e1-14		35

1939	A network diffusion model of disease progression in dementia. 2012 , 73, 1204-15	434
1938	Corticostriatal connectivity underlies individual differences in the balance between habitual and goal-directed action control. 2012 , 32, 12066-75	277
1937	New insights into the pathology of white matter tracts in cerebral palsy from diffusion magnetic resonance imaging: a systematic review. 2012 , 54, 684-96	82
1936	Fully automatic stitching of diffusion tensor images in spinal cord. 2012 , 209, 371-8	5
1935	The anatomical characteristics of superior longitudinal fasciculus I in human brain: Diffusion tensor tractography study. 2012 , 506, 146-8	22
1934	White matter connectivity between superior temporal sulcus and amygdala is associated with autistic trait in healthy humans. 2012 , 510, 154-8	33
1933	Termination differences in the primary sensorimotor cortex between the medial lemniscus and spinothalamic pathways in the human brain. 2012 , 516, 50-3	8
1932	The neural connectivity of the inferior olivary nucleus in the human brain: a diffusion tensor tractography study. 2012 , 523, 67-70	10
1931	Anatomical location of the corticospinal tract according to somatotopies in the centrum semiovale. 2012 , 523, 111-4	17
1930	The prefrontal cortex: comparative architectonic organization in the human and the macaque monkey brains. 2012 , 48, 46-57	208
1929	Neuroprotective lifestyles and the aging brain: activity, atrophy, and white matter integrity. 2012 , 79, 1802-8	138
1928	A role for the default mode network in the bases of disorders of consciousness. 2012 , 72, 335-43	171
1927	White matter structure changes as adults learn a second language. 2012 , 24, 1664-70	176
1926	Comparing structural and functional graph theory features in the human brain using multimodal MRI. 2012 , 33, 244-253	9
1925	Convergence and divergence of thickness correlations with diffusion connections across the human cerebral cortex. <i>NeuroImage</i> , 2012 , 59, 1239-48	232
1924	Cardiorespiratory fitness is positively correlated with cerebral white matter integrity in healthy seniors. <i>NeuroImage</i> , 2012 , 59, 1514-23	124
1923	Anatomical insights into disrupted small-world networks in schizophrenia. <i>NeuroImage</i> , 2012 , 59, 1085-9 3 .9	132
1922	Diffusion tractography of post-mortem human brains: optimization and comparison of spin echo and steady-state free precession techniques. <i>NeuroImage</i> , 2012 , 59, 2284-97	59

1921	The influence of complex white matter architecture on the mean diffusivity in diffusion tensor MRI of the human brain. <i>NeuroImage</i> , 2012 , 59, 2208-16	7.9	146
1920	Apparent Fibre Density: a novel measure for the analysis of diffusion-weighted magnetic resonance images. <i>NeuroImage</i> , 2012 , 59, 3976-94	7.9	341
1919	Bayesian inference in FMRI. <i>Neurolmage</i> , 2012 , 62, 801-10	7.9	37
1918	Hierarchical topological network analysis of anatomical human brain connectivity and differences related to sex and kinship. <i>NeuroImage</i> , 2012 , 59, 3784-804	7.9	52
1917	Diffusion MRI at 25: exploring brain tissue structure and function. <i>NeuroImage</i> , 2012 , 61, 324-41	7.9	305
1916	Corpus callosum alterations in very preterm infants: perinatal correlates and 2 year neurodevelopmental outcomes. <i>NeuroImage</i> , 2012 , 59, 3571-81	7.9	79
1915	Confirmation of functional zones within the human subthalamic nucleus: patterns of connectivity and sub-parcellation using diffusion weighted imaging. <i>NeuroImage</i> , 2012 , 60, 83-94	7.9	246
1914	The functional connectivity of the human caudate: an application of meta-analytic connectivity modeling with behavioral filtering. <i>NeuroImage</i> , 2012 , 60, 117-29	7.9	181
1913	Cortico-subthalamic white matter tract strength predicts interindividual efficacy in stopping a motor response. <i>NeuroImage</i> , 2012 , 60, 370-5	7.9	126
1912	k-space and q-space: combining ultra-high spatial and angular resolution in diffusion imaging using ZOOPPA at 7 T. <i>NeuroImage</i> , 2012 , 60, 967-78	7.9	109
1911	Ball and rackets: Inferring fiber fanning from diffusion-weighted MRI. <i>NeuroImage</i> , 2012 , 60, 1412-25	7.9	124
1910	Effects of image distortions originating from susceptibility variations and concomitant fields on diffusion MRI tractography results. <i>NeuroImage</i> , 2012 , 61, 275-88	7.9	156
1909	A multi-modal investigation of behavioral adjustment: post-error slowing is associated with white matter characteristics. <i>NeuroImage</i> , 2012 , 61, 195-205	7.9	14
1908	Quantitative assessment of a framework for creating anatomical brain networks via global tractography. <i>NeuroImage</i> , 2012 , 61, 1017-30	7.9	33
1907	NODDI: practical in vivo neurite orientation dispersion and density imaging of the human brain. <i>NeuroImage</i> , 2012 , 61, 1000-16	7.9	1589
1906	Determining functional connectivity using fMRI data with diffusion-based anatomical weighting. <i>NeuroImage</i> , 2012 , 62, 1769-79	7.9	54
1905	Grammar learning in older adults is linked to white matter microstructure and functional connectivity. <i>NeuroImage</i> , 2012 , 62, 1667-74	7.9	30
1904	Human cortical connectome reconstruction from diffusion weighted MRI: the effect of tractography algorithm. <i>NeuroImage</i> , 2012 , 62, 1732-49	7.9	143

(2012-2012)

1903	Anatomically-constrained tractography: improved diffusion MRI streamlines tractography through effective use of anatomical information. <i>NeuroImage</i> , 2012 , 62, 1924-38	7.9	520	
1902	A DTI tractography analysis of infralimbic and prelimbic connectivity in the mouse using high-throughput MRI. <i>NeuroImage</i> , 2012 , 63, 800-11	7.9	32	
1901	A robust method for investigating thalamic white matter tracts after traumatic brain injury. <i>NeuroImage</i> , 2012 , 63, 779-88	7.9	31	
1900	HOMOR: higher order model outlier rejection for high b-value MR diffusion data. <i>NeuroImage</i> , 2012 , 63, 835-42	7.9	37	
1899	A large deformation diffeomorphic metric mapping solution for diffusion spectrum imaging datasets. <i>NeuroImage</i> , 2012 , 63, 818-34	7.9	32	
1898	Tractography-based parcellation of the human left inferior parietal lobule. <i>NeuroImage</i> , 2012 , 63, 641-	52 7.9	77	
1897	Functional MRI-guided probabilistic tractography of cortico-cortical and cortico-subcortical language networks in children. <i>NeuroImage</i> , 2012 , 63, 1561-70	7.9	13	
1896	White matter integrity of the descending pain modulatory system is associated with interindividual differences in placebo analgesia. 2012 , 153, 2210-2217		85	
1895	White matter tract abnormalities in first-episode psychosis. 2012 , 141, 29-34		19	
1894	An investigation of a genomewide supported psychosis variant in ZNF804A and white matter integrity in the human brain. 2012 , 30, 1373-80		27	
1893	Anatomical connectivity patterns predict face selectivity in the fusiform gyrus. 2011 , 15, 321-7		216	
1892	Diffusion MRI of the neonate brain: acquisition, processing and analysis techniques. 2012 , 42, 1169-82		40	
1891	Diffusion magnetic resonance imaging for Brainnetome: a critical review. 2012 , 28, 375-88		11	
1890	Functional expansion of sensorimotor representation and structural reorganization of callosal connections in lower limb amputees. 2012 , 32, 3211-20		88	
1889	New Developments in the Visualization and Processing of Tensor Fields. 2012,		5	
1888	Learning a reliable estimate of the number of fiber directions in diffusion MRI. 2012 , 15, 493-500		18	
1887	Neuroanatomical patterns of cerebral white matter involvement in different motor neuron diseases as studied by diffusion tensor imaging analysis. 2012 , 13, 254-64		43	
1886	Comprehensive in vivo mapping of the human basal ganglia and thalamic connectome in individuals using 7T MRI. 2012 , 7, e29153		133	

1885	Improved sensitivity to cerebral white matter abnormalities in Alzheimer's disease with spherical deconvolution based tractography. 2012 , 7, e44074		66
1884	Increased cortical-limbic anatomical network connectivity in major depression revealed by diffusion tensor imaging. 2012 , 7, e45972		68
1883	Anatomical substrates of the alerting, orienting and executive control components of attention: focus on the posterior parietal lobe. 2012 , 7, e50590		40
1882	The Claustrum and Insula in Microcebus murinus: A High Resolution Diffusion Imaging Study. 2012 , 6, 21		33
1881	MR connectomics: a conceptual framework for studying the developing brain. 2012 , 6, 43		76
1880	The translational role of diffusion tensor image analysis in animal models of developmental pathologies. 2012 , 34, 5-19		16
1879	Brain white matter tract integrity as a neural foundation for general intelligence. 2012 , 17, 1026-30		219
1878	Validation of connectivity-based thalamic segmentation with direct electrophysiologic recordings from human sensory thalamus. <i>NeuroImage</i> , 2012 , 59, 2025-34	7.9	46
1877	Compensatory role of the cortico-rubro-spinal tract in motor recovery after stroke. 2012 , 79, 515-22		81
1876	Implementation and assessment of diffusion-weighted partial Fourier readout-segmented echo-planar imaging. 2012 , 68, 441-51		27
1875	Correction of vibration artifacts in DTI using phase-encoding reversal (COVIPER). 2012, 68, 882-9		38
1874	Model-based analysis of multishell diffusion MR data for tractography: how to get over fitting problems. 2012 , 68, 1846-55		222
1873	Predicting functional motor potential in chronic stroke patients using diffusion tensor imaging. 2012 , 33, 1040-51		182
1872	The effects of connection reconstruction method on the interregional connectivity of brain networks via diffusion tractography. 2012 , 33, 1894-913		75
1871	Probabilistic tractography recovers a rostrocaudal trajectory of connectivity variability in the human insular cortex. 2012 , 33, 2005-34		200
1870	Diffusion tensor imaging of the optic radiations after optic neuritis. 2012 , 33, 2047-61		37
1869	Parieto-frontal network in humans studied by cortico-cortical evoked potential. 2012 , 33, 2856-72		82
1868	Degeneration of corpus callosum and recovery of motor function after stroke: a multimodal magnetic resonance imaging study. 2012 , 33, 2941-56		92

(2012-2012)

1867	Reduced fractional anisotropy in the uncinate fasciculus in patients with major depression carrying the met-allele of the Val66Met brain-derived neurotrophic factor genotype. 2012 , 159B, 537-48	64
1866	Connectivity-based parcellation reveals interhemispheric differences in the insula. 2012 , 25, 264-71	90
1865	Human connectomics. 2012 , 22, 144-53	183
1864	Neural correlates supporting sensory discrimination after left hemisphere stroke. 2012 , 1460, 78-87	25
1863	Atypical hemispheric asymmetry in the arcuate fasciculus of completely nonverbal children with autism. 2012 , 1252, 332-7	45
1862	When right is all that is left: plasticity of right-hemisphere tracts in a young aphasic patient. 2012 , 1252, 237-45	53
1861	Modeling the orientation distribution function by mixtures of angular central Gaussian distributions. 2012 , 203, 200-11	12
1860	The effect of gradient sampling schemes on diffusion metrics derived from probabilistic analysis and tract-based spatial statistics. 2012 , 30, 402-12	13
1859	Globally optimized fiber tracking and hierarchical clustering a unified framework. 2012 , 30, 485-95	12
1858	White matter microstructural alterations in migraine: a diffusion-weighted MRI study. 2012 , 153, 651-656	61
1857	Diffeomorphic metric mapping of high angular resolution diffusion imaging based on Riemannian structure of orientation distribution functions. 2012 , 31, 1021-33	26
1856	Accurate localization of optic radiation during neurosurgery in an interventional MRI suite. 2012 , 31, 882-91	34
1855	Perceived helplessness is associated with individual differences in the central motor output system. 2012 , 35, 1481-7	36
1854	Modeling the interactions of Alzheimer-related genes from the whole brain microarray data and diffusion tensor images of human brain. 2012 , 13 Suppl 7, S10	8
1853	Direct optic nerve pulvinar connections defined by diffusion MR tractography in humans: implications for photophobia. 2012 , 33, 75-88	58
1852	Sensitive period for white-matter connectivity of superior temporal cortex in deaf people. 2012 , 33, 349-59	41
1851	MRtrix: Diffusion tractography in crossing fiber regions. 2012 , 22, 53-66	849
1850	Fast approximate stochastic tractography. 2012 , 10, 5-17	3

1849	Three-dimensional interactive and stereotactic human brain atlas of white matter tracts. 2012, 10, 33-55	32
1848	Preserved interhemispheric functional connectivity in a case of corpus callosum agenesis. 2012 , 54, 177-9	11
1847	Inferior frontal white matter asymmetry correlates with executive control of attention. 2013 , 34, 796-813	57
1846	Can spherical deconvolution provide more information than fiber orientations? Hindrance modulated orientational anisotropy, a true-tract specific index to characterize white matter diffusion. 2013 , 34, 2464-83	200
1845	Investigating the prevalence of complex fiber configurations in white matter tissue with diffusion magnetic resonance imaging. 2013 , 34, 2747-66	635
1844	Effects of chronic mild traumatic brain injury on white matter integrity in Iraq and Afghanistan war veterans. 2013 , 34, 2986-99	89
1843	Diffusion MR imaging: How to get the maximum from the experimental time. 2013, 4,	3
1842	Anatomical connection strength predicts dopaminergic drug effects on fronto-striatal function. 2013 , 227, 521-31	23
1841	Neuroimaging of Movement Disorders. 2013,	1
1840	Modeling in Computational Biology and Biomedicine. 2013,	1
1840 1839	Modeling in Computational Biology and Biomedicine. 2013, The organization of dorsal frontal cortex in humans and macaques. 2013, 33, 12255-74	281
1839	The organization of dorsal frontal cortex in humans and macaques. 2013 , 33, 12255-74 Diffusion tensor imaging reveals widespread white matter abnormalities in children and	281
1839 1838	The organization of dorsal frontal cortex in humans and macaques. 2013 , 33, 12255-74 Diffusion tensor imaging reveals widespread white matter abnormalities in children and adolescents with myotonic dystrophy type 1. 2013 , 260, 1122-31 Mapping of the mouse olfactory system with manganese-enhanced magnetic resonance imaging	281
1839 1838 1837	The organization of dorsal frontal cortex in humans and macaques. 2013, 33, 12255-74 Diffusion tensor imaging reveals widespread white matter abnormalities in children and adolescents with myotonic dystrophy type 1. 2013, 260, 1122-31 Mapping of the mouse olfactory system with manganese-enhanced magnetic resonance imaging and diffusion tensor imaging. 2013, 218, 527-37 An algorithm to estimate anatomical connectivity between brain regions using diffusion MRI. 2013,	281 37 19
1839 1838 1837	The organization of dorsal frontal cortex in humans and macaques. 2013, 33, 12255-74 Diffusion tensor imaging reveals widespread white matter abnormalities in children and adolescents with myotonic dystrophy type 1. 2013, 260, 1122-31 Mapping of the mouse olfactory system with manganese-enhanced magnetic resonance imaging and diffusion tensor imaging. 2013, 218, 527-37 An algorithm to estimate anatomical connectivity between brain regions using diffusion MRI. 2013, 31, 353-8	281 37 19
1839 1838 1837 1836	The organization of dorsal frontal cortex in humans and macaques. 2013, 33, 12255-74 Diffusion tensor imaging reveals widespread white matter abnormalities in children and adolescents with myotonic dystrophy type 1. 2013, 260, 1122-31 Mapping of the mouse olfactory system with manganese-enhanced magnetic resonance imaging and diffusion tensor imaging. 2013, 218, 527-37 An algorithm to estimate anatomical connectivity between brain regions using diffusion MRI. 2013, 31, 353-8 Central mechanisms of pain revealed through functional and structural MRI. 2013, 8, 518-34 Alzheimer's disease and amnestic mild cognitive impairment weaken connections within the	281 37 19 1

1831	Global tracking in human gliomas: a comparison with established tracking methods. 2013 , 23, 263-75		6
1830	Diffusion tensor MRI of chemotherapy-induced cognitive impairment in non-CNS cancer patients: a review. 2013 , 7, 409-35		73
1829	Thalamocortical tract between anterior thalamic nuclei and cingulate gyrus in the human brain: diffusion tensor tractography study. 2013 , 7, 236-41		27
1828	Fibromyalgia interacts with age to change the brain. 2013 , 3, 249-60		62
1827	Fronto-tectal white matter connectivity mediates facilitatory effects of non-invasive neurostimulation on visual detection. <i>NeuroImage</i> , 2013 , 82, 344-54	7.9	21
1826	White matter microstructural damage in Alzheimer's disease at different ages of onset. 2013 , 34, 2331-	40	32
1825	White matter microstructure asymmetry: effects of volume asymmetry on fractional anisotropy asymmetry. 2013 , 231, 1-12		25
1824	White-matter microstructure and language lateralization in left-handers: a whole-brain MRI analysis. 2013 , 82, 319-28		18
1823	Angular smoothing and radial regularization of ODF fields: application on deterministic crossing fiber tractography. 2013 , 29, 17-32		3
1822	Track-weighted functional connectivity (TW-FC): a tool for characterizing the structural-functional connections in the brain. <i>NeuroImage</i> , 2013 , 70, 199-210	7.9	34
1821	Parkinson's disease patients show reduced cortical-subcortical sensorimotor connectivity. 2013 , 28, 447	-54	99
1820	Parcellation of the human substantia nigra based on anatomical connectivity to the striatum. <i>NeuroImage</i> , 2013 , 81, 191-198	7.9	44
1819	Multimodal Brain Image Analysis. 2013 ,		6
1818	Advances in diffusion MRI acquisition and processing in the Human Connectome Project. <i>Neurolmage</i> , 2013 , 80, 125-43	7.9	596
1817	Delineation of motor and somatosensory thalamic subregions utilizing probabilistic diffusion tractography and electrophysiology. 2013 , 37, 600-9		16
1816	Developmental differences in diffusion tensor imaging parameters in borderline personality disorder. 2013 , 47, 1101-9		39
1815	Anatomical location of transcallosal sensorimotor fibers in the human brain: Diffusion tensor tractography study. 2013 , 4,		1
1814	Brain imaging predictors and the international study to predict optimized treatment for depression: study protocol for a randomized controlled trial. 2013 , 14, 224		31

1813	Walk the line: from diffusion imaging to the microstructure of the brain. 2013 , 23, 261-2		0
1812	Improvement of partial volume segmentation for brain tissue on diffusion tensor images using multiple-tensor estimation. 2013 , 26, 1131-40		4
1811	Connectivity-based parcellation of the postcentral gyrus using a spectral approach. 2013,		
1810	The WU-Minn Human Connectome Project: an overview. <i>NeuroImage</i> , 2013 , 80, 62-79	7.9	2585
1809	The structural connectome of the human brain in agenesis of the corpus callosum. <i>NeuroImage</i> , 2013 , 70, 340-55	7.9	60
1808	Functional organisation of visual pathways in a patient with no optic chiasm. 2013 , 51, 1260-72		10
1807	An exploratory study on the spatial relationship between regional cortical volume changes and white matter integrity in multiple sclerosis. 2013 , 3, 255-64		9
1806	Importance Sampling Spherical Harmonics to Improve Probabilistic Tractography. 2013,		
1805	Cerebellar networks with basal ganglia: feasibility for tracking cerebello-pallidal and subthalamo-cerebellar projections in the human brain. 2013 , 38, 3106-14		74
1804	De Leiden Lang Leven Studie: weerspiegelt het brein een lang leven?. 2013 , 17, 167-172		
1803	RubiX: combining spatial resolutions for Bayesian inference of crossing fibers in diffusion MRI. 2013 , 32, 969-82		29
1802	Functional organization of the neural language system: dorsal and ventral pathways are critical for syntax. 2013 , 23, 139-47		81
1801	Diffusion imaging in neurological disease. 2013 , 260, 335-42		7
1800	ADRB2, brain white matter integrity and cognitive ageing in the Lothian Birth Cohort 1936. 2013 , 43, 13-23		7
1799	The influence of preterm birth on the developing thalamocortical connectome. 2013 , 49, 1711-21		156
1798	Prenatal cocaine exposure alters functional activation in the ventral prefrontal cortex and its structural connectivity with the amygdala. 2013 , 213, 47-55		24
1797	Overlapping connections within the motor cortico-basal ganglia circuit: fMRI-tractography analysis. <i>NeuroImage</i> , 2013 , 78, 353-62	7.9	59
1796	Diffusion tensor imaging detects microstructural reorganization in the brain associated with chronic irritable bowel syndrome. 2013 , 154, 1528-1541		112

Using in vivo probabilistic tractography to reveal two segregated dorsal 'language-cognitive' pathways in the human brain. 2013 , 127, 230-40		18
Speech-induced striatal dopamine release is left lateralized and coupled to functional striatal circuits in healthy humans: a combined PET, fMRI and DTI study. <i>NeuroImage</i> , 2013 , 70, 21-32	7.9	40
Altered cortico-basal ganglia motor pathways reflect reduced volitional motor activity in schizophrenia. 2013 , 143, 269-76		79
Improving alignment in Tract-based spatial statistics: evaluation and optimization of image registration. <i>NeuroImage</i> , 2013 , 76, 400-11	7.9	120
Disruption of structural connectivity along the dorsal and ventral language pathways in patients with nonfluent and semantic variant primary progressive aphasia: a DT MRI study and a literature review. 2013 , 127, 157-66		58
A neural link between feeling and hearing. 2013 , 23, 1724-30		37
Anatomical location of the medial lemniscus and spinothalamic tract at the pons in the human brain: a diffusion tensor tractography study. 2013 , 30, 206-9		15
Classification of diffusion tensor images for the early detection of Alzheimer's disease. 2013 , 43, 1313-20)	29
Diffusion Magnetic Resonance Imaging and Fiber Tractography: The State of the Art and its Potential Impact on Patient Management. 2013 , 8, 279-93		
Subcortical substrates of TMS induced modulation of the cortico-cortical connectivity. 2013 , 6, 138-46		20
Functional responses and structural connections of cortical areas for processing faces and voices in the superior temporal sulcus. <i>NeuroImage</i> , 2013 , 76, 45-56	7.9	60
Neural connectivity of the posterior body of the fornix in the human brain: diffusion tensor imaging study. 2013 , 549, 116-9		11
Probabilistic tractography using Q-ball imaging and particle filtering: application to adult and in-utero fetal brain studies. 2013 , 17, 297-310		16
Subregions of the human superior frontal gyrus and their connections. <i>NeuroImage</i> , 2013 , 78, 46-58	7.9	220
Visual callosal topography in the absence of retinal input. <i>NeuroImage</i> , 2013 , 81, 325-334	7.9	23
Tractometer: towards validation of tractography pipelines. 2013 , 17, 844-57		140
Human and monkey ventral prefrontal fibers use the same organizational principles to reach their targets: tracing versus tractography. 2013 , 33, 3190-201		165
Early musical training and white-matter plasticity in the corpus callosum: evidence for a sensitive period. 2013 , 33, 1282-90		235
	pathways in the human brain. 2013, 127, 230-40 Speech-induced striatal dopamine release is left lateralized and coupled to functional striatal circuits in healthy humans: a combined PET, fMRI and DTI study. NeuroImage, 2013, 70, 21-32 Altered cortico-basal ganglia motor pathways reflect reduced volitional motor activity in schizophrenia. 2013, 143, 269-76 Improving alignment in Tract-based spatial statistics: evaluation and optimization of image registration. NeuroImage, 2013, 76, 400-11 Disruption of structural connectivity along the dorsal and ventral language pathways in patients with nonfluent and semantic variant primary progressive aphasia: a DT MRI study and a literature review. 2013, 127, 157-66 A neural link between feeling and hearing. 2013, 23, 1724-30 Anatomical location of the medial lemniscus and spinothalamic tract at the pons in the human brain: a diffusion tensor tractography study. 2013, 30, 206-9 Classification of diffusion tensor images for the early detection of Alzheimer's disease. 2013, 43, 1313-20 Diffusion Magnetic Resonance Imaging and Fiber Tractography: The State of the Art and its Potential Impact on Patient Management. 2013, 8, 279-93 Subcortical substrates of TMS induced modulation of the cortico-cortical connectivity. 2013, 6, 138-46 Functional responses and structural connections of cortical areas for processing faces and voices in the superior temporal sulcus. NeuroImage, 2013, 76, 45-56 Neural connectivity of the posterior body of the fornix in the human brain: diffusion tensor imaging study. 2013, 549, 116-9 Probabilistic tractography using Q-ball imaging and particle filtering: application to adult and in-utero fetal brain studies. 2013, 17, 297-310 Subregions of the human superior frontal gyrus and their connections. NeuroImage, 2013, 78, 46-58 Visual callosal topography in the absence of retinal input. NeuroImage, 2013, 81, 325-334 Tractometer: towards validation of tractography pipelines. 2013, 17, 844-57 Human and monkey ventral prefrontal fibers use the	pathways in the human brain. 2013, 127, 230-40 Speech-induced striatal dopamine release is left lateralized and coupled to functional striatal circuits in healthy humans: a combined PET, FMRI and DTI study. NeuroImage, 2013, 70, 21-32 Altered cortico-basal ganglia motor pathways reflect reduced volitional motor activity in schizophrenia. 2013, 143, 269-76 Improving alignment in Tract-based spatial statistics: evaluation and optimization of image registration. NeuroImage, 2013, 76, 400-11 Disruption of structural connectivity along the dorsal and ventral language pathways in patients with nonfluent and semantic variant primary progressive aphasia: a DT MRI study and a literature review. 2013, 127, 157-66 A neural link between feeling and hearing. 2013, 23, 1724-30 Anatomical location of the medial lemniscus and spinothalamic tract at the pons in the human brain: a diffusion tensor tractography study. 2013, 30, 206-9 Classification of diffusion tensor images for the early detection of Alzheimer's disease. 2013, 43, 1313-20 Diffusion Magnetic Resonance Imaging and Fiber Tractography: The State of the Art and its Potential Impact on Patient Management. 2013, 8, 279-93 Subcortical substrates of TMS induced modulation of the cortico-cortical connectivity. 2013, 6, 138-46 Functional responses and structural connections of cortical areas for processing faces and voices in the superior temporal sulcus. NeuroImage, 2013, 76, 45-56 Neural connectivity of the posterior body of the fornix in the human brain: diffusion tensor imaging study. 2013, 549, 116-9 Probabilistic tractography using Q-ball imaging and particle filtering: application to adult and in-utero fetal brain studies. 2013, 17, 297-310 Subregions of the human superior frontal gyrus and their connections. NeuroImage, 2013, 78, 46-58 7-9 Visual callosal topography in the absence of retinal input. NeuroImage, 2013, 81, 325-334 7-9 Tractometer: towards validation of tractography pipelines. 2013, 17, 844-57 Human and monkey ventral prefrontal fiber

1777	Thalamocortical disconnection in the orbitofrontal region associated with cortical thinning in schizophrenia. 2013 , 70, 12-21	55
1776	Connectivity-based parcellation of the human frontal pole with diffusion tensor imaging. 2013 , 33, 6782-90	80
1775	Biophysical network models and the human connectome. <i>NeuroImage</i> , 2013 , 80, 330-8 7.9	62
1774	Pathways to seeing music: enhanced structural connectivity in colored-music synesthesia. NeuroImage, 2013, 74, 359-66 7.9	43
1773	Microstructural white matter changes are correlated with the stage of psychiatric illness. 2013 , 3, e248	34
1772	Anatomical brain networks on the prediction of abnormal brain states. 2013 , 3, 1-21	33
1771	Test-retest reliability of computational network measurements derived from the structural connectome of the human brain. 2013 , 3, 160-76	62
1770	Graph analysis of the human connectome: promise, progress, and pitfalls. <i>NeuroImage</i> , 2013 , 80, 426-44 7.9	493
1769	White matter integrity, fiber count, and other fallacies: the do's and don'ts of diffusion MRI. NeuroImage, 2013, 73, 239-54 7-9	1584
1768	Two-tensor model-based bootstrapping on classified tensor morphologies: estimation of uncertainty in fiber orientation and probabilistic tractography. 2013 , 31, 296-312	1
1767	Differential effects of dual and unihemispheric motor cortex stimulation in older adults. 2013 , 33, 9176-83	124
1766	Networks of anatomical covariance. <i>NeuroImage</i> , 2013 , 80, 489-504 7.9	261
1765	The Speculative Neuroscience of the Future Human Brain. 2013 , 2, 209-252	1
1764	White matter fiber tractography: why we need to move beyond DTI. 2013 , 118, 1367-77	286
1763	Imaging human connectomes at the macroscale. 2013 , 10, 524-39	294
1762	The role of tissue microstructure and water exchange in biophysical modelling of diffusion in white matter. 2013 , 26, 345-70	102
1761	Toward global tractography. <i>NeuroImage</i> , 2013 , 80, 290-6 7.9	76
1760	Probabilistic diffusion tractography and graph theory analysis reveal abnormal white matter structural connectivity networks in drug-naive boys with attention deficit/hyperactivity disorder. 2013 , 33, 10676-87	140

(2013-2013)

1759	Linear transforms for Fourier data on the sphere: application to high angular resolution diffusion MRI of the brain. <i>NeuroImage</i> , 2013 , 71, 233-47	7.9	16
1758	Mapping putative hubs in human, chimpanzee and rhesus macaque connectomes via diffusion tractography. <i>Neurolmage</i> , 2013 , 80, 462-74	7.9	83
1757	Reconstruction of white matter tracts via repeated deterministic streamline trackinginitial experience. 2013 , 8, e63082		9
1756	Neuroimaging of Dystonia. 2013 , 165-184		
1755	White-matter microstructural changes in functional dyspepsia: a diffusion tensor imaging study. 2013 , 108, 260-9		54
1754	Abnormal temporal lobe white matter as a biomarker for genetic risk of bipolar disorder. 2013 , 73, 177-8	82	40
1753	Bayesian inference of structural brain networks. <i>NeuroImage</i> , 2013 , 66, 543-52	7.9	22
1752	A pitfall in the reconstruction of fibre ODFs using spherical deconvolution of diffusion MRI data. <i>NeuroImage</i> , 2013 , 65, 433-48	7.9	88
1751	Neural network connectivity differences in children who stutter. 2013 , 136, 3709-26		114
1750	Effects of cognitive remediation on cognitive dysfunction in partially or fully remitted patients with bipolar disorder: study protocol for a randomized controlled trial. 2013 , 14, 378		23
1749	Exploring Workflow Interoperability for Neuroimage Analysis on the SHIWA Platform. 2013 , 11, 505-522		7
1748	Logical foundations and fast implementation of probabilistic tractography. 2013 , 32, 1397-410		9
1747	Long-range connectomics. 2013 , 1305, 83-93		24
1746	The physics of functional magnetic resonance imaging (fMRI). 2013 , 76, 096601		117
1745	Asymmetric pedunculopontine network connectivity in parkinsonian patients with freezing of gait. 2013 , 136, 2405-18		165
1744	Diffusion magnetic resonance imaging in preterm brain injury. 2013 , 55 Suppl 2, 65-95		46
1743	Process versus product in social learning: comparative diffusion tensor imaging of neural systems for action execution-observation matching in macaques, chimpanzees, and humans. 2013 , 23, 1014-24		117
1742	Different characteristics of the corticospinal tract according to the cerebral origin: DTI study. 2013 , 34, 1359-63		64

1741	Impaired thalamocortical connectivity in autism spectrum disorder: a study of functional and anatomical connectivity. 2013 , 136, 1942-55	219
1740	Presurgical connectome and postsurgical seizure control in temporal lobe epilepsy. 2013 , 81, 1704-10	97
1739	Whole-brain magnetic resonance spectroscopic imaging measures are related to disability in ALS. 2013 , 80, 610-5	44
1738	White-matter changes correlate with cognitive functioning in Parkinson's disease. 2013 , 4, 37	40
1737	Motor and extramotor neurodegeneration in amyotrophic lateral sclerosis: a 3T high angular resolution diffusion imaging (HARDI) study. 2013 , 14, 553-61	24
1736	High angular resolution diffusion imaging probabilistic tractography of the auditory radiation. 2013 , 34, 1573-8	54
1735	A hitchhiker's guide to diffusion tensor imaging. 2013 , 7, 31	404
1734	Functional and structural connectivity of frontostriatal circuitry in Autism Spectrum Disorder. 2013 , 7, 430	93
1733	Relationship between somatosensory function and the spinothalamocortical pathway in chronic stroke patients. 2013 , 30, 197-200	6
1732	Structural connectivity in schizophrenia and its impact on the dynamics of spontaneous functional networks. 2013 , 23, 046111	43
1731	Less efficient information transfer in Cys-allele carriers of DISC1: a brain network study based on diffusion MRI. 2013 , 23, 1715-23	28
1730	White matter maturation supports the development of reasoning ability through its influence on processing speed. 2013 , 16, 941-51	41
1729	Preserved white matter integrity is a marker of familial longevity. 2013 , 74, 883-92	4
1728	HiFiVE: A Hilbert Space Embedding of Fiber Variability Estimates for Uncertainty Modeling and Visualization. 2013 , 32, 121-130	14
1727	Quantitative tractography and tract shape modeling in amyotrophic lateral sclerosis. 2013, 38, 1140-5	14
1726	White matter and visuospatial processing in autism: a constrained spherical deconvolution tractography study. 2013 , 6, 307-19	22
1725	Assessment of corticospinal tract (CST) damage in acute stroke patients: comparison of tract-specific analysis versus segmentation of a CST template. 2013 , 37, 836-45	24
1724	Determination of the appropriate b value and number of gradient directions for high-angular-resolution diffusion-weighted imaging. 2013 , 26, 1775-86	242

(2013-2013)

1723	Structural and functional changes across the visual cortex of a patient with visual form agnosia. 2013 , 33, 12779-91	54
1722	FATCAT: (an efficient) Functional and Tractographic Connectivity Analysis Toolbox. 2013 , 3, 523-35	125
1721	Mind wandering away from pain dynamically engages antinociceptive and default mode brain networks. 2013 , 110, 18692-7	254
1720	Brain white matter tract integrity and cognitive abilities in community-dwelling older people: the Lothian Birth Cohort, 1936. 2013 , 27, 595-607	28
1719	White matter microstructural abnormality in children with hydrocephalus detected by probabilistic diffusion tractography. 2013 , 34, 2379-85	20
1718	PANDA: a pipeline toolbox for analyzing brain diffusion images. 2013 , 7, 42	387
1717	The ascending reticular activating system from pontine reticular formation to the thalamus in the human brain. 2013 , 7, 416	84
1716	Local Tests for Identifying Anisotropic Diffusion Areas in Human Brain with DTI. 2013 , 7, 201-225	3
1715	Gray matter parcellation constrained full brain fiber bundling with diffusion tensor imaging. 2013 , 40, 072301	2
1714	Structural brain changes after 4 wk of unilateral strength training of the lower limb. 2013 , 115, 167-75	27
1713	Evaluation of Callosal Motor Fiber Location in the Human Brain by Diffusion Tensor Tractography Combined with Functional MRI. 2013 , 25, 387-389	1
1712	Precommissural fornix in the human brain: a diffusion tensor tractography study. 2013 , 54, 315-20	20
1711	Synesthesia, Hyper-Connectivity, and Diffusion Tensor Imaging. 2013,	1
1710	Robust tract skeleton extraction of cingulum based on active contour model from diffusion tensor MR imaging. 2013 , 8, e56113	2
1709	Principal networks. 2013 , 8, e60997	6
1708	Accelerating fibre orientation estimation from diffusion weighted magnetic resonance imaging using GPUs. 2013 , 8, e61892	101
1707	Local diffusion homogeneity (LDH): an inter-voxel diffusion MRI metric for assessing inter-subject white matter variability. 2013 , 8, e66366	24
1706	Assessment of structural connectivity in the preterm brain at term equivalent age using diffusion MRI and T2 relaxometry: a network-based analysis. 2013 , 8, e68593	25

1705	Optic radiation fiber tractography in glioma patients based on high angular resolution diffusion imaging with compressed sensing compared with diffusion tensor imaging - initial experience. 2013 , 8, e70973	35
1704	Increased global and local efficiency of human brain anatomical networks detected with FLAIR-DTI compared to non-FLAIR-DTI. 2013 , 8, e71229	5
1703	Time-optimized high-resolution readout-segmented diffusion tensor imaging. 2013 , 8, e74156	3
1702	A connectome-based comparison of diffusion MRI schemes. 2013 , 8, e75061	16
1701	Validation of DTI tractography-based measures of primary motor area connectivity in the squirrel monkey brain. 2013 , 8, e75065	39
1700	Fiber pathways of attention subnetworks revealed with tract-based spatial statistics (TBSS) and probabilistic tractography. 2013 , 8, e78831	21
1699	Differential contributions of dorso-ventral and rostro-caudal prefrontal white matter tracts to cognitive control in healthy older adults. 2013 , 8, e81410	12
1698	Multi-fiber tractography visualizations for diffusion MRI data. 2013 , 8, e81453	15
1697	Atlas-guided cluster analysis of large tractography datasets. 2013 , 8, e83847	25
1696	Prediction of selective serotonin reuptake inhibitor response using diffusion-weighted MRI. 2013 , 4, 5	31
1695	Broca's area and its striatal and thalamic connections: a diffusion-MRI tractography study. 2013 , 7, 8	68
1694	Structural changes in left fusiform areas and associated fiber connections in children with abacus training: evidence from morphometry and tractography. 2013 , 7, 335	28
1693	Imaging white matter in human brainstem. 2013 , 7, 400	32
1692	Differences of inter-tract correlations between neonates and children around puberty: a study based on microstructural measurements with DTI. 2013 , 7, 721	22
1691	Individual structural differences in left inferior parietal area are associated with schoolchildrens' arithmetic scores. 2013 , 7, 844	27
1690	Network efficiency in autism spectrum disorder and its relation to brain overgrowth. 2013 , 7, 845	32
1689	Dopaminergic drug effects during reversal learning depend on anatomical connections between the orbitofrontal cortex and the amygdala. 2013 , 7, 142	9
1688	Combined diffusion-weighted and functional magnetic resonance imaging reveals a temporal-occipital network involved in auditory-visual object processing. 2013 , 7, 5	35

1687	Tractography of the brainstem in major depressive disorder using diffusion tensor imaging. 2014 , 9, e84825	23
1686	Neural plasticity in human brain connectivity: the effects of long term deep brain stimulation of the subthalamic nucleus in Parkinson's disease. 2014 , 9, e86496	71
1685	Addressing the path-length-dependency confound in white matter tract segmentation. 2014 , 9, e96247	20
1684	Comparison of parameter threshold combinations for diffusion tensor tractography in chronic stroke patients and healthy subjects. 2014 , 9, e98211	11
1683	Altered inter-subregion connectivity of the default mode network in relapsing remitting multiple sclerosis: a functional and structural connectivity study. 2014 , 9, e101198	40
1682	Effects of VRK2 (rs2312147) on white matter connectivity in patients with schizophrenia. 2014 , 9, e103519	12
1681	Consensus between pipelines in structural brain networks. 2014 , 9, e111262	14
1680	Altered fronto-striatal fiber topography and connectivity in obsessive-compulsive disorder. 2014 , 9, e112075	20
1679	Quantifying uncertainty in brain network measures using Bayesian connectomics. 2014 , 8, 126	9
1678	Differences in neural connectivity between the substantia nigra and ventral tegmental area in the human brain. 2014 , 8, 41	28
1677	Diffusion imaging of cerebral white matter in persons who stutter: evidence for network-level anomalies. 2014 , 8, 54	63
1676	Injury of the mammillothalamic tract in patients with thalamic hemorrhage. 2014 , 8, 259	8
1675	Associations between Proprioceptive Neural Pathway Structural Connectivity and Balance in People with Multiple Sclerosis. 2014 , 8, 814	59
1674	Affective and cognitive prefrontal cortex projections to the lateral habenula in humans. 2014 , 8, 819	17
1673	DTIPrep: quality control of diffusion-weighted images. 2014 , 8, 4	172
1672	Isotropic non-white matter partial volume effects in constrained spherical deconvolution. 2014 , 8, 28	41
1671	The multi-modal Australian ScienceS Imaging and Visualization Environment (MASSIVE) high performance computing infrastructure: applications in neuroscience and neuroinformatics research. 2014 , 8, 30	38
1670	Diffusion-Weighted Imaging of the Spinal Cord. 2014 , 123-145	5

1669	Mapping Connections in Humans and Non-Human Primates. 2014 , 337-358	31
1668	Diffusion-Weighted MRI. 2014 , 81-97	8
1667	Diffusion tensor tractography for the dorsal spinocerebellar tract in the human brain. 2014 , 31, 7-10	8
1666	Assessment of the contralesional corticospinal tract in early-onset pediatric hemiplegia: Preliminary findings. 2014 , 2014, 5336-9	2
1665	Nonparametric Bayesian clustering of structural whole brain connectivity in full image resolution. 2014 ,	2
1664	Thalamo-cortical connectivity: what can diffusion tractography tell us about reading difficulties in children?. 2014 , 4, 428-39	12
1663	Computational Diffusion MRI. 2014 ,	3
1662	Connectivity strength of dissociable striatal tracts predict individual differences in temporal discounting. 2014 , 34, 10298-310	109
1661	The distribution of the cortical origin of the corticoreticular pathway in the human brain: a diffusion tensor imaging study. 2014 , 31, 204-8	17
1660	White matter changes linked to visual recovery after nerve decompression. 2014 , 6, 266ra173	16
1659	Network inefficiencies in autism spectrum disorder at 24 months. 2014 , 4, e388	73
1658	Handedness- and hemisphere-related differences in small-world brain networks: a diffusion tensor imaging tractography study. 2014 , 4, 145-56	32
1657	White matter changes associated with antipsychotic treatment in first-episode psychosis. 2014 , 39, 1324-31	91
1656	Brain Imaging Analysis. 2014 , 1, 61-85	26
1655	Are APOE e genotype and TOMM40 poly-T repeat length associations with cognitive ageing mediated by brain white matter tract integrity?. 2014 , 4, e449	16
1654	Connectivity-based parcellation of the human temporal pole using diffusion tensor imaging. 2014 , 24, 3365-78	84
1653	A direct amygdala-motor pathway for emotional displays to influence action: A diffusion tensor imaging study. 2014 , 35, 5974-83	81
1652	Subcortical, modality-specific pathways contribute to multisensory processing in humans. 2014 , 24, 2169-77	28

$_{1651}$ Implication of the anterior commissure in the allocation of attention to action. 2014 , 5, 432		10
Structure-function discrepancy: inhomogeneity and delays in synchronized neural networks. 2014 , 10, e1003736		26
1649 Fiber Visualization with LIC Maps Using Multidirectional Anisotropic Glyph Samples. 2014 , 2014, 4018	319	2
1648 Moving Beyond DTI. 2014 , 65-78		3
1647 Fiber-Tracking: 3-Dimensional Tract Reconstruction. 2014 , 79-96		
1646 Large deformation diffeomorphic registration of diffusion-weighted imaging data. 2014 , 18, 1290-8		15
Improving diffusion-weighted imaging of post-mortem human brains: SSFP at 7 T. <i>NeuroImage</i> , 2014 , 102 Pt 2, 579-89	7.9	29
Relating structure and function in the human brain: relative contributions of anatomy, stationary dynamics, and non-stationarities. 2014 , 10, e1003530		151
Quantifying the pattern of optic tract degeneration in human hemianopia. 2014 , 85, 379-86		23
Injury of the mammillothalamic tract in patients with subarachnoid haemorrhage: a retrospective diffusion tensor imaging study. 2014 , 4, e005613		22
1641 White matter tractography in early psychosis: clinical and neurocognitive associations. 2014 , 39, 417-	·27	24
1640 Semi-supervised clustering for parcellating brain regions based on resting state fMRI data. 2014 ,		1
1639 Cross-Subject Comparison of Local Diffusion MRI Parameters. 2014 , 209-239		2
Altered white matter integrity in the corpus callosum in fibromyalgia patients identified by tract-based spatial statistical analysis. 2014 , 66, 3190-9		20
1637 Task switching in traumatic brain injury relates to cortico-subcortical integrity. 2014 , 35, 2459-69		27
Cerebral small vessel disease affects white matter microstructure in mild cognitive impairment. 2014 , 35, 2836-51		45
1635 PCLR: phase-constrained low-rank model for compressive diffusion-weighted MRI. 2014 , 72, 1330-13	41	20
Transcallosal connection patterns of opposite dorsal premotor regions support a lateralized specialization for action and perception. 2014 , 40, 2980-6		4

1633	Tracking on the Product Manifold of Shape and Orientation for Tractography from Diffusion MRI. 2014 , 2014, 3051-3056	7
1632	Characterizing white matter changes in cigarette smokers via diffusion tensor imaging. 2014 , 145, 134-42	41
1631	Intraoperative dorsal language network mapping by using single-pulse electrical stimulation. 2014 , 35, 4345-61	88
1630	Cerebral correlates of visuospatial neglect: a direct cerebral stimulation study. 2014 , 35, 1334-50	73
1629	High-resolution MRI and diffusion-weighted imaging of the human habenula at 7 tesla. 2014 , 39, 1018-26	45
1628	Altered white matter microstructure underlies listening difficulties in children suspected of auditory processing disorders: a DTI study. 2014 , 4, 531-43	15
1627	Sex dimorphism in the white matter: fractional anisotropy and brain size. 2014 , 39, 917-23	25
1626	Brain tissue properties differentiate between motor and limbic basal ganglia circuits. 2014 , 35, 5083-92	63
1625	Association between structural and functional connectivity in the verb generation network. 2014 , 4, 221-9	2
1624	Spatial Mapping of Translational Diffusion Coefficients Using Diffusion Tensor Imaging: A Mathematical Description. 2014 , 43, 1-27	1
1623	Age-related reduced prefrontal-amygdala structural connectivity is associated with lower trait anxiety. 2014 , 28, 631-42	26
1622	Anatomical location and somatotopic organization of the corticospinal tract in the corona radiata of the normal human brain: a diffusion tensor tractography study. 2014 , 25, 710-4	8
1621	The role of probabilistic tractography in the surgical treatment of thalamic gliomas. 2014 , 10 Suppl 2, 262-72; discussion 272	17
1620	Multi-tissue constrained spherical deconvolution for improved analysis of multi-shell diffusion MRI data. <i>NeuroImage</i> , 2014 , 103, 411-426	605
1619	Structural loop between the cerebellum and the superior temporal sulcus: evidence from diffusion tensor imaging. 2014 , 24, 626-32	77
1618	Changes to memory structures in children treated for posterior fossa tumors. 2014 , 20, 168-80	48
1617	Stochastic geometric network models for groups of functional and structural connectomes. NeuroImage, 2014, 101, 473-84 7-9	13
1616	Automatic method for thalamus parcellation using multi-modal feature classification. 2014 , 17, 169-76	8

1615	Diffusion imaging of auditory and auditory-limbic connectivity in tinnitus: preliminary evidence and methodological challenges. 2014 , 2014, 145943	31
1614	Beyond crossing fibers: bootstrap probabilistic tractography using complex subvoxel fiber geometries. 2014 , 5, 216	8
1613	Can musical training influence brain connectivity? Evidence from diffusion tensor MRI. 2014 , 4, 405-27	42
1612	Presurgical Tractography Applications. 2014 , 531-567	1
1611	Connectivity Fingerprinting of Gray Matter. 2014 , 481-509	1
1610	Validation of Tractography. 2014 , 453-480	4
1609	Common cerebral networks associated with distinct deep brain stimulation targets for cluster headache. 2014 , 34, 224-30	16
1608	Microstructural brain tissue damage in metabolic syndrome. 2014 , 37, 493-500	38
1607	Social subordination stress and serotonin transporter polymorphisms: associations with brain white matter tract integrity and behavior in juvenile female macaques. 2014 , 24, 3334-49	25
1606	Auditory tracts identified with combined fMRI and diffusion tractography. <i>NeuroImage</i> , 2014 , 84, 562-74 _{7.9}	52
1605	Gray and white matter correlates of navigational ability in humans. 2014 , 35, 2561-72	31
1604	A macroscopic view of microstructure: using diffusion-weighted images to infer damage, repair, and plasticity of white matter. 2014 , 276, 14-28	80
1603	Subdivision of the occipital lobes: an anatomical and functional MRI connectivity study. 2014 , 56, 121-37	50
1602	Autism as a disconnection syndrome: A qualitative and quantitative review of diffusion tensor imaging studies. 2014 , 8, 387-412	25
1601	Sex differences in connectivity of the subgenual anterior cingulate cortex. 2014 , 155, 755-763	55
1600	White matter microstructure changes induced by motor skill learning utilizing a body machine interface. <i>NeuroImage</i> , 2014 , 88, 32-40	27
1599	Preterm birth affects the developmental synergy between cortical folding and cortical connectivity observed on multimodal MRI. <i>NeuroImage</i> , 2014 , 89, 23-34	29
1598	Towards quantitative connectivity analysis: reducing tractography biases. <i>NeuroImage</i> , 2014 , 98, 266-78 7.9	178

1597	Connectivity between right inferior frontal gyrus and supplementary motor area predicts after-effects of right frontal cathodal tDCS on picture naming speed. 2014 , 7, 122-9	35
1596	Structural connectivity differences in left and right temporal lobe epilepsy. <i>NeuroImage</i> , 2014 , 100, 135- 4 4)	136
1595	White matter pathway organization of the reward system is related to positive and negative symptoms in schizophrenia. 2014 , 153, 136-42	56
1594	The structural and functional connectivity of the posterior cingulate cortex: comparison between deterministic and probabilistic tractography for the investigation of structure-function 7.9 relationships. <i>NeuroImage</i> , 2014 , 102 Pt 1, 118-27	121
1593	Neural connectivity of the anterior body of the fornix in the human brain: diffusion tensor imaging study. 2014 , 559, 72-5	8
1592	Altered intrahemispheric structural connectivity in Gilles de la Tourette syndrome. 2014 , 4, 174-81	48
1591	An investigation of the white matter microstructure in motion detection using diffusion MRI. 2014 , 1570, 35-42	6
1590	An improved OPDT model in high angular resolution diffusion imaging. 2014 , 48, 385-395	2
1589	Structural asymmetries of language-related gray and white matter and their relationship to language function in young children with ASD. 2014 , 8, 60-72	54
1588	Cortico-subthalamic connection predicts individual differences in value-driven choice bias. 2014 , 219, 1239-49	14
1587	Cerebello-cerebral connectivity deficits in Friedreich ataxia. 2014 , 219, 969-81	33
1586	Altered structural networks and executive deficits in traumatic brain injury patients. 2014 , 219, 193-209	110
1585	Comprehensive morphometry of subcortical grey matter structures in early-stage Parkinson's disease. 2014 , 35, 1681-90	66
1584	Distributed corpus callosum involvement in amyotrophic lateral sclerosis: a deterministic tractography study using q-ball imaging. 2014 , 261, 27-36	11
1583	An investigation into the functional and structural connectivity of the Default Mode Network. NeuroImage, 2014, 90, 381-9 7.9	36
1582	Regional alterations in cortical thickness and white matter integrity in amyotrophic lateral sclerosis. 2014 , 261, 412-21	28
1581	Clinical, cognitive, and behavioural correlates of white matter damage in progressive supranuclear palsy. 2014 , 261, 913-24	43
1580	Potential and limitations of diffusion MRI tractography for the study of language. 2014 , 131, 65-73	41

1579	Connectivity-based functional analysis of dopamine release in the striatum using diffusion-weighted MRI and positron emission tomography. 2014 , 24, 1165-77		203
1578	Tractography of the corticobulbar tract. 2014 , 339, 237-8		
1577	Structural and functional brain rewiring clarifies preserved interhemispheric transfer in humans born without the corpus callosum. 2014 , 111, 7843-8		75
1576	Fiber connectivity between the striatum and cortical and subcortical regions is associated with temperaments in Chinese males. <i>NeuroImage</i> , 2014 , 89, 226-34	7.9	31
1575	Cognitive flexibility depends on white matter microstructure of the basal ganglia. 2014 , 53, 171-7		23
1574	How delays matter in an oscillatory whole-brain spiking-neuron network model for MEG alpha-rhythms at rest. <i>NeuroImage</i> , 2014 , 87, 383-94	7.9	29
1573	Test-retest reliability of structural brain networks from diffusion MRI. <i>NeuroImage</i> , 2014 , 86, 231-43	7.9	102
1572	Computational Diffusion MRI and Brain Connectivity. 2014,		1
1571	Comparison of human ventral frontal cortex areas for cognitive control and language with areas in monkey frontal cortex. 2014 , 81, 700-13		275
1570	A computational modelling study of transcranial direct current stimulation montages used in depression. <i>NeuroImage</i> , 2014 , 87, 332-44	7.9	109
1569	Spurious group differences due to head motion in a diffusion MRI study. <i>NeuroImage</i> , 2014 , 88, 79-90	7.9	360
1568	Functional Brain Tumor Imaging. 2014,		1
1567	Resting state functional connectivity alterations in primary lateral sclerosis. 2014 , 35, 916-25		30
1566	Advanced neuroimaging techniques for central neuromodulation. 2014 , 25, 173-85		2
1565	Human brain asymmetry in microstructural connectivity demonstrated by diffusional kurtosis imaging. 2014 , 1588, 73-80		8
1564	Magnetic resonance diffusion tractography of the preterm infant brain: a systematic review. 2014 , 56, 113-24		35
1563	Contralateral interictal spikes are related to tapetum damage in left temporal lobe epilepsy. 2014 , 55, 1406-14		13
1562	Fast identification of optimal fascicle configurations from standard clinical diffusion MRI using Akaike information criterion. 2014 ,		2

1561	Estimation of the CSA-ODF using Bayesian compressed sensing of multi-shell HARDI. 2014 , 72, 1471-85		14
1560	Multi-label segmentation of white matter structures: application to neonatal brains. <i>NeuroImage</i> , 2014 , 102 Pt 2, 913-22	7.9	16
1559	Hemispheric lateralization of topological organization in structural brain networks. 2014 , 35, 4944-57		64
1558	Functional parcellation of the hippocampus by clustering resting state fMRI signals. 2014,		5
1557	Anatomical accuracy of brain connections derived from diffusion MRI tractography is inherently limited. 2014 , 111, 16574-9		499
1556	Preserved mid-fusiform activation for visual words in a patient with a visual word recognition impairment. 2014 , 65, 113-24		2
1555	Integration of resting-state FMRI and diffusion-weighted MRI connectivity analyses of the human brain: limitations and improvement. 2014 , 24, 176-86		11
1554	Aberrant white matter microstructure in children with 16p11.2 deletions. 2014 , 34, 6214-23		53
1553	White matter microstructure in transsexuals and controls investigated by diffusion tensor imaging. 2014 , 34, 15466-75		76
1552	MR Diffusion Tractography. 2014 , 429-451		7
1551	Unraveling the secrets of white matterbridging the gap between cellular, animal and human imaging studies. 2014 , 276, 2-13		103
1550	Visualization and Processing of Tensors and Higher Order Descriptors for Multi-Valued Data. 2014 ,		4
1549	FIBRASCAN: a novel method for 3D white matter tract reconstruction in MR space from cadaveric dissection. <i>NeuroImage</i> , 2014 , 103, 106-118	7.9	36
1548	Beyond fractional anisotropy: extraction of bundle-specific structural metrics from crossing fiber models. <i>NeuroImage</i> , 2014 , 100, 176-91	7.9	35
1547	Neural connectivity of the lateral geniculate body in the human brain: diffusion tensor imaging study. 2014 , 578, 66-70		6
1546	Functional network mirrored in the prefrontal cortex, caudate nucleus, and thalamus: high-resolution functional imaging and structural connectivity. 2014 , 34, 9202-12		44
1545	Insular cortex mediates increased pain tolerance in yoga practitioners. 2014 , 24, 2732-40		79
1544	The neural connectivity of the intralaminar thalamic nuclei in the human brain: a diffusion tensor tractography study. 2014 , 579, 140-4		48

1543	Resting-state networks link invasive and noninvasive brain stimulation across diverse psychiatric and neurological diseases. 2014 , 111, E4367-75	348
1542	Fiber tract associated with autistic traits in healthy adults. 2014 , 59, 117-24	13
1541	TBSS and probabilistic tractography reveal white matter connections for attention to object features. 2014 , 219, 2159-71	12
1540	White matter abnormalities and cognitive impairment in early-onset schizophrenia-spectrum disorders. 2014 , 53, 362-72.e1-2	65
1539	Advantages of QBI in TBSS analyses. 2014 , 32, 184-9	7
1538	Visualizing Meyer's loop: A comparison of deterministic and probabilistic tractography. 2014 , 108, 481-90	40
1537	Study protocol: The Whitehall II imaging sub-study. 2014 , 14, 159	58
1536	Alterations of hippocampal projections in adult macaques with neonatal hippocampal lesions: a Diffusion Tensor Imaging study. <i>NeuroImage</i> , 2014 , 102 Pt 2, 828-37	14
1535	Neurocognitive enhancement in older adults: comparison of three cognitive training tasks to test a hypothesis of training transfer in brain connectivity. <i>NeuroImage</i> , 2014 , 85 Pt 3, 1027-39	87
1534	Multiple thalamo-cortical disconnections in anterior thalamic infarction: implications for thalamic mechanisms of memory and language. 2014 , 53, 264-73	31
1533	Structurally-informed Bayesian functional connectivity analysis. <i>NeuroImage</i> , 2014 , 86, 294-305 7.9	35
1532	Rich-club organization of the newborn human brain. 2014 , 111, 7456-61	217
1531	Genome-wide schizophrenia variant at MIR137 does not impact white matter microstructure in healthy participants. 2014 , 574, 6-10	15
1530	Diffusion tensor imaging and MR morphometry of the central auditory pathway and auditory cortex in aging. 2014 , 260, 87-97	63
1529	A flocking based method for brain tractography. 2014 , 18, 515-30	12
1528	Diffusion configuration of water molecules in diffusion weighted imaging. 2014 , 125, 2123-2128	
1527	Abnormal structural networks characterize major depressive disorder: a connectome analysis. 2014 , 76, 567-74	217
1526	Diffusion tensor tractography reveals disrupted structural connectivity in childhood absence epilepsy. 2014 , 108, 125-38	65

1525	The importance of using a proper technique and accurate seeding of regions-of-interest in diffusion tensor tractography. 2014 , 339, 235-6		6
1524	Abnormal cingulum bundle development in autism: a probabilistic tractography study. 2014 , 221, 63-8		44
1523	Connectivity patterns of pallidal DBS electrodes in focal dystonia: a diffusion tensor tractography study. <i>NeuroImage</i> , 2014 , 84, 435-42	1	39
1522	White matter integrity of motor connections related to training gains in healthy aging. 2014 , 35, 1404-11		25
1521	Disrupted white matter in language and motor tracts in developmental stuttering. 2014 , 131, 25-35		74
1520	Exploring mechanisms of spontaneous functional connectivity in MEG: how delayed network interactions lead to structured amplitude envelopes of band-pass filtered oscillations. <i>NeuroImage</i> , 7.9 2014 , 90, 423-35		175
1519	Plausibility Tracking: a method to evaluate anatomical connectivity and microstructural properties along fiber pathways. <i>NeuroImage</i> , 2014 , 90, 163-78	1	23
1518	Anatomy is strategy: skilled reading differences associated with structural connectivity differences in the reading network. 2014 , 133, 1-13		32
1517	Connectivity-based parcellation of the human posteromedial cortex. 2014 , 24, 719-27		52
1516	Individual differences in white matter anatomy predict dissociable components of reading skill in adults. <i>NeuroImage</i> , 2014 , 96, 261-75		26
1515	Microstructural differences in the thalamus and thalamic radiations in the congenitally deaf. NeuroImage, 2014 , 100, 347-57)	19
1514	Neural signatures of the interaction between the 5-HTTLPR genotype and stressful life events in healthy women. 2014 , 223, 157-63		13
1513	Alzheimer's disease susceptibility genes APOE and TOMM40, and brain white matter integrity in the Lothian Birth Cohort 1936. 2014 , 35, 1513.e25-33		47
1512	Intrahemispheric and interhemispheric structural network abnormalities in PLS and ALS. 2014 , 35, 1710-22		64
1511	White matter microstructural organization and gait stability in older adults. 2014 , 6, 104		52
1510	Reading skill in adult survivors of childhood brain tumor: a theory-based neurocognitive model. 2014 , 28, 448-58		12
1509	Geometric Distortions in Diffusion MRI. 2014 , 63-85		7
1508	Multiple Fibers. 2014 , 105-123		12

1507	3D multi-slab diffusion-weighted readout-segmented EPI with real-time cardiac-reordered K-space acquisition. 2014 , 72, 1565-79	30
1506	Perpendicular fibre tracking for neural fibre bundle analysis using diffusion MRI. 2014 , 10, 75-92	
1505	Anatomical location of the frontopontine fibers in the internal capsule in the human brain: a diffusion tensor tractography study. 2014 , 25, 117-21	6
1504	Brain network analysis. 2014 , 15, 30-38	27
1503	Differential structural and resting state connectivity between insular subdivisions and other pain-related brain regions. 2014 , 155, 2047-55	96
1502	Resilience and corpus callosum microstructure in adolescence. 2015 , 45, 2285-94	30
1501	White matter microstructure between the pre-SMA and the cingulum bundle is related to response conflict in healthy subjects. 2015 , 5, e00375	7
1500	Validation of tractography: Comparison with manganese tracing. 2015 , 36, 4116-34	92
1499	Following the Spreading of Brain Structural Changes in Alzheimer's Disease: A Longitudinal, Multimodal MRI Study. 2015 , 47, 995-1007	15
1498	Estimation of diffusion properties in three-way fiber crossings without overfitting. 2015 , 60, 9123-44	4
1498 1497	Estimation of diffusion properties in three-way fiber crossings without overfitting. 2015 , 60, 9123-44 Right external globus pallidus changes are associated with altered causal awareness in youth with depression. 2015 , 5, e653	4
.,	Right external globus pallidus changes are associated with altered causal awareness in youth with depression. 2015 , 5, e653	
1497	Right external globus pallidus changes are associated with altered causal awareness in youth with depression. 2015 , 5, e653 Diffusion tensor imaging of dolphin brains reveals direct auditory pathway to temporal lobe. 2015 ,	4
1497 1496	Right external globus pallidus changes are associated with altered causal awareness in youth with depression. 2015 , 5, e653 Diffusion tensor imaging of dolphin brains reveals direct auditory pathway to temporal lobe. 2015 , 282, Connectivity between the superior colliculus and the amygdala in humans and macaque monkeys:	4 26
1497 1496 1495	Right external globus pallidus changes are associated with altered causal awareness in youth with depression. 2015, 5, e653 Diffusion tensor imaging of dolphin brains reveals direct auditory pathway to temporal lobe. 2015, 282, Connectivity between the superior colliculus and the amygdala in humans and macaque monkeys: virtual dissection with probabilistic DTI tractography. 2015, 114, 1947-62 Abnormal hippocampal-thalamic white matter tract development and positive symptom course in	4 26 77
1497 1496 1495	Right external globus pallidus changes are associated with altered causal awareness in youth with depression. 2015, 5, e653 Diffusion tensor imaging of dolphin brains reveals direct auditory pathway to temporal lobe. 2015, 282, Connectivity between the superior colliculus and the amygdala in humans and macaque monkeys: virtual dissection with probabilistic DTI tractography. 2015, 114, 1947-62 Abnormal hippocampal-thalamic white matter tract development and positive symptom course in individuals at ultra-high risk for psychosis. 2015, 1,	4 26 77 24
1497 1496 1495 1494 1493	Right external globus pallidus changes are associated with altered causal awareness in youth with depression. 2015, 5, e653 Diffusion tensor imaging of dolphin brains reveals direct auditory pathway to temporal lobe. 2015, 282, Connectivity between the superior colliculus and the amygdala in humans and macaque monkeys: virtual dissection with probabilistic DTI tractography. 2015, 114, 1947-62 Abnormal hippocampal-thalamic white matter tract development and positive symptom course in individuals at ultra-high risk for psychosis. 2015, 1, Visualizing crossing probabilistic tracts. 2015,	4 26 77 24

1489	Quantitative representation and description of intravoxel fiber complexity in HARDI. 2015, 60, 8417-36	1
1488	Comparison of diffusion tractography and tract-tracing measures of connectivity strength in rhesus macaque connectome. 2015 , 36, 3064-75	100
1487	Measuring embeddedness: Hierarchical scale-dependent information exchange efficiency of the human brain connectome. 2015 , 36, 3653-65	10
1486	Toward tract-specific fractional anisotropy (TSFA) at crossing-fiber regions with clinical diffusion MRI. 2015 , 74, 1768-79	16
1485	A data-driven approach to extract connectivity structures from diffusion tensor imaging data. 2015,	2
1484	Structural and functional connectivity in the default mode network in 22q11.2 deletion syndrome. 2015 , 7, 23	37
1483	Functional and diffusion tensor magnetic resonance imaging of the sheep brain. 2015 , 11, 262	12
1482	Brain structural and functional connectivity in Parkinson's disease with freezing of gait. 2015 , 36, 5064-78	97
1481	Connectivity-based whole brain dual parcellation by group ICA reveals tract structures and decreased connectivity in schizophrenia. 2015 , 36, 4681-701	21
1480	A new template to study callosal growth shows specific growth in anterior and posterior regions of the corpus callosum in early childhood. 2015 , 42, 1675-84	4
1479	The Relation Between Injury of the Spinothalamocortical Tract and Central Pain in Chronic Patients With Mild Traumatic Brain Injury. 2015 , 30, E40-6	44
1478	Functional Mapping of the Human Auditory Cortex: fMRI Investigation of a Patient with Auditory Agnosia from Trauma to the Inferior Colliculus. 2015 , 28, 160-80	13
1477	Reduced structural connectivity within a prefrontal-motor-subcortical network in amyotrophic lateral sclerosis. 2015 , 41, 1342-52	26
1476	Diffusion Tensor Imaging of TBI: Potentials and Challenges. 2015 , 24, 241-51	34
1475	Postmortem diffusion MRI of the human brainstem and thalamus for deep brain stimulator electrode localization. 2015 , 36, 3167-78	61
1474	A network of amygdala connections predict individual differences in trait anxiety. 2015 , 36, 4819-30	44
1473	Thalamic Reorganization in Chronic Patients With Intracerebral Hemorrhage: A Retrospective Cross-Sectional Study. 2015 , 94, e1391	2
1472	Disconnection of the hippocampus and amygdala associated with lesion load in relapsing-remitting multiple sclerosis: a structural and functional connectivity study. 2015 , 11, 1749-65	9

(2015-2015)

1471	Altered Structural and Functional Connectivity in Late Preterm Preadolescence: An Anatomic Seed-Based Study of Resting State Networks Related to the Posteromedial and Lateral Parietal Cortex. 2015 , 10, e0130686	20
1470	Comparison of nine tractography algorithms for detecting abnormal structural brain networks in Alzheimer's disease. 2015 , 7, 48	79
1469	White matter microstructure contributes to age-related declines in task-induced deactivation of the default mode network. 2015 , 7, 194	17
1468	Parcellation of the primary cerebral cortices based on local connectivity profiles. 2015 , 9, 50	8
1467	Automatic target validation based on neuroscientific literature mining for tractography. 2015 , 9, 66	7
1466	Unraveling the multiscale structural organization and connectivity of the human brain: the role of diffusion MRI. 2015 , 9, 77	22
1465	A multiscale approach for the reconstruction of the fiber architecture of the human brain based on 3D-PLI. 2015 , 9, 118	27
1464	Asymmetric projections of the arcuate fasciculus to the temporal cortex underlie lateralized language function in the human brain. 2015 , 9, 119	27
1463	Synchronous Changes of Cortical Thickness and Corresponding White Matter Microstructure During Brain Development Accessed by Diffusion MRI Tractography from Parcellated Cortex. 2015 , 9, 158	18
1462	Evidence from a rare case study for Hebbian-like changes in structural connectivity induced by long-term deep brain stimulation. 2015 , 9, 167	14
1461	Individual variability in the anatomical distribution of nodes participating in rich club structural networks. 2015 , 9, 16	9
1460	A multimodal approach for determining brain networks by jointly modeling functional and structural connectivity. 2015 , 9, 22	23
1459	Multi-Modal Imaging of Neural Correlates of Motor Speed Performance in the Trail Making Test. 2015 , 6, 219	6
1458	Functional networks and structural connectivity of visuospatial and visuoperceptual working memory. 2015 , 9, 340	12
1457	Automatic analysis (aa): efficient neuroimaging workflows and parallel processing using Matlab and XML. 2014 , 8, 90	86
1456	Ontology-based approach for in vivo human connectomics: the medial Brodmann area 6 case study. 2015 , 9, 9	2
1455	Boosting brain connectome classification accuracy in Alzheimer's disease using higher-order singular value decomposition. 2015 , 9, 257	18
1454	Probabilistic clustering of the human connectome identifies communities and hubs. 2015 , 10, e0117179	22

1453	The semantic variant of primary progressive aphasia: clinical and neuroimaging evidence in single subjects. 2015 , 10, e0120197	30
1452	Evaluating the accuracy of diffusion MRI models in white matter. 2015 , 10, e0123272	42
1451	Organization of the Human Frontal Pole Revealed by Large-Scale DTI-Based Connectivity: Implications for Control of Behavior. 2015 , 10, e0124797	34
1450	Structural connectivity of the developing human amygdala. 2015 , 10, e0125170	26
1449	Development of the Corticospinal and Callosal Tracts from Extremely Premature Birth up to 2 Years of Age. 2015 , 10, e0125681	21
1448	The microstructural status of the corpus callosum is associated with the degree of motor function and neurological deficit in stroke patients. 2015 , 10, e0122615	38
1447	Reproducibility of the Structural Brain Connectome Derived from Diffusion Tensor Imaging. 2015 , 10, e0135247	59
1446	Improved Framework for Tractography Reconstruction of the Optic Radiation. 2015 , 10, e0137064	24
1445	Unifying Inference of Meso-Scale Structures in Networks. 2015 , 10, e0143133	12
1444	Detection of the arcuate fasciculus in congenital amusia depends on the tractography algorithm. 2015 , 6, 9	33
1443	Change of Neural Connectivity of the Red Nucleus in Patients with Striatocapsular Hemorrhage: A Diffusion Tensor Tractography Study. 2015 , 2015, 679815	10
1442	The Plasticity of Brain Gray Matter and White Matter following Lower Limb Amputation. 2015 , 2015, 823185	34
1441	Delay of gratification is associated with white matter connectivity in the dorsal prefrontal cortex: a diffusion tensor imaging study in chimpanzees (Pan troglodytes). 2015 , 282, 20150764	10
1440	Shared white-matter dysconnectivity in schizophrenia and bipolar disorder with psychosis. 2015 , 45, 759-70	62
1439	White Matter Connectivity of the Thalamus Delineates the Functional Architecture of Competing Thalamocortical Systems. 2015 , 25, 4477-89	41
1438	Overcoming the effects of false positives and threshold bias in graph theoretical analyses of neuroimaging data. <i>NeuroImage</i> , 2015 , 118, 313-33	85
1437	White Matter Integrity of Specific Dentato-Thalamo-Cortical Pathways is Associated with Learning Gains in Precise Movement Timing. 2015 , 25, 1707-14	19
1436	From Local Q-Ball Estimation to Fibre Crossing Tractography. 2015 , 455-473	2

(2015-2015)

1435	epilepsy based on structural connectome data. <i>NeuroImage</i> , 2015 , 118, 219-30	95
1434	Left-hemisphere lateralization for language and interhemispheric fiber tracking in patients with schizophrenia. 2015 , 165, 30-7	22
1433	Coupled changes in brain white matter microstructure and fluid intelligence in later life. 2015 , 35, 8672-82	69
1432	Amygdala subnuclei connectivity in response to violence reveals unique influences of individual differences in psychopathic traits in a nonforensic sample. 2015 , 36, 1417-28	46
1431	Tract-based analysis of white matter degeneration in Alzheimer's disease. 2015 , 301, 79-89	47
1430	Advanced fiber tracking in early acquired brain injury causing cerebral palsy. 2015 , 36, 181-7	12
1429	Beyond a bigger brain: Multivariable structural brain imaging and intelligence. 2015 , 51, 47-56	77
1428	Aphasia severity in chronic stroke patients: a combined disconnection in the dorsal and ventral language pathways. 2015 , 29, 287-95	24
1427	Structural plasticity of remote cortical brain regions is determined by connectivity to the primary lesion in subcortical stroke. 2015 , 35, 1507-14	37
1426	Connectivity-based segmentation of the periaqueductal gray matter in human with brainstem optimized diffusion MRI. 2015 , 36, 3459-71	49
1425	Sparse Reconstruction Challenge for diffusion MRI: Validation on a physical phantom to determine which acquisition scheme and analysis method to use?. 2015 , 26, 316-31	53
1424	Bayesian predictive modeling based on multidimensional connectivity profiling. 2015 , 28, 5-11	4
1423	A Bayesian approach to distinguishing interdigitated tongue muscles from limited diffusion magnetic resonance imaging. 2015 , 45, 63-74	11
1422	An inverse relationship between serum macrophage inhibitory cytokine-1 levels and brain white matter integrity in community-dwelling older individuals. 2015 , 62, 80-8	10
1421	Altered PDE10A expression detectable early before symptomatic onset in Huntington's disease. 2015 , 138, 3016-29	71
1420	Fetal Cerebral Magnetic Resonance Imaging Beyond Morphology. 2015 , 36, 465-75	16
1419	Estimating diffusion properties in complex fiber configurations based on structure-adaptive multi-valued tensor-field filtering. 2015 ,	
1418	Scan time reduction for readout-segmented EPI using simultaneous multislice acceleration: Diffusion-weighted imaging at 3 and 7 Tesla. 2015 , 74, 136-149	46

1417	High resolution whole brain diffusion imaging at 7T for the Human Connectome Project. <i>NeuroImage</i> , 2015 , 122, 318-31	7.9	114
1416	MEM-diffusion MRI framework to solve MEEG inverse problem. 2015 ,		1
1415	SVM-Based Classification of Diffusion Tensor Imaging Data for Diagnosing Alzheimer Disease and Mild Cognitive Impairment. 2015 , 489-499		2
1414	Tracking the Neurodevelopmental Correlates of Mental State Inference in Early Childhood. 2015 , 40, 379-94		5
1413	Does diffusion MRI tell us anything about the white matter? An overview of methods and pitfalls. 2015 , 161, 133-41		70
1412	A potential biomarker in sports-related concussion: brain functional connectivity alteration of the default-mode network measured with longitudinal resting-state fMRI over thirty days. 2015 , 32, 327-41		91
1411	Differences of the medial lemniscus and spinothalamic tract according to the cortical termination areas: A diffusion tensor tractography study. 2015 , 32, 67-71		13
1410	Virtual dissection and comparative connectivity of the superior longitudinal fasciculus in chimpanzees and humans. <i>NeuroImage</i> , 2015 , 108, 124-37	7.9	112
1409	Aging and large-scale functional networks: white matter integrity, gray matter volume, and functional connectivity in the resting state. 2015 , 290, 369-78		69
1408	The anatomical location of the corticobulbar tract at the corona radiata in the human brain: diffusion tensor tractography study. 2015 , 590, 80-3		16
1407	Connectomics: comprehensive approaches for whole-brain mapping. 2015 , 64, 57-67		21
1406	Fiber estimation and tractography in diffusion MRI: development of simulated brain images and comparison of multi-fiber analysis methods at clinical b-values. <i>NeuroImage</i> , 2015 , 109, 341-56	7.9	67
1405	Tractography from HARDI using an intrinsic unscented Kalman filter. 2015 , 34, 298-305		3
1404	The ascending reticular activating system from pontine reticular formation to the hypothalamus in the human brain: a diffusion tensor imaging study. 2015 , 590, 58-61		38
1403	Linked alterations in gray and white matter morphology in adults with high-functioning autism spectrum disorder: a multimodal brain imaging study. 2015 , 7, 155-69		54
1402	Convergent functional architecture of the superior parietal lobule unraveled with multimodal neuroimaging approaches. 2015 , 36, 238-57		121
1401	Cerebro-cerebellar connectivity is increased in primary lateral sclerosis. 2015 , 7, 288-96		28
1400	34. Structural connectivity of eloquent speech areas defined by direct cortical stimulation mapping. 2015 , 126, e41-e42		

1399	Hyperconnectivity in juvenile myoclonic epilepsy: a network analysis. 2015 , 7, 98-104		34
1398	Informed constrained spherical deconvolution (iCSD). 2015 , 24, 269-281		27
1397	Predicting functional connectivity from structural connectivity via computational models using MRI: an extensive comparison study. <i>NeuroImage</i> , 2015 , 111, 65-75	7.9	60
1396	White matter disruption at the prodromal stage of Alzheimer's disease: relationships with hippocampal atrophy and episodic memory performance. 2015 , 7, 482-92		52
1395	Simultaneous multi-scale diffusion estimation and tractography guided by entropy spectrum pathways. 2015 , 34, 1177-93		14
1394	Determination of the posterior boundary of Wernicke's area based on multimodal connectivity profiles. 2015 , 36, 1908-24		45
1393	Effective electric fields along realistic DTI-based neural trajectories for modelling the stimulation mechanisms of TMS. 2015 , 60, 453-71		27
1392	Understanding structural-functional relationships in the human brain: a large-scale network perspective. 2015 , 21, 290-305		113
1391	Brain function during cognitive flexibility and white matter integrity in alcohol-dependent patients, problematic drinkers and healthy controls. 2015 , 20, 979-89		21
1390	EEG functional connectivity is partially predicted by underlying white matter connectivity. <i>NeuroImage</i> , 2015 , 108, 23-33	7.9	59
1389	A Connectome Computation System for discovery science of brain. 2015 , 60, 86-95		82
1388	Diffusion tensor imaging for understanding brain development in early life. 2015, 66, 853-76		129
1387	The prefrontal cortex achieves inhibitory control by facilitating subcortical motor pathway connectivity. 2015 , 35, 786-94		133
1386	Edge density imaging: mapping the anatomic embedding of the structural connectome within the white matter of the human brain. <i>NeuroImage</i> , 2015 , 109, 402-17	7.9	25
1385	Bilateral dorsal and ventral fiber pathways for the processing of affective prosody identified by probabilistic fiber tracking. <i>NeuroImage</i> , 2015 , 109, 27-34	7.9	38
1384	Deafferentation in thalamic and pontine areas in severe traumatic brain injury. 2015 , 42, 202-11		13
1383	Novel fingerprinting method characterises the necessary and sufficient structural connectivity from deep brain stimulation electrodes for a successful outcome. 2015 , 17, 015001		20
1382	Role of fronto-striatal tract and frontal aslant tract in movement and speech: an axonal mapping study. 2015 , 220, 3399-412		162

1381	Contralateral cerebello-thalamo-cortical pathways with prominent involvement of associative areas in humans in vivo. 2015 , 220, 3369-84		99
1380	Convergence and divergence across construction methods for human brain white matter networks: an assessment based on individual differences. 2015 , 36, 1995-2013		37
1379	Deficiency of brain structural sub-network underlying post-ischaemic stroke apathy. 2015 , 22, 341-7		19
1378	Imaging white-matter pathways of the auditory system with diffusion imaging tractography. 2015 , 129, 277-88		6
1377	A cortical-subcortical syntax pathway linking Broca's area and the striatum. 2015 , 36, 2270-83		31
1376	Gray matter axonal connectivity maps. 2015 , 6, 35		8
1375	Audio-visual integration through the parallel visual pathways. 2015, 1624, 71-77		8
1374	White matter integrity and cognitive performance in school-age children: A population-based neuroimaging study. <i>NeuroImage</i> , 2015 , 119, 119-28	7.9	50
1373	Superficial white matter as a novel substrate of age-related cognitive decline. 2015 , 36, 2094-106		45
1372	The Visual Word Form Area remains in the dominant hemisphere for language in late-onset left occipital lobe epilepsies: A postsurgery analysis of two cases. 2015 , 46, 91-8		4
1371	Aneurysmal subarachnoid hemorrhage causes injury of the ascending reticular activating system: relation to consciousness. 2015 , 36, 667-71		24
1370	Edge-Centered DTI Connectivity Analysis: Application to Schizophrenia. 2015 , 13, 501-9		5
1369	Tract shape modeling detects changes associated with preterm birth and neuroprotective treatment effects. 2015 , 8, 51-8		14
1368	Thalamocortical Connectivity Predicts Cognition in Children Born Preterm. 2015 , 25, 4310-8		150
1367	Structural Connectivity Networks of Transgender People. 2015 , 25, 3527-34		59
1366	Connectivity-based fixel enhancement: Whole-brain statistical analysis of diffusion MRI measures in the presence of crossing fibres. <i>NeuroImage</i> , 2015 , 117, 40-55	7.9	163
1365	Tract-specific white matter degeneration in aging: the Rotterdam Study. 2015 , 11, 321-30		127
1364	Real-Time Strategy Video Game Experience and Visual Perceptual Learning. 2015 , 35, 10485-92		31

1363 Fiber Tracking with DWI. **2015**, 265-269

1362	Tissue Microstructure Imaging with Diffusion MRI. 2015 , 277-285		2
1361	Tract-Based Spatial Statistics and Other Approaches for Cross-Subject Comparison of Local Diffusion MRI Parameters. 2015 , 437-464		2
1360	Bayesian Model Inversion. 2015 , 509-516		
1359	The influence of construction methodology on structural brain network measures: A review. 2015 , 253, 170-82		55
1358	Differential adaptation of descending motor tracts in musicians. 2015 , 25, 1490-8		46
1357	Temporal lobe epilepsy and affective disorders: the role of the subgenual anterior cingulate cortex. 2015 , 86, 144-51		22
1356	Microstructural changes in white matter associated with freezing of gait in Parkinson's disease. 2015 , 30, 567-76		72
1355	Challenges of microtome-based serial block-face scanning electron microscopy in neuroscience. 2015 , 259, 137-142		46
1354	Connectivity-based parcellation of the thalamus in multiple sclerosis and its implications for cognitive impairment: A multicenter study. 2015 , 36, 2809-25		55
1353	The organisation of the elderly connectome. <i>NeuroImage</i> , 2015 , 114, 414-26	7.9	47
1352	Lower Blood Pressure and Gray Matter Integrity Loss in Older Persons. 2015 , 17, 630-7		10
1351	Emotion regulation and trait anxiety are predicted by the microstructure of fibers between amygdala and prefrontal cortex. 2015 , 35, 6020-7		80
1350	White matter fractional anisotropy over two time points in early onset schizophrenia and adolescent cannabis use disorder: A naturalistic diffusion tensor imaging study. 2015 , 232, 34-41		26
1349	Structural connectivity of neural reward networks in youth at risk for substance use disorders. 2015 , 232, 2217-26		10
1348	Structural connectivity analysis reveals abnormal brain connections in agenesis of the corpus callosum in children. 2015 , 25, 1471-8		16
1347	Brain structural abnormalities in patients with major depression with or without generalized anxiety disorder comorbidity. 2015 , 262, 1255-65		44
1346	Tractography of Meyer's loop for temporal lobe resection alidation by prediction of postoperative visual field outcome????. 2015 , 157, 947-56; discussion 956		10

1345	Fibromyalgia is characterized by altered frontal and cerebellar structural covariance brain networks. 2015 , 7, 667-77	35
1344	Superficial white matter fiber systems impede detection of long-range cortical connections in diffusion MR tractography. 2015 , 112, E2820-8	267
1343	Connectivity reveals relationship of brain areas for reward-guided learning and decision making in human and monkey frontal cortex. 2015 , 112, E2695-704	229
1342	MRI assessment of the effects of acetazolamide and external lumbar drainage in idiopathic normal pressure hydrocephalus. 2015 , 12, 9	22
1341	Assessment of a method to determine deep brain stimulation targets using deterministic tractography in a navigation system. 2015 , 38, 739-50; discussion 751	28
1340	Disrupted developmental organization of the structural connectome in fetuses with corpus callosum agenesis. <i>NeuroImage</i> , 2015 , 111, 277-88	50
1339	Imaging White Matter Anatomy for Brain Tumor Surgery. 2015 , 91-121	1
1338	Handbook of Biomedical Imaging. 2015,	5
1337	Segmentation of the Cerebellar Peduncles Using a Random Forest Classifier and a Multi-object Geometric Deformable Model: Application to Spinocerebellar Ataxia Type 6. 2015 , 13, 367-81	15
1336	Three distinct fiber pathways of the bed nucleus of the stria terminalis to the amygdala and prefrontal cortex. 2015 , 66, 60-8	58
1335	Longitudinal alterations to brain function, structure, and cognitive performance in healthy older adults: A fMRI-DTI study. 2015 , 71, 225-35	35
1334	Comparative diffusion tractography of corticostriatal motor pathways reveals differences between humans and macaques. 2015 , 113, 2164-72	21
1333	Understanding fiber mixture by simulation in 3D Polarized Light Imaging. <i>NeuroImage</i> , 2015 , 111, 464-757.9	35
1332	HERITABILITY OF BRAIN NETWORK TOPOLOGY IN 853 TWINS AND SIBLINGS. 2015 , 2015, 449-453	4
1331	A Neural Basis for Developmental Topographic Disorientation. 2015 , 35, 12954-69	28
1330	Selective vulnerability of Rich Club brain regions is an organizational principle of structural connectivity loss in Huntington's disease. 2015 , 138, 3327-44	66
1329	Human Frontal-Subcortical Circuit and Asymmetric Belief Updating. 2015 , 35, 14077-85	44
1328	Predicting the laterality of temporal lobe epilepsy from PET, MRI, and DTI: A multimodal study. 2015 , 9, 20-31	29

(2015-2015)

1327	57, 1093-102	12
1326	Validating Neuro-Computational Models of Neurological and Psychiatric Disorders. 2015,	5
1325	Fiber Orientation and Compartment Parameter Estimation From Multi-Shell Diffusion Imaging. 2015 , 34, 2320-32	38
1324	The effect of Gibbs ringing artifacts on measures derived from diffusion MRI. <i>NeuroImage</i> , 2015 , 120, 441-55	62
1323	Diffusion MRI and its Role in Neuropsychology. 2015 , 25, 250-71	20
1322	Neuroanatomy of intergroup bias: A white matter microstructure study of individual differences. NeuroImage, 2015 , 122, 345-54 7.9	20
1321	Clinical Applications of fMRI. 2015 , 611-632	1
1320	Group-wise consistent sulcal fundi segmentation based on DMRI-derived ODF features. 2015,	
1319	Corticospinal tract anatomy and functional connectivity of primary motor cortex in autism. 2015 , 54, 859-67	34
1318	Boosting Classification Accuracy of Diffusion MRI Derived Brain Networks for the Subtypes of Mild Cognitive Impairment Using Higher Order Singular Value Decomposition. 2015 , 2015, 131-135	2
1317	Intelligent Computing Theories and Methodologies. 2015,	
1316	A multimodal neuroimaging study of a case of crossed nonfluent/agrammatic primary progressive aphasia. 2015 , 262, 2336-45	19
1315	In vivo histology of the myelin g-ratio with magnetic resonance imaging. <i>NeuroImage</i> , 2015 , 118, 397-405/.9	177
1314	Identification of the Corticobulbar Tracts of the Tongue and Face Using Deterministic and Probabilistic DTI Fiber Tracking in Patients with Brain Tumor. 2015 , 36, 2036-41	24
1313	A Diffusion MRI Tractography Connectome of the Mouse Brain and Comparison with Neuronal Tracer Data. 2015 , 25, 4628-37	132
1312	Separate Brain Circuits Support Integrative and Semantic Priming in the Human Language System. 2016 , 26, 3169-82	10
1311	The direct pathway from the brainstem reticular formation to the cerebral cortex in the ascending reticular activating system: A diffusion tensor imaging study. 2015 , 606, 200-3	15
1310	The anatomical location of the corticoreticular pathway at the subcortical white matter in the human brain: A diffusion tensor imaging study. 2015 , 32, 106-9	6

1309	Compensation or inhibitory failure? Testing hypotheses of age-related right frontal lobe involvement in verbal memory ability using structural and diffusion MRI. 2015 , 63, 4-15		16
1308	A greater involvement of posterior brain areas in interhemispheric transfer in autism: fMRI, DWI and behavioral evidences. 2015 , 8, 267-80		19
1307	White matter compartment models for in vivo diffusion MRI at 300mT/m. <i>NeuroImage</i> , 2015 , 118, 468-8	8 3 7.9	47
1306	Attention in spina bifida myelomeningocele: Relations with brain volume and integrity. 2015 , 8, 72-8		11
1305	L2-Proficiency-Dependent Laterality Shift in Structural Connectivity of Brain Language Pathways. 2015 , 5, 349-61		18
1304	Postshunt lateral ventricular volume, white matter integrity, and intellectual outcomes in spina bifida and hydrocephalus. 2015 , 15, 410-9		14
1303	Strengths and weaknesses of state of the art fiber tractography pipelinesA comprehensive in-vivo and phantom evaluation study using Tractometer. 2015 , 26, 287-305		49
1302	Microstructure of frontoparietal connections predicts individual resistance to sleep deprivation. <i>NeuroImage</i> , 2015 , 106, 123-33	7.9	36
1301	Role of white-matter pathways in coordinating alpha oscillations in resting visual cortex. <i>NeuroImage</i> , 2015 , 106, 328-39	7.9	29
1300	Aging of corticospinal tract fibers according to the cerebral origin in the human brain: a diffusion tensor imaging study. 2015 , 585, 77-81		18
1299	Development of human brain structural networks through infancy and childhood. 2015 , 25, 1389-404		118
1298	Multimodal frontostriatal connectivity underlies individual differences in self-esteem. 2015 , 10, 364-70		52
1297	DISC1 Ser704Cys impacts thalamic-prefrontal connectivity. 2015 , 220, 91-100		19
1296	Connectomics: a new paradigm for understanding brain disease. 2015 , 25, 733-48		137
1295	Acceleration of high angular and spatial resolution diffusion imaging using compressed sensing with multichannel spiral data. 2015 , 73, 126-38		31
1294	Preferential detachment during human brain development: age- and sex-specific structural connectivity in diffusion tensor imaging (DTI) data. 2015 , 25, 1477-89		82
1293	A comparative analysis of mouse and human medial geniculate nucleus connectivity: a DTI and anterograde tracing study. <i>Neurolmage</i> , 2015 , 105, 53-66	7.9	23
1292	Cortical and subcortical connections of the human claustrum revealed in vivo by constrained spherical deconvolution tractography. 2015 , 25, 406-14		67

1291	Relating structural and functional connectivity in MRI: a simple model for a complex brain. 2015 , 34, 27-37	14
1290	Orbitofrontal cortex volume and brain reward response in obesity. 2015 , 39, 214-21	84
1289	Human thalamus regulates cortical activity via spatially specific and structurally constrained phase-amplitude coupling. 2015 , 25, 1618-28	34
1288	Acquisition of Paleolithic toolmaking abilities involves structural remodeling to inferior frontoparietal regions. 2015 , 220, 2315-31	70
1287	Connectivity-based parcellation of the human frontal polar cortex. 2015 , 220, 2603-16	36
1286	Critical Review and Comparison of Axonal Structures in MRI/DTI and Histology. 2016 , 337-347	1
1285	APPLICATION OF A NOVEL QUANTITATIVE TRACTOGRAPHY-BASED ANALYSIS OF DIFFUSION TENSOR IMAGING TO EXAMINE FIBER BUNDLE LENGTH IN HUMAN CEREBRAL WHITE MATTER. 2016 , 18, 21-29	2
1284	Serial Diffusion Tensor Imaging of the Optic Radiations after Acute Optic Neuritis. 2016 , 2016, 2764538	13
1283	Differences in Cortical Representation and Structural Connectivity of Hands and Feet between Professional Handball Players and Ballet Dancers. 2016 , 2016, 6817397	21
1282	Simultaneous Assessment of White Matter Changes in Microstructure and Connectedness in the Blind Brain. 2016 , 2016, 6029241	24
1281	9 Diffusion Tensor Imaging. 2016 ,	
1280	Fundamentals of Functional Neuroimaging. 41-73	
		3
1279	Recent Progress in Magnetic Resonance Imaging of the Embryonic and Neonatal Mouse Brain. 2016 , 10, 18	14
	Recent Progress in Magnetic Resonance Imaging of the Embryonic and Neonatal Mouse Brain. 2016	
	Recent Progress in Magnetic Resonance Imaging of the Embryonic and Neonatal Mouse Brain. 2016 , 10, 18	14
1278	Recent Progress in Magnetic Resonance Imaging of the Embryonic and Neonatal Mouse Brain. 2016, 10, 18 Toward Developmental Connectomics of the Human Brain. 2016, 10, 25 The Neuroanatomical Basis for Posterior Superior Parietal Lobule Control Lateralization of	14 78
1278	Recent Progress in Magnetic Resonance Imaging of the Embryonic and Neonatal Mouse Brain. 2016, 10, 18 Toward Developmental Connectomics of the Human Brain. 2016, 10, 25 The Neuroanatomical Basis for Posterior Superior Parietal Lobule Control Lateralization of Visuospatial Attention. 2016, 10, 32	14 78 45

1273	Sex Differences in Fiber Connection between the Striatum and Subcortical and Cortical Regions. 2016 , 10, 100	7
1272	Intrinsic Functional Plasticity of the Thalamocortical System in Minimally Disabled Patients with Relapsing-Remitting Multiple Sclerosis. 2016 , 10, 2	11
1271	Connectivity-Based Predictions of Hand Motor Outcome for Patients at the Subacute Stage After Stroke. 2016 , 10, 101	11
1270	Decreased Cerebellar-Orbitofrontal Connectivity Correlates with Stuttering Severity: Whole-Brain Functional and Structural Connectivity Associations with Persistent Developmental Stuttering. 2016 , 10, 190	22
1269	Reduced Volume of the Arcuate Fasciculus in Adults with High-Functioning Autism Spectrum Conditions. 2016 , 10, 214	12
1268	A Direct Cortico-Nigral Pathway as Revealed by Constrained Spherical Deconvolution Tractography in Humans. 2016 , 10, 374	28
1267	A Symmetry-Based Method to Infer Structural Brain Networks from Probabilistic Tractography Data. 2016 , 10, 46	3
1266	Structural Brain Network Characteristics Can Differentiate CIS from Early RRMS. 2016 , 10, 14	47
1265	Multimodal Imaging Signatures of Parkinson's Disease. 2016 , 10, 131	20
1264	Exploring Patterns of Alteration in Alzheimer's Disease Brain Networks: A Combined Structural and Functional Connectomics Analysis. 2016 , 10, 380	24
1263	Diffusion Capillary Phantom vs. Human Data: Outcomes for Reconstruction Methods Depend on Evaluation Medium. 2016 , 10, 407	6
1262	Converting Multi-Shell and Diffusion Spectrum Imaging to High Angular Resolution Diffusion Imaging. 2016 , 10, 418	7
1261		
1201	The Inverse Relationship between the Microstructural Variability of Amygdala-Prefrontal Pathways and Trait Anxiety Is Moderated by Sex. 2016 , 10, 93	17
1260	and Trait Anxiety Is Moderated by Sex. 2016 , 10, 93	3
	and Trait Anxiety Is Moderated by Sex. 2016 , 10, 93	
1260	and Trait Anxiety Is Moderated by Sex. 2016 , 10, 93 Cortical surface parcellation via dMRI using mutual nearest neighbor condition. 2016 , Structural Brain Alterations in Motor Subtypes of Parkinson's Disease: Evidence from Probabilistic	3
1260 1259	and Trait Anxiety Is Moderated by Sex. 2016 , 10, 93 Cortical surface parcellation via dMRI using mutual nearest neighbor condition. 2016 , Structural Brain Alterations in Motor Subtypes of Parkinson's Disease: Evidence from Probabilistic Tractography and Shape Analysis. 2016 , 11, e0157743 Reliable Dual Tensor Model Estimation in Single and Crossing Fibers Based on Jeffreys Prior. 2016 ,	3 19

1255	Imaging Data. 2016 , 7, 114	3
1254	Periventricular Nodular Heterotopia: Detection of Abnormal Microanatomic Fiber Structures with Whole-Brain Diffusion MR Imaging Tractography. 2016 , 281, 896-906	13
1253	Structural brain correlates of cognitive and behavioral impairment in MND. 2016 , 37, 1614-26	64
1252	Structural connectivity of the human anterior temporal lobe: A diffusion magnetic resonance imaging study. 2016 , 37, 2210-22	34
1251	Longitudinal development in the preterm thalamus and posterior white matter: MRI correlations between diffusion weighted imaging and T2 relaxometry. 2016 , 37, 2479-92	22
1250	Connectome sensitivity or specificity: which is more important?. <i>NeuroImage</i> , 2016 , 142, 407-420 7.9	184
1249	Individualized Map of White Matter Pathways: Connectivity-Based Paradigm for Neurosurgical Planning. 2016 , 79, 568-77	28
1248	Application of probabilistic fiber-tracking method of MR imaging to measure impact of cranial irradiation on structural brain connectivity in children treated for medulloblastoma. 2016 ,	1
1247	Changes of Brain Connectivity in the Primary Motor Cortex After Subcortical Stroke: A Multimodal Magnetic Resonance Imaging Study. 2016 , 95, e2579	27
1246	FIBER DIRECTION ESTIMATION, SMOOTHING AND TRACKING IN DIFFUSION MRI. 2016 , 10, 1137-1156	5
1245	Individual differences in reasoning and visuospatial attention are associated with prefrontal and parietal white matter tracts in healthy older adults. 2016 , 30, 558-67	8
1244	Neuroimaging evidence of deficient axon myelination in Wolfram syndrome. 2016 , 6, 21167	23
1243	Abnormal topological organization of the white matter network in Mandarin speakers with congenital amusia. 2016 , 6, 26505	9
1242	Effects of delaying binge drinking on adolescent brain development: a longitudinal neuroimaging study. 2016 , 16, 445	13
1241	Ageing and brain white matter structure in 3,513 UK Biobank participants. 2016 , 7, 13629	207
1240	Microstructure Imaging of Crossing (MIX) White Matter Fibers from diffusion MRI. 2016 , 6, 38927	34
1239	Functional complexity emerging from anatomical constraints in the brain: the significance of network modularity and rich-clubs. 2016 , 6, 38424	48
1238	Effects of vocal training in a musicophile with congenital amusia. 2016 , 22, 526-537	13

1237	Network effects and pathways in Deep brain stimulation in Parkinson's disease. 2016 , 2016, 5533-5536	8
1236	Corticospinal tract modeling for neurosurgical planning by tracking through regions of peritumoral edema and crossing fibers using two-tensor unscented Kalman filter tractography. 2016 , 11, 1475-86	28
1235	Neural connections foster social connections: a diffusion-weighted imaging study of social networks. 2016 , 11, 721-7	29
1234	Reducing Computation Time by Monte Carlo Method: An Application in Determining Axonal Orientation Distribution Function. 2016 , 95-105	
1233	The Human Brainnetome Atlas: A New Brain Atlas Based on Connectional Architecture. 2016 , 26, 3508-26	964
1232	Voxel-based lesion-symptom mapping of stroke lesions underlying somatosensory deficits. 2016 , 10, 257-66	53
1231	Associations between mobility, cognition and callosal integrity in people with parkinsonism. 2016 , 11, 415-422	18
1230	Reduced white matter integrity in amateur boxers. 2016 , 58, 911-20	13
1229	Visualization of MRI Diffusion Data by a Multi-Kernel LIC Approach with Anisotropic Glyph Samples. 2016 , 157-177	1
1228	Global Diffusion Tractography by Simulated Annealing. 2017 , 64, 649-660	1
1227	Supraspinal control of automatic postural responses in people with multiple sclerosis. 2016 , 47, 92-5	8
1226	Visualization in Medicine and Life Sciences III. 2016,	
1225	Modern Methods for Interrogating the Human Connectome. 2016 , 22, 105-19	19
1224	Crossing Versus Fanning: Model Comparison Using HCP Data. 2016 , 159-169	2
1223	Connectivity Profiles Reveal a Transition Subarea in the Parahippocampal Region That Integrates the Anterior Temporal-Posterior Medial Systems. 2016 , 36, 2782-95	28
1222	Edge correlations in spatial networks. 2016 , 4, 1-14	3
1221	Global and regional cortical connectivity maturation index (CCMI) of developmental human brain with quantification of short-range association tracts. 2016 , 9788,	5
1220	The Disconnected Brain and Executive Function Decline in Aging. 2017 , 27, 2303-2317	83

1219	Fusion in diffusion MRI for improved fibre orientation estimation: An application to the 3T and 7T data of the Human Connectome Project. <i>NeuroImage</i> , 2016 , 134, 396-409	7.9	67
1218	Alzheimer Disease Classification with Novel Microstructural Metrics from Diffusion-Weighted MRI. 2016 , 41-54		3
1217	Estimation of Fiber Orientations Using Neighborhood Information. 2016 , 87-96		
1216	Neurobiology of knowledge and misperception of lyrics. <i>NeuroImage</i> , 2016 , 134, 12-21	7.9	1
1215	Clarifying Human White Matter. 2016 , 39, 103-28		72
1214	Computational Diffusion MRI. 2016 ,		1
1213	Limited microstructural and connectivity deficits despite subcortical volume reductions in school-aged children born preterm with very low birth weight. <i>NeuroImage</i> , 2016 , 130, 24-34	7.9	24
1212	Abnormal frontostriatal connectivity in adolescent-onset schizophrenia and its relationship to cognitive functioning. 2016 , 35, 32-8		24
1211	Symmetrical Location Characteristics of Corticospinal Tract Associated With Hand Movement in the Human Brain: A Probabilistic Diffusion Tensor Tractography. 2016 , 95, e3317		5
1210	Corticolimbic anatomical characteristics predetermine risk for chronic pain. 2016 , 139, 1958-70		183
1209	Mapping Brain Anatomical Connectivity Using Diffusion Magnetic Resonance Imaging: Structural connectivity of the human brain. 2016 , 33, 36-51		8
1208	Concurrent white and gray matter degeneration of disease-specific networks in early-stage Alzheimer's disease and behavioral variant frontotemporal dementia. 2016 , 43, 119-28		15
1207	Bi-directional changes in fractional anisotropy after experiment TBI: Disorganization and reorganization?. <i>NeuroImage</i> , 2016 , 133, 129-143	7.9	44
1206	Clinically Anxious Individuals Show Disrupted Feedback between Inferior Frontal Gyrus and Prefrontal-Limbic Control Circuit. 2016 , 36, 4708-18		16
1205	Tractography Study of Deep Brain Stimulation of the Anterior Cingulate Cortex in Chronic Pain: Key to Improve the Targeting. 2016 , 86, 361-70.e1-3		18
1204	Feasibility of the Combined Application of Navigated Probabilistic Fiber Tracking and Navigated Ultrasonography in Brain Tumor Surgery. 2016 , 90, 306-314		5
1203	Fiber Orientation Distribution Estimation Using a PeacemanRachford Splitting Method. 2016 , 9, 573-60)4	5
1202	Correlation of Fractional Anisotropy With Motor Recovery in Patients With Stroke After Postacute Rehabilitation. 2016 , 97, 1487-1495		21

1201	Group-wise parcellation of the cortex through multi-scale spectral clustering. <i>NeuroImage</i> , 2016 , 136, 68-83	7.9	31
1200	Characterising brain network topologies: A dynamic analysis approach using heat kernels. <i>Neurolmage</i> , 2016 , 141, 490-501	7.9	19
1199	References. 2016 , 433-472		
1198	Impact of region-of-interest method on quantitative analysis of DTI data in the optic tracts. 2016 , 16, 42		11
1197	EP 135. Boosting cognitive control with transcranial alternating current stimulation. 2016 , 127, e297-e	298	
1196	EP 134. Effect of transcranial random noise stimulation depends on sensitivity to sham stimulation. 2016 , 127, e297		
1195	Multi-compartment microscopic diffusion imaging. <i>NeuroImage</i> , 2016 , 139, 346-359	7.9	186
1194	Detection of small colon bleeding in wireless capsule endoscopy videos. 2016 , 54, 16-26		25
1193	A Bayesian approach to fiber orientation estimation guided by volumetric tract segmentation. 2016 , 54, 35-47		1
1192	Processing Time Reduction: an Application in Living Human High-Resolution Diffusion Magnetic Resonance Imaging Data. 2016 , 40, 243		1
1191	Diffusion tensor distribution function metrics boost power to detect deficits in Alzheimer's disease. 2016 ,		0
1190	Structural Network Disorganization in Subjects at Clinical High Risk for Psychosis. 2017 , 43, 583-591		31
1189	Diffusion Tensor Imaging (DTI) and Tractography. 2016 , 411-442		2
1188	Associations between education and brain structure at age 73 years, adjusted for age 11 IQ. 2016 , 87, 1820-1826		26
1187	Natural variation in sensory-motor white matter organization influences manifestations of Huntington's disease. 2016 , 37, 4615-4628		15
1186	Nodes and Edges. 2016 , 37-88		
1185	Connectivity precedes function in the development of the visual word form area. 2016 , 19, 1250-5		214
1184	Tractography-Based Ventral Intermediate Nucleus Targeting: Novel Methodology and Intraoperative Validation. 2016 , 31, 1217-25		108

1183	Structural connectivity analyses in motor recovery research after stroke. 2016 , 3, 233-44	52
1182	Testosterone affects language areas of the adult human brain. 2016 , 37, 1738-48	27
1181	The cumulative effect of genetic polymorphisms on depression and brain structural integrity. 2016 , 37, 2173-84	8
1180	Involvement of the caudate nucleus head and its networks in sporadic amyotrophic lateral sclerosis-frontotemporal dementia continuum. 2016 , 17, 571-579	14
1179	High-resolution diffusion MRI at 7T using a three-dimensional multi-slab acquisition. <i>NeuroImage</i> , 2016 , 143, 1-14	41
1178	Age-related white-matter correlates of motor sequence learning and consolidation. 2016 , 48, 13-22	15
1177	EP 133. Structural connectivity of eloquent speech areas defined by direct cortical stimulation mapping. 2016 , 127, e296-e297	
1176	Structural parcellation of the thalamus using shortest-path tractography. 2016 ,	О
1175	White matter microstructure alterations in primary dysmenorrhea assessed by diffusion tensor imaging. 2016 , 6, 25836	7
1174	Identification of the stria medullaris thalami using diffusion tensor imaging. 2016 , 12, 852-857	7
1173	Grit Is Associated with Structure of Nucleus Accumbens and Gains in Cognitive Training. 2016 , 28, 1688-1699	16
1172	Periventricular White Matter Is a Nexus for Network Connectivity in the Human Brain. 2016 , 6, 548-57	14
1171	Altered striatal circuits underlie characteristic personality traits in Parkinson's disease. 2016 , 263, 1828-39	15
1170	Cardiac fiber tracking using adaptive particle filtering based on tensor rotation invariant in MRI. 2016 , 61, 1888-903	1
1169	Functional topography of the right inferior parietal lobule structured by anatomical connectivity profiles. 2016 , 37, 4316-4332	39
1168	Brain networks modulated by subthalamic nucleus deep brain stimulation. 2016 , 139, 2503-15	88
1167	Glial activation colocalizes with structural abnormalities in amyotrophic lateral sclerosis. 2016 , 87, 2554-2561	67
1166	Ipsilesional anodal tDCS enhances the functional benefits of rehabilitation in patients after stroke. 2016 , 8, 330re1	124

1165 Species Preserved and Exclusive Structural Connections Revealed by Sparse CCA. 2016, 123-131

1164	Alterations in amygdala-prefrontal circuits in infants exposed to prenatal maternal depression. 2016 , 6, e935	91
1163	Scaling in topological properties of brain networks. 2016 , 6, 24926	15
1162	Using CForest to Analyze Diffusion Tensor Imaging Data: A Study of White Matter Integrity in Healthy Aging. 2016 , 6, 747-758	5
1161	Discriminative fusion of multiple brain networks for early mild cognitive impairment detection. 2016 ,	4
1160	A Case of Hearing Loss after Bilateral Putaminal Hemorrhage: A Diffusion-tensor Imaging Study. 2016 , 1, 20160003	2
1159	Specialization of the Right Intraparietal Sulcus for Processing Mathematics During Development. 2017 , 27, 4436-4446	9
1158	Neural injury of the Papez circuit following hypoxic-ischemic brain injury: A case report. 2016 , 95, e5173	5
1157	Relation between injury of the periaqueductal gray and central pain in patients with mild traumatic brain injury: Observational study. 2016 , 95, e4017	26
1156	Characterizing brain tissue by assessment of the distribution of anisotropic microstructural environments in diffusion-compartment imaging (DIAMOND). 2016 , 76, 963-77	7 ²
1155	Speed of saccade execution and inhibition associated with fractional anisotropy in distinct fronto-frontal and fronto-striatal white matter pathways. 2016 , 37, 2811-22	13
1154	Functional organization of the fusiform gyrus revealed with connectivity profiles. 2016 , 37, 3003-16	48
1153	Anatomy and lateralization of the human corticobulbar tracts: an fMRI-guided tractography study. 2016 , 221, 3337-45	9
1152	Treatment of dysphasia with rTMS and language therapy after childhood stroke: Multimodal imaging of plastic change. 2016 , 159, 23-34	14
1151	Probabilistic Fiber-Tracking Reveals Degeneration of the Contralateral Auditory Pathway in Patients with Vestibular Schwannoma. 2016 , 37, 1610-6	12
1150	The 100 most-cited articles in neuroimaging: A bibliometric analysis. <i>NeuroImage</i> , 2016 , 139, 149-156 7.9	46
1149	Using Diffusion Tractography to Predict Cortical Connection Strength and Distance: A Quantitative Comparison with Tracers in the Monkey. 2016 , 36, 6758-70	225
1148	Multivariate Connectome-Based Symptom Mapping in Post-Stroke Patients: Networks Supporting Language and Speech. 2016 , 36, 6668-79	101

1147	Estimation of fiber orientations using neighborhood information. 2016 , 32, 243-56		18
1146	Dentatorubrothalamic tract localization with postmortem MR diffusion tractography compared to histological 3D reconstruction. 2016 , 221, 3487-501		31
1145	The extreme capsule fiber complex in humans and macaque monkeys: a comparative diffusion MRI tractography study. 2016 , 221, 4059-4071		71
1144	Brain imaging correlates of recovered swallowing after dysphagic stroke: A fMRI and DWI study. 2016 , 12, 1013-1021		29
1143	A connectivity-based approach to the pathophysiology of hemiballism. 2016 , 6, 107-113		
1142	Tract-specific white matter microstructure and gait in humans. 2016 , 43, 164-73		24
1141	Early diffusion evidence of retrograde transsynaptic degeneration in the human visual system. 2016 , 87, 198-205		12
1140	Reduced frontal-subcortical white matter connectivity in association with suicidal ideation in major depressive disorder. 2016 , 6, e835		52
1139	A comprehensive tractography study of patients with bipolar disorder and their unaffected siblings. 2016 , 37, 3474-85		27
1138	Structural and functional connectivity mapping of the vestibular circuitry from human brainstem to cortex. 2016 , 221, 1291-308		101
1137	Structural Connectivity Fingerprints Predict Cortical Selectivity for Multiple Visual Categories across Cortex. 2016 , 26, 1668-83		95
1136	Brain Events Underlying Episodic Memory Changes in Aging: A Longitudinal Investigation of Structural and Functional Connectivity. 2016 , 26, 1272-1286		67
1135	Vanderbilt University Institute of Imaging Science Center for Computational Imaging XNAT: A multimodal data archive and processing environment. <i>NeuroImage</i> , 2016 , 124, 1097-1101	7.9	27
1134	Deep brain stimulation of the posterior gyrus rectus region for treatment resistant depression. 2016 , 194, 33-7		33
1133	Structural and functional connectivity of the subthalamic nucleus during vocal emotion decoding. 2016 , 11, 349-56		23
1132	MumfordBhah and Potts Regularization for Manifold-Valued Data. 2016 , 55, 428-445		17
1131	Probabilistic Tractography Using Particle Filtering and Clustered Directional Data. 2016 , 47-62		
1130	Role of the left frontal aslant tract in stuttering: a brain stimulation and tractographic study. 2016 , 263, 157-67		71

1129	Functional Brain Activation Associated with Inhibitory Control Deficits in Older Adults. 2016 , 26, 12-22		56
1128	Comparing brains by matching connectivity profiles. 2016 , 60, 90-7	;	71
1127	Advances in Neurotechnology, Electronics and Informatics. 2016,		
1126	Altered Thalamo-Cortical White Matter Connectivity: Probabilistic Tractography Study in Clinical-High Risk for Psychosis and First-Episode Psychosis. 2016 , 42, 723-31	(65
1125	Network specific change in white matter integrity in mesial temporal lobe epilepsy. 2016 , 120, 65-72	-	13
1124	Individual differences in frontolimbic circuitry and anxiety emerge with adolescent changes in endocannabinoid signaling across species. 2016 , 113, 4500-5		48
1123	A COMPREHENSIVE EXAMINATION OF WHITE MATTER TRACTS AND CONNECTOMETRY IN MAJOR DEPRESSIVE DISORDER. 2016 , 33, 56-65	,	32
1122	Multimodal description of whole brain connectivity: A comparison of resting state MEG, fMRI, and DWI. 2016 , 37, 20-34		44
1121	White matter development and tobacco smoking in young adults: A systematic review with recommendations for future research. 2016 , 162, 26-33	;	28
1120	Trade-off between angular and spatial resolutions in in vivo fiber tractography. <i>NeuroImage</i> , 2016 , 129, 117-132) :	22
1119	Comparison of 3D orientation distribution functions measured with confocal microscopy and diffusion MRI. <i>NeuroImage</i> , 2016 , 129, 185-197)]	71
1118	Limb-kinetic apraxia due to injury of corticofugal tracts from secondary motor area in patients with corona radiata infarct. 2016 , 116, 467-472		12
1117	Neural correlates of unihemispheric and bihemispheric motor cortex stimulation in healthy young adults. <i>NeuroImage</i> , 2016 , 140, 141-9) :	27
1116	Shared neuroanatomical substrates of impaired phonological working memory across reading disability and autism. 2016 , 1, 169-177		4
1115	Modeling transcranial magnetic stimulation from the induced electric fields to the membrane potentials along tractography-based white matter fiber tracts. 2016 , 13, 026028	-	17
1114	Training shortest-path tractography: Automatic learning of spatial priors. NeuroImage, 2016 , 130, 63-76 $_{7.9}$)	5
1113	Brain MR Imaging in Patients with Lower Motor Neuron-Predominant Disease. 2016 , 280, 545-56	:	28
1112	Human Choice Strategy Varies with Anatomical Projections from Ventromedial Prefrontal Cortex to Medial Striatum. 2016 , 36, 2857-67		22

1111	Recovery of Hypersomnia Concurrent With Recovery of an Injured Ascending Reticular Activating System in a Stroke Patient: A Case Report. 2016 , 95, e2484		10
1110	Kernel regression estimation of fiber orientation mixtures in diffusion MRI. <i>NeuroImage</i> , 2016 , 127, 158-	- 1 752	27
1109	A survey of current trends in diffusion MRI for structural brain connectivity. 2016 , 13, 011001		8
1108	Increased Default Mode Network Connectivity in Individuals at High Familial Risk for Depression. 2016 , 41, 1759-67		56
1107	DTI Analysis Methods: Fibre Tracking and Connectivity. 2016 , 205-228		1
1106	High Angular Resolution Diffusion Imaging. 2016 , 383-406		3
1105	Investigating Brain Network Characteristics Interrupted by Covert White Matter Injury in Patients with Moyamoya Disease: Insights from Graph Theoretical Analysis. 2016 , 89, 654-665.e2		5
1104	PCA-based groupwise image registration for quantitative MRI. 2016 , 29, 65-78		84
1103	Joint reconstruction of white-matter pathways from longitudinal diffusion MRI data with anatomical priors. <i>NeuroImage</i> , 2016 , 127, 277-286	7.9	38
1102	Corpus Callosum Diffusion and Connectivity Features in High Functioning Subjects With Pyridoxine-Dependent Epilepsy. 2016 , 54, 43-8		5
1101	The Structural Connectome of the Human Central Homeostatic Network. 2016 , 6, 187-200		51
1100	Differential motor and prefrontal cerebello-cortical network development: Evidence from multimodal neuroimaging. <i>NeuroImage</i> , 2016 , 124, 591-601	7.9	37
1099	Hippocampal-medial prefrontal circuit supports memory updating during learning and post-encoding rest. 2016 , 134 Pt A, 91-106		67
1098	A probabilistic atlas of the cerebellar white matter. <i>NeuroImage</i> , 2016 , 124, 724-732	7.9	54
1097	Connectivity-Based Brain Parcellation: A Connectivity-Based Atlas for Schizophrenia Research. 2016 , 14, 83-97		10
1096	Variability and anatomical specificity of the orbitofrontothalamic fibers of passage in the ventral capsule/ventral striatum (VC/VS): precision care for patient-specific tractography-guided targeting of deep brain stimulation (DBS) in obsessive compulsive disorder (OCD). 2016 , 10, 1054-1067		91
1095	A cross-modal, cross-species comparison of connectivity measures in the primate brain. <i>NeuroImage</i> , 2016 , 125, 311-331	7.9	50
1094	Changes in white matter microstructure in the developing brainA longitudinal diffusion tensor imaging study of children from 4 to 11years of age. <i>NeuroImage</i> , 2016 , 124, 473-486	7.9	117

1093	Open Environment for Multimodal Interactive Connectivity Visualization and Analysis. 2016 , 6, 109-21	13
1092	Injury of the corticobulbar tract in patients with dysarthria following cerebral infarct: diffusion tensor tractography study. 2016 , 126, 361-5	11
1091	MGH-USC Human Connectome Project datasets with ultra-high b-value diffusion MRI. <i>NeuroImage</i> , 2016 , 124, 1108-1114	144
1090	Distinct hippocampal functional networks revealed by tractography-based parcellation. 2016 , 221, 2999-3012	56
1089	Test-retest reliability of high angular resolution diffusion imaging acquisition within medial temporal lobe connections assessed via tract based spatial statistics, probabilistic tractography and a novel graph theory metric. 2016 , 10, 533-47	10
1088	Greater Insula White Matter Fiber Connectivity in Women Recovered from Anorexia Nervosa. 2016 , 41, 498-507	43
1087	Visual exploration of HARDI fibers with probabilistic tracking. 2016 , 330, 483-494	3
1086	Structural integrity of frontostriatal connections predicts longitudinal changes in self-esteem. 2017 , 12, 280-286	11
1085	Shared microstructural features of behavioral and substance addictions revealed in areas of crossing fibers. 2017 , 2, 188-195	61
1084	Impaired topological architecture of brain structural networks in idiopathic Parkinson's disease: a DTI study. 2017 , 11, 113-128	35
1083	Altered white matter integrity in whole brain and segments of corpus callosum, in young social drinkers with binge drinking pattern. 2017 , 22, 490-501	30
1082	Clinical Application of Fiber Visualization with LIC Maps Using Multidirectional Anisotropic Glyph Samples (A-Glyph LIC). 2017 , 27, 263-273	3
1081	White Matter Tract Injury is Associated with Deep Gray Matter Iron Deposition in Multiple Sclerosis. 2017 , 27, 107-113	15
1080	A seed-based cross-modal comparison of brain connectivity measures. 2017 , 222, 1131-1151	17
1079	Multimodal investigation of triple network connectivity in patients with 22q11DS and association with executive functions. 2017 , 38, 2177-2189	17
1078	Changes in the cerebellar and cerebro-cerebellar circuit in type 2 diabetes. 2017 , 130, 95-100	20
1077	Development, validation and application of a new fornix template for studies of aging and preclinical Alzheimer's disease. 2017 , 13, 106-115	26
1076	Functional and structural connectivity of the amygdala in obsessive-compulsive disorder. 2017 , 13, 246-255	22

(2017-2017)

1075	lupus erythematosus identified by probabilistic tractography and connectivity-based analyses. 2017 , 13, 349-360		8	
1074	White matter integrity and symptom dimensions of schizophrenia: A diffusion tensor imaging study. 2017 , 184, 59-68		35	
1073	Using probabilistic tractography to target the subcallosal cingulate cortex in patients with treatment resistant depression. 2017 , 261, 72-74		20	
1072	Effects of aging on functional and structural brain connectivity. <i>NeuroImage</i> , 2017 , 160, 32-40	7.9	213	
1071	Structural Connectivity Variances Underlie Functional and Behavioral Changes During Pain Relief Induced by Neuromodulation. 2017 , 7, 41603		30	
1070	The effect of diffusion gradient direction number on corticospinal tractography in the human brain: an along-tract analysis. 2017 , 30, 265-280		3	
1069	Topological Organization of Whole-Brain White Matter in HIV Infection. 2017 , 7, 115-122		9	
1068	Connectivity of the Cingulate Sulcus Visual Area (CSv) in the Human Cerebral Cortex. 2018 , 28, 713-725		20	
1067	White matter changes in microstructure associated with a maladaptive response to stress in rats. 2017 , 7, e1009		20	
1066	A comparison of structural connectivity in anxious depression versus non-anxious depression. 2017 , 89, 38-47		20	
1065	Symmetry of the arcuate fasciculus and its impact on language performance of patients with brain tumors in the language-dominant hemisphere. 2017 , 127, 1407-1416		15	
1064	Fiber up-sampling and quality assessment of tractograms - towards quantitative brain connectivity. 2017 , 7, e00588		12	
1063	White Matter Tract Pathology in Pediatric Anoxic Brain Injury from Drowning. 2017, 38, 814-819		7	
1062	Anterior hippocampal dysconnectivity in posttraumatic stress disorder: a dimensional and multimodal approach. 2017 , 7, e1045		35	
1061	Dissociable frontostriatal white matter connectivity underlies reward and motor impulsivity. <i>NeuroImage</i> , 2017 , 150, 336-343	7.9	25	
1060	Improved clinical diffusion MRI reliability using a tensor distribution function compared to a single tensor. 2017 ,			
1059	Structural and Functional Abnormalities in Children with Attention-Deficit/Hyperactivity Disorder: A Focus on Subgenual Anterior Cingulate Cortex. 2017 , 7, 106-114		14	
1058	Brain fingerprints of olfaction: a novel structural method for assessing olfactory cortical networks in health and disease. 2017 , 7, 42534		39	

1057	Aberrant interhemispheric homotopic functional and structural connectivity in amyotrophic lateral sclerosis. 2017 , 88, 369-370	28
1056	Probabilistic vs. deterministic fiber tracking and the influence of different seed regions to delineate cerebellar-thalamic fibers in deep brain stimulation. 2017 , 45, 1623-1633	28
1055	Evaluations of diffusion tensor image registration based on fiber tractography. 2017 , 16, 9	12
1054	Vesicular monoamine transporter 1 gene polymorphism and white matter integrity in major depressive disorder. 2017 , 77, 138-145	5
1053	Akinetic mutism in a patient with mild traumatic brain injury: A diffusion tensor tractography study. 2017 , 31, 1159-1163	10
1052	Transcriptional signatures of connectomic subregions of the human striatum. 2017 , 16, 647-663	24
1051	How structure sculpts function: Unveiling the contribution of anatomical connectivity to the brain's spontaneous correlation structure. 2017 , 27, 047409	42
1050	Connectome imaging for mapping human brain pathways. 2017 , 22, 1230-1240	71
1049	Disrupted topological organization of structural networks revealed by probabilistic diffusion tractography in Tourette syndrome children. 2017 , 38, 3988-4008	19
1048	Risk and protective factors for structural brain ageing in the eighth decade of life. 2017 , 222, 3477-3490	31
1047	Dissociable corticostriatal circuits underlie goal-directed vs. cue-elicited habitual food seeking after satiation: evidence from a multimodal MRI study. 2017 , 46, 1815-1827	34
1046	Empirical consideration of the effects of acquisition parameters and analysis model on clinically feasible q-ball imaging. 2017 , 40, 62-74	4
1045	Magnetic resonance imaging connectivity for the prediction of seizure outcome in temporal lobe epilepsy. 2017 , 58, 1251-1260	43
1044	Differential Hemispheric Predilection of Microstructural White Matter and Functional Connectivity Abnormalities between Respectively Semantic and Behavioral Variant Frontotemporal Dementia. 2017 , 56, 789-804	9
1043	Impact of Gradient Number and Voxel Size on Diffusion Tensor Imaging Tractography for Resective Brain Surgery. 2017 , 105, 923-934.e2	6
1042	Deconstructing white matter connectivity of human amygdala nuclei with thalamus and cortex subdivisions in vivo. 2017 , 38, 3927-3940	38
1041	Structural connectivity differences in motor network between tremor-dominant and nontremor Parkinson's disease. 2017 , 38, 4716-4729	39
1040	Population-averaged macaque brain atlas with high-resolution ex vivo DTI integrated into in vivo space. 2017 , 222, 4131-4147	24

1039	Diffusion MRI microstructure models with in vivo human brain Connectome data: results from a multi-group comparison. 2017 , 30, e3734	26
1038	Disrupted white matter structural networks in healthy older adult APOE $\bar{\mu}4$ carriers - An international multicenter DTI study. 2017 , 357, 119-133	23
1037	Altered Brain Wiring in Parkinson's Disease: A Structural Connectome-Based Analysis. 2017 , 7, 347-356	20
1036	Modular Segregation of Structural Brain Networks Supports the Development of Executive Function in Youth. 2017 , 27, 1561-1572.e8	178
1035	Multimodal connectivity-based parcellation reveals a shell-core dichotomy of the human nucleus accumbens. 2017 , 38, 3878-3898	24
1034	Brain structural alterations in obese children with and without Prader-Willi Syndrome. 2017 , 38, 4228-4238	18
1033	Brain grey and white matter predictors of verbal ability traits in older age: The Lothian Birth Cohort 1936. <i>NeuroImage</i> , 2017 , 156, 394-402	14
1032	Multiparametric MRI to distinguish early onset Alzheimer's disease and behavioural variant of frontotemporal dementia. 2017 , 15, 428-438	33
1031	Structural and functional brain signatures of C9orf72 in motor neuron disease. 2017 , 57, 206-219	35
1030	Altered structural connectivity of pain-related brain network in burning mouth syndrome-investigation by graph analysis of probabilistic tractography. 2017 , 59, 525-532	22
1029	Persistent amygdala novelty response is associated with less anterior cingulum integrity in trauma-exposed women. 2017 , 14, 250-259	3
1028	Role of corpus callosum integrity in arm function differs based on motor severity after stroke. 2017 , 14, 641-647	24
1027	White matter microstructure in children with autistic traits. 2017 , 263, 127-134	14
1026	Neural Reorganization Due to Neonatal Amygdala Lesions in the Rhesus Monkey: Changes in Morphology and Network Structure. 2017 , 27, 3240-3253	9
1025	The origins of the vocal brain in humans. 2017 , 77, 177-193	67
1024	Linking optic radiation volume to visual perception in schizophrenia and bipolar disorder. 2017 , 190, 102-106	9
1023	Dissociable diffusion MRI patterns of white matter microstructure and connectivity in Alzheimer's disease spectrum. 2017 , 7, 45131	28
1022	Fractional anisotropy derived from the diffusion tensor distribution function boosts power to detect Alzheimer's disease deficits. 2017 , 78, 2322-2333	15

1021	Mechanisms of circumferential gyral convolution in primate brains. 2017 , 42, 217-229		15
1020	White-matter crossing-fiber microstructure in adolescents prenatally exposed to cocaine. 2017 , 174, 23-29		7
1019	Abnormal structural connectivity between the basal ganglia, thalamus, and frontal cortex in patients with disorders of consciousness. 2017 , 90, 71-87		29
1018	Single or multiple frequency generators in on-going brain activity: A mechanistic whole-brain model of empirical MEG data. <i>NeuroImage</i> , 2017 , 152, 538-550	7.9	87
1017	Assessing connectivity related injury burden in diffuse traumatic brain injury. 2017 , 38, 2913-2922		13
1016	The Emergence of Network Inefficiencies in Infants With Autism Spectrum Disorder. 2017 , 82, 176-185		65
1015	A systematic evaluation of intraoperative white matter tract shift in pediatric epilepsy surgery using high-field MRI and probabilistic high angular resolution diffusion imaging tractography. 2017 , 19, 592-605		10
1014	Altered microstructure rather than morphology in the corpus callosum after lower limb amputation. 2017 , 7, 44780		9
1013	CIVILITY: Cloud based Interactive Visualization of Tractography Brain Connectome. 2017, 10137,		3
1012	Individual classification of Alzheimer's disease with diffusion magnetic resonance imaging. <i>NeuroImage</i> , 2017 , 152, 476-481	7.9	40
1011	A Bayesian Double Fusion Model for Resting-State Brain Connectivity Using Joint Functional and Structural Data. 2017 , 7, 219-227		12
1010	Modular-level alterations of structure-function coupling in schizophrenia connectome. 2017 , 38, 2008-2	025	23
1009	Comparison of probabilistic and deterministic fiber tracking of cranial nerves. 2017 , 127, 613-621		21
1008	White matter lesions relate to tract-specific reductions in functional connectivity. 2017 , 51, 97-103		24
1007	Tracking thoughts: Exploring the neural architecture of mental time travel during mind-wandering. <i>NeuroImage</i> , 2017 , 147, 272-281	7.9	64
1006	White Matter Disruption and Connected Speech in Non-Fluent and Semantic Variants of Primary Progressive Aphasia. 2017 , 7, 52-73		20
1005	Pure word deafness following left temporal damage: Behavioral and neuroanatomical evidence from a new case. 2017 , 97, 240-254		18
1004	Callosal microstructure affects the timing of electrophysiological left-right differences. <i>NeuroImage</i> , 2017 , 163, 310-318	7.9	12

1003	Structural connectomics of anxious arousal in early adolescence: Translating clinical and ethological findings. 2017 , 16, 604-609	5
1002	Traumatic axonal injury despite clinical phenotype of mild traumatic brain injury: a case report. 2017 , 31, 1534-1537	1
1001	Age-Related Changes in Topological Degradation of White Matter Networks and Gene Expression in Chronic Schizophrenia. 2017 , 7, 574-589	7
1000	Evaluation of striatonigral connectivity using probabilistic tractography in Parkinson's disease. 2017 , 16, 557-563	32
999	A Sparse Bayesian Learning Algorithm for White Matter Parameter Estimation from Compressed Multi-shell Diffusion MRI. 2017 , 10433, 602-610	
998	Short-range connections in the developmental connectome during typical and atypical brain maturation. 2017 , 83, 109-122	46
997	Recovery of an injured prefronto-caudate tract in a patient with traumatic brain injury: A diffusion tensor tractography study. 2017 , 31, 1548-1551	4
996	Direct Electrical Stimulation in the Human Brain Disrupts Melody Processing. 2017 , 27, 2684-2691.e7	16
995	Neural Substrate for Metacognitive Accuracy of Tactile Working Memory. 2017 , 27, 5343-5352	10
994	Segmentation of the inferior longitudinal fasciculus in the human brain: A white matter dissection and diffusion tensor tractography study. 2017 , 1675, 102-115	63
993	Central and non-central networks, cognition, clinical symptoms, and polygenic risk scores in schizophrenia. 2017 , 38, 5919-5930	13
992	Altered topology of structural brain networks in patients with Gilles de la Tourette syndrome. 2017 , 7, 10606	6
991	Subject-Specific Structural Parcellations Based on Randomized AB-divergences. 2017 , 10433, 407-415	2
990	A flexible graphical model for multi-modal parcellation of the cortex. <i>NeuroImage</i> , 2017 , 162, 226-248 $_{7.9}$	5
989	Connectivity-based parcellation of the anterior limb of the internal capsule. 2017 , 38, 6107-6117	34
988	Can increased spatial resolution solve the crossing fiber problem for diffusion MRI?. 2017 , 30, e3787	38
987	Recovery of an injured corticobulbar tract in a patient with stroke: A case report. 2017 , 96, e7636	5
986	The association between substance P and white matter integrity in medication-naive patients with major depressive disorder. 2017 , 7, 9707	9

985	Disrupted topological organization of structural brain networks in childhood absence epilepsy. 2017 , 7, 11973	13
984	Chronic post-stroke aphasia severity is determined by fragmentation of residual white matter networks. 2017 , 7, 8188	25
983	Supervoxel-based statistical analysis of diffusion tensor imaging in schizotypal personality disorder. NeuroImage, 2017, 163, 368-378	4
982	Analysis of structure-function network decoupling in the brain systems of spastic diplegic cerebral palsy. 2017 , 38, 5292-5306	20
981	Structural connectivity differences in essential tremor with and without resting tremor. 2017, 264, 1865-1874	22
980	Fiber tractography using machine learning. <i>NeuroImage</i> , 2017 , 158, 417-429 7.9	36
979	Relationships between the integrity and function of lumbar nerve roots as assessed by diffusion tensor imaging and neurophysiology. 2017 , 59, 893-903	4
978	The anatomical scaffold underlying the functional centrality of known cortical hubs. 2017 , 38, 5141-5160	8
977	Single Nucleotide Polymorphisms Associated with Reading Ability Show Connection to Socio-Economic Outcomes. 2017 , 47, 469-479	8
976	Subthalamic deep brain stimulation sweet spots and hyperdirect cortical connectivity in Parkinson's disease. <i>NeuroImage</i> , 2017 , 158, 332-345	131
975	High angular resolution diffusion imaging abnormalities in the early stages of amyotrophic lateral sclerosis. 2017 , 380, 215-222	9
974	Temporal lobe networks supporting the comprehension of spoken words. 2017 , 140, 2370-2380	61
973	Injury of the dentato-rubro-thalamic tract in patients with cerebellar infarct: Case report. 2017, 96, e7220	4
972	Structurofunctional resting-state networks correlate with motor function in chronic stroke. 2017 , 16, 610-623	9
971	Altered structural network architecture is predictive of the presence of psychotic symptoms in patients with 22q11.2 deletion syndrome. 2017 , 16, 142-150	15
970	Picture free recall performance linked to the brain's structural connectome. 2017 , 7, e00721	3
969	Probabilistic Tractography of the Cranial Nerves in Vestibular Schwannoma. 2017 , 107, 47-53	15
968	AxTract: Toward microstructure informed tractography. 2017 , 38, 5485-5500	39

967	White Matter Connectivity Pattern Associate with Characteristics of Scalp EEG Signals. 2017, 30, 797-809	3
966	Investigating the maturation of microstructure and radial orientation in the preterm human cortex with diffusion MRI. NeuroImage, 2017 , 162, 65-72 7.9	16
965	Sparse registration of diffusion weighted images. 2017 , 151, 33-43	3
964	Tractography-Based Score for Learning Effective Connectivity From Multimodal Imaging Data Using Dynamic Bayesian Networks. 2018 , 65, 1057-1068	7
963	Bayesian Diffusion Tensor Estimation with Spatial Priors. 2017 , 372-383	2
962	Whole brain functional connectivity predicted by indirect structural connections. 2017,	3
961	Predicting Cognitive Recovery of Stroke Patients from the Structural MRI Connectome Using a NaMe Bayesian Tree Classifier. 2017 ,	О
960	Effects of natural medicinal on emotional brain response. 2017 , 27, S704-S705	
959	White matter structural connectivity and episodic memory in early childhood. 2017 , 28, 41-53	16
958	Altered Structural Connectivity of the Left Visual Thalamus in Developmental Dyslexia. 2017, 27, 3692-3698.	2 432
957	Intact hemisphere and corpus callosum compensate for visuomotor functions after early visual cortex damage. 2017 , 114, E10475-E10483	39
956	Task-relevant brain networks identified with simultaneous PET/MR imaging of metabolism and connectivity. 2018 , 223, 1369-1378	27
955	Amygdala-midbrain connectivity indicates a role for the mammalian parental care system in human altruism. 2017 , 284,	13
954	Reading on the right when there's nothing left? Probabilistic tractography reveals hemispheric asymmetry in pure alexia. 2017 , 23, 201-209	1
953	A translational study on looming-evoked defensive response and the underlying subcortical pathway in autism. 2017 , 7, 14755	9
952	White matter tractography for neurosurgical planning: A topography-based review of the current state of the art. 2017 , 15, 659-672	98
951	Longitudinal analysis of diffusion-weighted MRI with a ball-and-sticks model. 2017,	
950	Structural neuroimaging correlates of alcohol and cannabis use in adolescents and adults. 2017 , 112, 2144-2154	23

949	Enhancing Diffusion MRI Measures By Integrating Grey and White Matter Morphometry With Hyperbolic Wasserstein Distance. 2017 , 2017, 520-524	3
948	Right-sided dominance of the bilateral vestibular system in the upper brainstem and thalamus. 2017 , 264, 55-62	34
947	Diffusion Magnetic Resonance Imaging in Diffuse Low-Grade Gliomas. 2017 , 375-410	
946	Cognitive performance in healthy older adults relates to spontaneous switching between states of functional connectivity during rest. 2017 , 7, 5135	110
945	Zoomed MRI Guided by Combined EEG/MEG Source Analysis: A Multimodal Approach for Optimizing Presurgical Epilepsy Work-up and its Application in a Multi-focal Epilepsy Patient Case Study. 2017 , 30, 417-433	29
944	Estimation of individual axon bundle properties by a Multi-Resolution Discrete-Search method. 2017 , 42, 26-43	4
943	Improved tractography using asymmetric fibre orientation distributions. <i>NeuroImage</i> , 2017 , 158, 205-218/9.9	29
942	Performance of unscented Kalman filter tractography in edema: Analysis of the two-tensor model. 2017 , 15, 819-831	24
941	Intrainsular connectivity and somatosensory responsiveness in young children with ASD. 2017, 8, 25	15
940	Calretinin interneuron density in the caudate nucleus is lower in autism spectrum disorder. 2017 , 140, 2028-2040	23
939	Restoration of the ascending reticular activating system compressed by hematoma in a stroke patient. 2017 , 96, e6103	3
938	Microstructure of the Default Mode Network in Preterm Infants. 2017, 38, 343-348	14
937	White matter integrity in brain networks relevant to anxiety and depression: evidence from the human connectome project dataset. 2017 , 11, 1604-1615	21
936	A Comparative evaluation of voxel-based spatial mapping in diffusion tensor imaging. <i>NeuroImage</i> , 7.9	20
935	Differential Impairment of Thalamocortical Structural Connectivity in Amyotrophic Lateral Sclerosis. 2017 , 23, 155-161	5
934	The role of the pallidothalamic fibre tracts in deep brain stimulation for dystonia: A diffusion MRI tractography study. 2017 , 38, 1224-1232	15
933	Microstructural changes of brain in patients with aromatic L-amino acid decarboxylase deficiency. 2017 , 38, 1532-1540	10
932	Microstructural Integrity of Hippocampal Subregions Is Impaired after Mild Traumatic Brain Injury. 2017 , 34, 1402-1411	11

931	The most relevant human brain regions for functional connectivity: Evidence for a dynamical workspace of binding nodes from whole-brain computational modelling. <i>NeuroImage</i> , 2017 , 146, 197-210.	32
930	Recovery from Posttraumatic Stress Requires Dynamic and Sequential Shifts in Amygdalar Connectivities. 2017 , 42, 454-461	12
929	Atypical white-matter microstructure in congenitally deaf adults: Alregion of interest and tractography study using diffusion-tensor imaging. 2017 , 343, 72-82	19
928	Connectivity-based parcellation of the macaque frontal cortex, and its relation with the cytoarchitectonic distribution described in current atlases. 2017 , 222, 1331-1349	15
927	The pace of vocabulary growth during preschool predicts cortical structure at school age. 2017 , 98, 13-23	11
926	Rapid recovery from aphasia after infarction of Wernicke's area. 2017 , 31, 951-980	17
925	Associations between autistic traits and fractional anisotropy values in white matter tracts in a nonclinical sample of young adults. 2017 , 235, 259-267	8
924	In vivo detection of connectivity between cortical and white matter lesions in early MS. 2017 , 23, 973-981	2
923	A diffusion tensor imaging atlas of white matter in tree shrew. 2017 , 222, 1733-1751	9
922	Altered whole-brain connectivity in albinism. 2017 , 38, 740-752	5
921	The structural connectivity of higher order association cortices reflects human functional brain networks. 2017 , 97, 221-239	49
920	Automated white matter fiber tract identification in patients with brain tumors. 2017, 13, 138-153	79
919	White matter integrity between left basal ganglia and left prefrontal cortex is compromised in gambling disorder. 2017 , 22, 1590-1600	7
918	Probabilistic tractography using Lasso bootstrap. 2017 , 35, 544-553	3
917	Investigating white matter fibre density and morphology using fixel-based analysis. <i>NeuroImage</i> , 2017 , 144, 58-73	249
916	Relationship between structural and functional connectivity change across the adult lifespan: A longitudinal investigation. 2017 , 38, 561-573	48
915	Delayed degeneration of the left fornical crus with verbal memory impairment in a patient with mild traumatic brain injury: A case report. 2017 , 96, e9219	3
914	Plasticity in deep and superficial white matter: a DTI study in world class gymnasts. 2018 , 223, 1849-1862	12

Which white matter bundles are associated with treatment efficacy in deep brain stimulation of the ventral internal capsule for OCD and major depressive disorder?. **2017**, 27, S705

912	A neuroanatomical predictor of mirror self-recognition in chimpanzees. 2017 , 12, 37-48	50
911	Limb-kinetic apraxia in a patient with mild traumatic brain injury: A case report. 2017 , 96, e9008	6
910	Mutations in the netrin-1 gene cause congenital mirror movements. 2017 , 127, 3923-3936	30
909	White Matter Correlates of Musical Anhedonia: Implications for Evolution of Music. 2017, 8, 1664	26
908	Endothelial Function Is Associated with White Matter Microstructure and Executive Function in Older Adults. 2017 , 9, 255	10
907	Asymmetry of Hemispheric Network Topology Reveals Dissociable Processes between Functional and Structural Brain Connectome in Community-Living Elders. 2017 , 9, 361	16
906	Exploration of the Connectivity between the Subthalamic Nucleus and the Globus Pallidus in the Human Brain Using Multi-Fiber Tractography. 2016 , 10, 119	15
905	Microstructural Alterations in Asymptomatic and Symptomatic Patients with Spinocerebellar Ataxia Type 3: A Tract-Based Spatial Statistics Study. 2017 , 8, 714	12
904	White Matter Integrity and Treatment-Based Change in Speech Performance in Minimally Verbal Children with Autism Spectrum Disorder. 2017 , 11, 175	19
903	Functional and Structural Network Recovery after Mild Traumatic Brain Injury: A 1-Year Longitudinal Study. 2017 , 11, 280	36
902	Cortex Parcellation Associated Whole White Matter Parcellation in Individual Subjects. 2017 , 11, 352	5
901	Reproducible Large-Scale Neuroimaging Studies with the OpenMOLE Workflow Management System. 2017 , 11, 21	2
900	ATPP: A Pipeline for Automatic Tractography-Based Brain Parcellation. 2017 , 11, 35	10
899	Running Neuroimaging Applications on Amazon Web Services: How, When, and at What Cost?. 2017 , 11, 63	12
898	Bayesian Tractography Using Geometric Shape Priors. 2017 , 11, 483	3
897	Uniformity and Deviation of Intra-axonal Cross-sectional Area Coverage of the Gray-to-White Matter Interface. 2017 , 11, 729	2
896	Deafferentation of the Superior Colliculus Abolishes Spatial Summation of Redundant Visual Signals. 2017 , 11, 9	3

895	Complex Brain Network Analysis and Its Applications to Brain Disorders: A Survey. 2017, 2017, 1-27	46
894	Thalamocortical Connectivity and Microstructural Changes in Congenital and Late Blindness. 2017 , 2017, 9807512	21
893	The visual white matter: The application of diffusion MRI and fiber tractography to vision science. 2017 , 17, 4	41
892	A Novel Richardson-Lucy Model with Dictionary Basis and Spatial Regularization for Isolating Isotropic Signals. 2017 , 12, e0168864	1
891	Reconstruction of the Cortical Maps of the Tasmanian Tiger and Comparison to the Tasmanian Devil. 2017 , 12, e0168993	8
890	Similar white matter changes in schizophrenia and bipolar disorder: A tract-based spatial statistics study. 2017 , 12, e0178089	47
889	Brain network eigenmodes provide a robust and compact representation of the structural connectome in health and disease. 2017 , 13, e1005550	29
888	Injury of ascending reticular activating system associated with delayed post-hypoxic leukoencephalopathy: a case report. 2017 , 17, 139	4
887	Multiscale network analysis through tail-greedy bottom-up approximation, with applications in neuroscience. 2017 ,	
886	Cerebellum and neurodegenerative diseases: Beyond conventional magnetic resonance imaging. 2017 , 9, 371-388	28
885	Predictors of Memory in Healthy Aging: Polyunsaturated Fatty Acid Balance and Fornix White Matter Integrity. 2017 , 8, 372-383	19
884	Subthalamic Nucleus Deep Brain Stimulation: Basic Concepts and Novel Perspectives. 2017, 4,	69
883	Decreased uncinate fasciculus tract integrity in male and female patients with PTSD: a diffusion tensor imaging study. 2017 , 42, 331-342	35
882	Alterations of White Matter Integrity in Patients with Chronic Obstructive Pulmonary Disease: Tract-Based Analysis Using TRActs Constrained by UnderLying Anatomy. 2017 , 77, 148	O
881	The structural and functional brain networks that support human social networks. 2018, 355, 12-23	54
880	Identification of Stria Medullaris Fibers in the Massa Intermedia Using Diffusion Tensor Imaging. 2018 , 112, e497-e504	10
879	Auditory structural connectivity in preterm and healthy term infants during the first postnatal year. 2018 , 60, 256-264	5
878	Connectivity profiles of the insular network for speech control in healthy individuals and patients with spasmodic dysphonia. 2018 , 223, 2489-2498	7

877	Altered anatomical connections of associative and limbic cortico-basal-ganglia circuits in obsessive-compulsive disorder. 2018 , 51, 1-8	15
876	Minimum spanning tree analysis of the human connectome. 2018 , 39, 2455-2471	33
875	The impact of in-scanner head motion on structural connectivity derived from diffusion MRI. NeuroImage, 2018 , 173, 275-286 7-9	57
874	Bayesian Optimisation of Large-Scale Biophysical Networks. <i>NeuroImage</i> , 2018 , 174, 219-236 7.9	7
873	Structural connectome with high angular resolution diffusion imaging MRI: assessing the impact of diffusion weighting and sampling on graph-theoretic measures. 2018 , 60, 497-504	4
872	Microstructural parcellation of the human brain. <i>NeuroImage</i> , 2018 , 182, 219-231 7.9	15
871	A gyral coordinate system predictive of fibre orientations. <i>NeuroImage</i> , 2018 , 176, 417-430 7.9	7
870	White matter pathways and social cognition. 2018 , 90, 350-370	40
869	Natural biological variation of white matter microstructure is accentuated in Huntington's disease. 2018 , 39, 3516-3527	11
868	Alterations in the microstructure of white matter in children and adolescents with Tourette syndrome measured using tract-based spatial statistics and probabilistic tractography. 2018 , 104, 75-89	15
867	Substance-use initiation moderates the effect of stress on white-matter microstructure in adolescents. 2018 , 27, 217-224	
866	Brain Parcellation and Connectivity Mapping Using Wasserstein Geometry. 2018 , 165-174	
865	Amygdala Functional and Structural Connectivity Predicts Individual Risk Tolerance. 2018 , 98, 394-404.e4	40
864	Computational Diffusion MRI. 2018 ,	
863	Connectivity of the ventral visual cortex is necessary for object recognition in patients. 2018 , 39, 2786-2799	3
862	Bayesian uncertainty quantification in linear models for diffusion MRI. <i>NeuroImage</i> , 2018 , 175, 272-285 7.9	7
861	Promise and pitfalls of g-ratio estimation with MRI. <i>NeuroImage</i> , 2018 , 182, 80-96 7.9	64
860	Recovery of an injured corticofugal tract from the supplementary motor area in a patient with traumatic brain injury: A case report. 2018 , 97, e9063	7

859	Diffusion tensor imaging in metachromatic leukodystrophy. 2018 , 265, 659-668	9
858	Connectivity derived thalamic segmentation in deep brain stimulation for tremor. 2018 , 18, 130-142	98
857	Applications of community detection techniques to brain graphs: Algorithmic considerations and implications for neural function. 2018 , 106, 846-867	55
856	No evidence for systematic white matter correlates of dyslexia and dyscalculia. 2018 , 18, 356-366	9
855	Post-mortem inference of the human hippocampal connectivity and microstructure using ultra-high field diffusion MRI at 11.7 T. 2018 , 223, 2157-2179	28
854	Preliminary mapping of the structural effects of age in pediatric bipolar disorder with multimodal MR imaging. 2018 , 273, 54-62	7
853	Anatomy of aphasia revisited. 2018, 141, 848-862	145
852	PAGANI Toolkit: Parallel graph-theoretical analysis package for brain network big data. 2018 , 39, 1869-1885	8
851	Spectral mapping of brain functional connectivity from diffusion imaging. 2018, 8, 1411	47
850	Functional Segmentation of the Anterior Limb of the Internal Capsule: Linking White Matter Abnormalities to Specific Connections. 2018 , 38, 2106-2117	78
849	Association of Heritable Cognitive Ability and Psychopathology With White Matter Properties in Children and Adolescents. 2018 , 75, 287-295	55
848	Decreased Number of Self-Paced Saccades in Post-Concussion Syndrome Associated with Higher Symptom Burden and Reduced White Matter Integrity. 2018 , 35, 719-729	20
847	Structural connectivity of the amygdala in young adults with autism spectrum disorder. 2018 , 39, 1270-1282	26
846	Analytic tractography: A closed-form solution for estimating local white matter connectivity with diffusion MRI. NeuroImage, 2018 , 169, 473-484 7.9	8
845	The potential value of probabilistic tractography-based for MR-guided focused ultrasound thalamotomy for essential tremor. 2018 , 17, 1019-1027	28
844	Quantifying axonal responses in patient-specific models of subthalamic deep brain stimulation. NeuroImage, 2018 , 172, 263-277 7.9	52
843	White matter integrity in the fronto-striatal accumbofrontal tract predicts impulsivity. 2018 , 12, 1524-1528	11
842	Changes in Frontoparietotemporal Connectivity following Do-As-I-Do Imitation Training in Chimpanzees (Pan troglodytes). 2018 , 30, 421-431	14

841	Fibre-specific white matter reductions in Alzheimer's disease and mild cognitive impairment. 2018 , 141, 888-902	139
840	A method for pre-operative single-subject thalamic segmentation based on probabilistic tractography for essential tremor deep brain stimulation. 2018 , 60, 303-309	20
839	Structural connectivity of right frontal hyperactive areas scales with stuttering severity. 2018 , 141, 191-204	48
838	Default mode network abnormalities in posttraumatic stress disorder: A novel network-restricted topology approach. <i>NeuroImage</i> , 2018 , 176, 489-498	81
837	Towards Portable Large-Scale Image Processing with High-Performance Computing. 2018 , 31, 304-314	16
836	Mesocorticolimbic Connectivity and Volumetric Alterations in Mutation Carriers. 2018 , 38, 4655-4665	16
835	The Ipsilateral Vestibulothalamic Tract in the Human Brain. 2018 , 9, 22-25	1
834	Segmentation of the Globus Pallidus Internus Using Probabilistic Diffusion Tractography for Deep Brain Stimulation Targeting in Parkinson Disease. 2018 , 39, 1127-1134	28
833	Tensor Eigenvalues and Their Applications. 2018,	62
832	Topography of the human acoustic radiation as revealed by ex vivo fibers micro-dissection and in vivo diffusion-based tractography. 2018 , 223, 449-459	26
831	White Matter Connectivity of the Visual-Vestibular Cortex Examined by Diffusion-Weighted Imaging. 2018 , 8, 235-244	18
830	A Role for the Frontal Aslant Tract in Speech Planning: A Neurosurgical Case Study. 2018 , 30, 752-769	32
829	Cerebellar Growth Impairment Characterizes School-Aged Children Born Preterm without Perinatal Brain Lesions. 2018 , 39, 956-962	12
828	Connectivity-based segmentation of the brainstem by probabilistic tractography. 2018, 1690, 74-88	3
827	Rotationally-invariant mapping of scalar and orientational metrics of neuronal microstructure with diffusion MRI. <i>NeuroImage</i> , 2018 , 174, 518-538	117
826	Individualized parcellation of the subthalamic nucleus in patients with Parkinson's disease with 7T MRI. NeuroImage, 2018 , 168, 403-411 7.9	65
825	Concurrent white matter bundles and grey matter networks using independent component analysis. <i>NeuroImage</i> , 2018 , 170, 296-306	26
824	Brain white matter structural networks in patients with non-neuropsychiatric systemic lupus erythematosus. 2018 , 12, 142-155	6

(2021-2018)

823	The heterogeneity of the left dorsal premotor cortex evidenced by multimodal connectivity-based parcellation and functional characterization. <i>NeuroImage</i> , 2018 , 170, 400-411	7.9	44
822	Tests of cortical parcellation based on white matter connectivity using diffusion tensor imaging. <i>NeuroImage</i> , 2018 , 170, 321-331	7.9	7
821	Brain structural and functional signatures of impulsive-compulsive behaviours in Parkinson's disease. 2018 , 23, 459-466		38
820	Structural connectivity in spatial attention network: reconstruction from left hemispatial neglect. 2018 , 12, 309-323		16
819	High resolution anatomical and quantitative MRI of the entire human occipital lobe ex vivo at 9.4T. <i>NeuroImage</i> , 2018 , 168, 162-171	7.9	17
818	Diffusion tensor imaging and tractography of the white matter in normal aging: The rate-of-change differs between segments within tracts. 2018 , 45, 113-119		17
817	Tracking Training-Related Plasticity by Combining fMRI and DTI: The Right Hemisphere Ventral Stream Mediates Musical Syntax Processing. 2018 , 28, 1209-1218		20
816	Disrupted frontostriatal connectivity in primary insomnia: a DTI study. 2021 , 15, 2524-2531		2
815	Structural connectome quantifies tumor invasion and predicts survival in glioblastoma patients.		4
814	Diffusion Kurtosis Imaging Fiber Tractography of Major White Matter Tracts in Neurosurgery. 2021 , 11,		O
813	qModeL: A plug-and-play model-based reconstruction for highly accelerated multi-shot diffusion MRI using learned priors. 2021 , 86, 835-851		2
812	White Matter Connectivity and Gray Matter Volume Changes Following Donepezil Treatment in Patients With Mild Cognitive Impairment: A Preliminary Study Using Probabilistic Tractography. 2020 , 12, 604940		3
811	Diffusion imaging changes in the treated tract following focused ultrasound thalamotomy for tremor. 2021 , 1, 100010		О
810	Quantifying structural connectivity in brain tumor patients.		2
809	Tract-specific statistics based on diffusion-weighted probabilistic tractography.		
808	Chronic musculoskeletal impairment is associated with alterations in brain regions responsible for the production and perception of movement. 2021 , 599, 2255-2272		3
807	Functional and structural brain connectivity in congenital deafness. 2021 , 226, 1323-1333		2
806	Shift Toward Randomness in Brain Networks of Patients With Anorexia Nervosa: The Role of Malnutrition. 2021 , 15, 645139		3

805	Anatomical location of the spinothalamic tract in the subcortical white matter in the human brain: A diffusion tensor imaging study. 2021 , 34, 736-741	2
804	Structural brain connectivity in children with developmental dyscalculia.	
803	Validation of Olfactory Network Based on Brain Structural Connectivity and Its Association With Olfactory Test Scores. 2021 , 15, 638053	1
802	Splenial white matter integrity is associated with memory impairments in posterior cortical atrophy. 2021 , 3, fcab060	O
801	White matter abnormalities in adults with bipolar disorder type-II and unipolar depression. 2021 , 11, 7541	2
800	Hodology of the superior longitudinal system of the human brain: a historical perspective, the current controversies, and a proposal. 2021 , 226, 1363-1384	11
799	A quality control pipeline for probabilistic reconstruction of white-matter pathways. 2021 , 353, 109099	0
798	Comparison of structural MRI brain measures between 1.5T and 3T: data from the Lothian Birth Cohort 1936.	
797	Elasticnetisdr to Reconstruct Both Sparse Brain Activity and Effective Connectivity. 2021,	
796	Exercise-induced fluid shifts are distinct to exercise mode and intensity: a comparison of blood flow-restricted and free-flow resistance exercise. 2021 , 130, 1822-1835	1
795	Altered Thalamocortical Connectivity in 6-Week-Old Infants at High Familial Risk for Autism Spectrum Disorder. 2021 , 31, 4191-4205	6
794	In-vivo diffusion MRI protocol optimization for the chimpanzee brain and examination of aging effects on the primate optic nerve at 3T. 2021 , 77, 194-203	3
793	In vivo human whole-brain Connectom diffusion MRI dataset at 760 μ m isotropic resolution. 2021 , 8, 122	8
792	A graph neural network framework for causal inference in brain networks. 2021 , 11, 8061	1
791	Nature and nurture shape structural connectivity in the face processing brain network. <i>NeuroImage</i> , 2021 , 229, 117736	0
790	The impact of susceptibility correction on diffusion metrics in adolescents. 2021 , 51, 1471-1480	O
789	An MRI protocol for anatomical and functional evaluation of the California sea lion brain. 2021 , 353, 109097	1
788	Enhanced structural connectivity within the motor loop in professional boxers prior to a match. 2021 , 11, 9015	O

(2021-2021)

787	Preliminary Comparison of Subcortical Structures in Elderly Subclinical Depression: Structural Analysis with 3T MRI. 2021 , 30, 183-202		O
786	White matter microstructural differences underlying beta oscillations during speech in adults who stutter. 2021 , 215, 104921		1
7 ⁸ 5	Supplementary and Premotor Aspects of the Corticospinal Tract Show Links with Restricted and Repetitive Behaviors in Middle-Aged Adults with Autism Spectrum Disorder. 2021 , 31, 3962-3972		2
784	Delayed access to conscious processing in multiple sclerosis: Reduced cortical activation and impaired structural connectivity. 2021 , 42, 3379-3395		1
783	Myelin development in visual scene-network tracts beyond late childhood: A multimethod neuroimaging study. 2021 , 137, 18-34		3
782	Functional and diffusion MRI reveal the neurophysiological basis of neonates' noxious-stimulus evoked brain activity. 2021 , 12, 2744		4
781	Cognitive impairment after focal brain lesions is better predicted by damage to structural than functional network hubs. 2021 , 118,		13
780	Graph Models of Pathology Spread in Alzheimer's Disease: An Alternative to Conventional Graph Theoretic Analysis. 2021 , 11, 799-814		2
779	Comparison of structural MRI brain measures between 1.5 and 3 T: Data from the Lothian Birth Cohort 1936. 2021 , 42, 3905-3921		2
778	Cortical ripples provide the conditions for consolidation during NREM sleep in humans.		2
777	White matter abnormalities associated with ADHD outcomes in adulthood. 2021,		4
776	Blood-based epigenome-wide analyses of cognitive abilities.		2
775	A causal role for the pulvinar in coordinating task-independent cortico-cortical interactions. 2021 , 529, 3772-3784		О
774	Application of Diffusion Weighted Imaging and Diffusion Tensor Imaging in the Pretreatment and Post-treatment of Brain Tumor. 2021 , 59, 335-347		1
773	Limbic and Executive Meso- and Nigrostriatal Tracts Predict Impulsivity Differences in Attention-Deficit/Hyperactivity Disorder. 2021 ,		1
772	Diffusion Magnetic Resonance Imaging-Based Biomarkers for Neurodegenerative Diseases. 2021 , 22,		4
771	Structural alterations in cortical and thalamocortical white matter tracts after recovery from prefrontal cortex lesions in macaques. <i>NeuroImage</i> , 2021 , 232, 117919	7.9	1
770	Effects of amyloid pathology and the APOE \$\tilde{\mu}\$4 allele on the association between cerebrospinal fluid AB8 and AB0 and brain morphology in cognitively normal 70-years-olds. 2021 , 101, 1-12		O

769	Localization and Identification of Brain Microstructural Abnormalities in Paediatric Concussion. 2021 , 15, 657374	1
768	Diffusion-Weighted Imaging of Intelligence. 2021 , 191-209	O
767	Ventral Intermediate Nucleus structural connectivity-derived segmentation: anatomical reliability and variability.	
766	Single-participant structural similarity matrices lead to greater accuracy in classification of participants than function in autism in MRI. 2021 , 12, 34	4
765	Neuroimaging Methods and Findings. 2021 , 189-324	
764	Diffusion Tensor Imaging: A Promising New Technique for Accurate Identification of the Stria Medullaris and Habenula. 2021 , 14, 1-7	
763	Comparison of multiple tractography methods for reconstruction of the retinogeniculate visual pathway using diffusion MRI. 2021 , 42, 3887-3904	4
762	Topological Aberrance of Structural Brain Network Provides Quantitative Substrates of Post-Traumatic Brain Injury Attention Deficits in Children. 2021 , 11, 651-662	3
761	Impaired Structural Connectivity in Parkinson's Disease Patients with Mild Cognitive Impairment: A Study Based on Probabilistic Tractography. 2021 , 11, 380-392	2
760	Developmental Topographical Disorientation With Concurrent Face Recognition Deficit: A Case Report. 2021 , 12, 654071	1
759	The Digital Brain Bank, an open access platform for post-mortem datasets.	2
75 ⁸	Perturbation of resting-state network nodes preferentially propagates to structurally rather than functionally connected regions. 2021 , 11, 12458	1
757	Meditation-induced effects on whole-brain structural and effective connectivity.	1
756	Human cortical areas are sparsely connected: Combining histology with diffusion MRI to estimate the absolute number of axons.	1
755	Parcellation of the Hippocampus According to Its Connection Probability with Prefrontal Cortex Subdivisions in a Malaysian Malay Population: Preliminary Findings. 2021 , 28, 65-76	1
754	Structural Differences Between Healthy Subjects and Patients With Schizophrenia or Schizoaffective Disorder: A Graph and Control Theoretical Perspective. 2021 , 12, 669783	O
753	Fiber orientation distribution from diffusion MRI: Effects of inaccurate response function calibration. 2021 , 31, 1082-1098	O
752	Prevalence of white matter pathways coming into a single diffusion MRI voxel orientation: the bottleneck issue in tractography.	O

751	A Progressive Approach for Uncertainty Visualization in Diffusion Tensor Imaging. 2021 , 40, 411-422		1
750	Uncertainty-aware Visualization in Medical Imaging - A Survey. 2021 , 40, 665-689		3
749	The Association Between Poor Sleep and Accelerated Brain Ageing.		
748	Structural connectivity changes in the cerebral pain matrix in burning mouth syndrome: a multi-shell, multi-tissue-constrained spherical deconvolution model analysis. 2021 , 63, 2005-2012		O
747	The Forget-Me-Not dHCP study: 7 Tesla high resolution diffusion imaging in the unfixed post-mortem neonatal brain.		2
746	Using diffusion MRI data acquired with ultra-high gradients to improve tractography in routine-quality data.		1
745	Reduced frontal white matter microstructure in healthy older adults with low tactile recognition performance. 2021 , 11, 11689		Ο
744	Biological constraints on neural network models of cognitive function. 2021 , 22, 488-502		12
743	Deterioration of the Corticobulbar Tract in Older Dysphagic Patients Without Neurologic Diseases 2022 , 101, 353-357		О
742	Comparison of corticospinal tract integrity measures extracted from standard versus native space in chronic stroke. 2021 , 359, 109216		1
741	Diffusion magnetic resonance imaging data: development of methods and tools for diagnosis and treatment of brain diseases. 2021 , 20, 191-201		
740	Structural Neuroplasticity Following Cognitive Behavioral Therapy for the Treatment of Chronic Musculoskeletal Pain: A Randomized Controlled Trial with Secondary MRI Outcomes.		
739	Empty Sella Syndrome as a Window Into the Neuroprotective Effects of Prolactin. 2021, 8, 680602		O
738	White Matter Microstructural Differences in Youth With Classical Congenital Adrenal Hyperplasia. 2021 , 106, 3196-3212		1
737	Longitudinal diffusion MRI analysis using Segis-Net: A single-step deep-learning framework for simultaneous segmentation and registration. <i>NeuroImage</i> , 2021 , 235, 118004	7.9	3
736	Quantifying myelin in crossing fibers using diffusion-prepared phase imaging: Theory and simulations. 2021 , 86, 2618-2634		1
735	Structural connectivity-based segmentation of the human entorhinal cortex.		0
734	Inflammatory markers and tract-based structural connectomics in older adults with a preliminary exploration of associations by race. 2021 , 1		

733	Perturbations in dynamical models of whole-brain activity dissociate between the level and stability of consciousness. 2021 , 17, e1009139	8
732	Nonequilibrium brain dynamics as a signature of consciousness. 2021 , 104, 014411	2
731	Diffusion MRI data, sulcal anatomy, and tractography for eight species from the Primate Brain Bank. 2021 , 226, 2497-2509	6
730	Morphological, Structural, and Functional Networks Highlight the Role of the Cortical-Subcortical Circuit in Individuals With Subjective Cognitive Decline. 2021 , 13, 688113	3
729	Diffusion MRI tractography for neurosurgery: the basics, current state, technical reliability and challenges. 2021 , 66,	5
728	BAI-Net: Individualized Human Cerebral Cartography using Graph Convolutional Network.	1
727	Exploring brain connectivity changes in major depressive disorder using functional-structural data fusion: A CAN-BIND-1 study. 2021 , 42, 4940-4957	3
726	Structural and functional network-level reorganization in the coding of auditory motion directions and sound source locations in the absence of vision.	1
725	White matter changes in the trigeminal spinal tract in chronic migraineurs: an ex vivo study combining ultra-high-field diffusion tensor imaging and polarized light imaging microscopy. 2021 ,	1
724	Aberrant cortico-thalamic structural connectivity in premature-born adults. 2021 , 141, 347-362	2
723	Structural Connectivity Patterns of Side Effects Induced by Subthalamic Deep Brain Stimulation for Parkinson's Disease. 2021 ,	1
722	An Age-Specific Atlas for Delineation of White Matter Pathways in Children Aged 6-8 Years. 2021 ,	1
721	The Social Cerebellum: A Large-Scale Investigation of Functional and Structural Specificity and Connectivity. 2021 ,	4
720	Local and distant responses to single pulse electrical stimulation reflect different forms of connectivity. <i>NeuroImage</i> , 2021 , 237, 118094	4
719	Alterations in brain structure and function in patients with osteonecrosis of the femoral head: a multimodal MRI study. 2021 , 9, e11759	0
718	Track-to-Learn: A general framework for tractography with deep reinforcement learning. 2021 , 72, 102093	O
717	Disconnectome of the migraine brain: a "connectopathy" model. 2021 , 22, 102	2
716	A machine learning-based method for estimating the number and orientations of major fascicles in diffusion-weighted magnetic resonance imaging. 2021 , 72, 102129	4

7 ¹ 5	Contributions of Brain Function and Structure to Three Different Domains of Cognitive Control in Normal Aging. 2021 , 1-22	3
714	Soma and Neurite Density MRI (SANDI) of the in-vivo mouse brain.	Ο
713	A large-scale structural and functional connectome of social mentalizing. <i>NeuroImage</i> , 2021 , 236, 11811 5 .9	3
712	Childhood exercise predicts response inhibition in later life via changes in brain connectivity and structure. <i>NeuroImage</i> , 2021 , 237, 118196 7.9	4
711	Minimal specifications for non-human primate MRI: Challenges in standardizing and harmonizing data collection. <i>NeuroImage</i> , 2021 , 236, 118082	6
710	Functional redundancy of the premotor network in hemispherotomy patients. 2021 , 8, 1796-1808	O
709	Diffusion tensor-based analysis of white matter in the healthy aging canine brain. 2021, 105, 129-136	Ο
708	Topographic Evolution of Anterior Cerebral Artery Infarction and Its Impact on Motor Impairment. 2021 , 1-11	
707	Temporo-cerebellar connectivity underlies timing constraints in audition. 2021 , 10,	2
706	Age-dependent relationship of cardiorespiratory fitness and white matter integrity. 2021, 105, 48-56	О
705	Population-Average Brain Templates and Application to Automated Voxel-Wise Analysis Pipelines for Cynomolgus Macaque. 2021 , 1	
704	A critical review of connectome validation studies. 2021 , 34, e4605	2
703	Mapping brain-wide excitatory projectome of primate prefrontal cortex at submicron resolution: relevance to diffusion tractography.	
702	Karawun: assisting evaluation of advances in multimodal imaging for neurosurgical planning and intraoperative neuronavigation.	1
701	Connectivity gradients on tractography data: Pipeline and example applications. 2021, 42, 5827-5845	1
700	A connectomic analysis of deep brain stimulation for treatment-resistant depression. 2021 , 14, 1226-1233	2
699	Cortical Morphology and White Matter Tractography of Three Phylogenetically Distant Primates: Evidence for a Simian Elaboration. 2021 ,	2
698	Overconnectivity of the right Heschl's and inferior temporal gyrus correlates with symptom severity in preschoolers with autism spectrum disorder. 2021 , 14, 2314-2329	2

697 Aging of the Nigrostriatal Tract in the Human Brain: A Diffusion Tensor Imaging Study. **2021**, 57,

696	Isolating the white matter circuitry of the dorsal language stream: Connectome-Symptom Mapping in stroke induced aphasia. 2021 , 42, 5689-5702		3
695	Disrupted structural connectome and neurocognitive functions in Duchenne muscular dystrophy: classifying and subtyping based on Dp140 dystrophin isoform. 2021 , 1		О
694	Frontal cortical regions associated with attention connect more strongly to central than peripheral V1. <i>NeuroImage</i> , 2021 , 238, 118246	7.9	2
693	Atypical age-related changes in the structure of the mentalizing network in children with refractory focal epilepsy. 2021 , 175, 106701		О
692	Disruptions in white matter microstructure associated with impaired visual associative memory in schizophrenia-spectrum illness. 2021 , 1		O
691	Independent contributions of structural and functional connectivity: Evidence from a stroke model 2021 , 5, 911-928		O
690	Optimization of epilepsy surgery through virtual resections on individual structural brain networks. 2021 , 11, 19025		2
689	Using connectomics for predictive assessment of brain parcellations. <i>NeuroImage</i> , 2021 , 238, 118170	7.9	4
688	Impact of Locus Coeruleus and Its Projections on Memory and Aging. 2021,		1
687	Loss of consciousness reduces the stability of brain hubs and the heterogeneity of brain dynamics. 2021 , 4, 1037		2
686	MESMERISED: Super-accelerating T relaxometry and diffusion MRI with STEAM at 7 T for quantitative multi-contrast and diffusion imaging. <i>NeuroImage</i> , 2021 , 239, 118285	7.9	2
685	Small variation in dynamic functional connectivity in cerebellar networks. 2021, 461, 751-761		O
684	Current and Future Challenges of Functional MRI and Diffusion Tractography in the Surgical Setting: From Eloquent Brain Mapping to Neural Plasticity. 2021 , 42, 474-489		2
683	Diffusion MRI and anatomic tracing in the same brain reveal common failure modes of tractography. <i>NeuroImage</i> , 2021 , 239, 118300	7.9	17
682	Scan-rescan repeatability of axonal imaging metrics using high-gradient diffusion MRI and statistical implications for study design. <i>NeuroImage</i> , 2021 , 240, 118323	7.9	4
681	Neurite density and arborization is associated with reading skill and phonological processing in children. <i>NeuroImage</i> , 2021 , 241, 118426	7.9	3
680	Microstructural properties within the amygdala and affiliated white matter tracts across adolescence. <i>NeuroImage</i> , 2021 , 243, 118489	7.9	2

679	Fixel-based Analysis of Diffusion MRI: Methods, Applications, Challenges and Opportunities. NeuroImage, 2021, 241, 118417	.9	17
678	Deep sr-DDL: Deep structurally regularized dynamic dictionary learning to integrate multimodal and dynamic functional connectomics data for multidimensional clinical characterizations. 7 NeuroImage, 2021, 241, 118388	.9	2
677	The specificity of thalamic alterations in Korsakoff's syndrome: Implications for the study of amnesia. 2021 , 130, 292-300		1
676	Ventral intermediate nucleus structural connectivity-derived segmentation: anatomical reliability and variability. <i>NeuroImage</i> , 2021 , 243, 118519	.9	1
675	Species and individual differences and connectional asymmetry of Broca's area in humans and macaques. <i>NeuroImage</i> , 2021 , 244, 118583	.9	О
674	Identifying brain regions supporting amygdalar functionality: Application of a novel graph theory technique. <i>Neurolmage</i> , 2021 , 244, 118614	.9	1
673	Fiber tractography-assisted deep brain stimulation surgery: Connectomics in the operating room. 2022 , 465-481		
672	Brain Imaging and Substance Use Disorders: Focus on White Matter Microstructural Integrity. 2022 , 652-6	73	, O
671	Increased structural connectivity of thalamic stimulation sites to motor cortex relates to tremor suppression. 2021 , 30, 102628		1
670	Uncertainty in the DTI Visualization Pipeline. 2021 , 125-148		Ο
669	Connectivity Patterns of Deep Brain Stimulation Targets in Patients with Gilles de la Tourette Syndrome. 2021 , 11,		3
668	White matter abnormalities in misophonia. 2021 , 32, 102787		2
667	Two cortical representations of voice control are differentially involved in speech fluency. 2021 , 3, fcaa23	2	3
666	Modulations of local synchrony over time lead to resting-state functional connectivity in a parsimonious large-scale brain model.		1
665	Transcranial Magnetic Stimulation and Aphasia Research. 679-699		1
664	Issues in Translating Imaging Technology and Presurgical Diffusion Tensor Imaging. 2011 , 731-765		2
663	Advanced Diffusion MR Tractography for Surgical Planning. 2014 , 183-194		1
662	Fuzzy Fibers: Uncertainty in dMRI Tractography. 2014 , 79-92		6

661	A Comparative Analysis of Cellular Morphological Differentiation Within the Cerebral Cortex Using Diffusion Tensor Imaging. 2011 , 329-351	8
660	DT-MRI Connectivity and/or Tractography?: Two New Algorithms. 2009 , 335-353	1
659	Measures of Tractography Convergence. 2019 , 295-307	1
658	Finite Element Modelling Framework for Electroconvulsive Therapy and Other Transcranial Stimulations. 2019 , 27-47	1
657	Integrating Heterogeneous Brain Networks for Predicting Brain Disease Conditions. 2019, 214-222	6
656	Entrack: A Data-Driven Maximum-Entropy Approach to Fiber Tractography. 2019 , 232-244	3
655	Multidimensional Neuroimaging Processing in ReCaS Datacenter. 2019 , 468-477	2
654	A Dynamical Clustering Model of Brain Connectivity Inspired by the -Body Problem. 2013 , 8159, 129-137	5
653	Tractography-Driven Groupwise Multi-scale Parcellation of the Cortex. 2015, 24, 600-12	15
652	Towards a Quantified Network Portrait of a Population. 2015 , 24, 650-61	2
651	Multi-Modal Visualization of Probabilistic Tractography. 2016 , 195-218	1
650	Sparse Bayesian Inference of White Matter Fiber Orientations from Compressed Multi-resolution Diffusion MRI. 2015 , 9349, 117-124	4
649	Reliability of Structural Connectivity Examined with Four Different Diffusion Reconstruction Methods at Two Different Spatial and Angular Resolutions. 2016 , 219-231	2
648	GraMPa: Graph-Based Multi-modal Parcellation of the Cortex Using Fusion Moves. 2016 , 148-156	6
647	Learning from Diffusion-Weighted Magnetic Resonance Images Using Graph Kernels. 2017, 39-48	1
646	Bayesian Heteroscedastic Regression for Diffusion Tensor Imaging. 2017 , 257-282	4
645	A Novel Anatomically-Constrained Global Tractography Approach to Monitor Sharp Turns in Gyri. 2017 , 532-539	2
644	A comparison of methods for recovering intra-voxel white matter fiber architecture from clinical diffusion imaging scans. 2008 , 11, 305-12	7

643	Neural tractography using an unscented Kalman filter. 2009 , 21, 126-38	24
642	Brain connectivity using geodesics in HARDI. 2009 , 12, 482-9	9
641	Probabilistic anatomical connectivity using completion fields. 2010 , 13, 566-73	2
640	Biomarkers for identifying first-episode schizophrenia patients using diffusion weighted imaging. 2010 , 13, 657-65	9
639	Multi-diffusion-tensor fitting via spherical deconvolution: a unifying framework. 2010 , 13, 674-81	24
638	ODF maxima extraction in spherical harmonic representation via analytical search space reduction. 2010 , 13, 84-91	5
637	Large deformation diffeomorphic metric mapping of orientation distribution functions. 2011 , 22, 448-62	9
636	A polynomial approach for maxima extraction and its application to tractography in HARDI. 2011 , 22, 723-34	3
635	Classification Study of DTI and HARDI Anisotropy Measures for HARDI Data Simplification. 2012, 229-251	2
634	Tractography via the ensemble average propagator in diffusion MRI. 2012 , 15, 339-46	2
633	Beyond crossing fibers: tractography exploiting sub-voxel fibre dispersion and neighbourhood structure. 2013 , 23, 402-13	15
632	Model selection and estimation of multi-compartment models in diffusion MRI with a Rician noise model. 2013 , 23, 644-55	3
631	Reliable selection of the number of fascicles in diffusion images by estimation of the generalization error. 2013 , 23, 742-53	12
630	Diffusion propagator estimation from sparse measurements in a tractography framework. 2013 , 16, 510-7	16
629	Higher-Order Tensors in Diffusion Imaging. 2014 , 129-161	6
628	Local striatal reward signals can be predicted from corticostriatal connectivity. <i>NeuroImage</i> , 2017 , 159, 9-17	10
627	Topographic organization of connections between prefrontal cortex and mediodorsal thalamus: Evidence for a general principle of indirect thalamic pathways between directly connected cortical 7.9 areas. <i>NeuroImage</i> , 2019 , 189, 832-846	16
626	Predicting reading ability from brain anatomy and function: From areas to connections. NeuroImage , 2020 , 218, 116966 7.9	2

625	Quantitative MRI outcomes in child and adolescent leukemia survivors: Evidence for global alterations in gray and white matter. 2020 , 28, 102428	5
624	Brain Network Analysis. 2019 ,	2
623	Reaction time variability and brain white matter integrity. 2019 , 33, 642-657	2
622	Neurosurgical applications of tractography in the UK. 2020 , 1-6	5
621	Individual Cortical Entropy Profile: Test-Retest Reliability, Predictive Power for Cognitive Ability, and Neuroanatomical Foundation. 2020 , 1, tgaa015	7
620	Brain imaging signature of neuropathic pain phenotypes in small-fiber neuropathy: altered thalamic connectome and its associations with skin nerve degeneration. 2021 , 162, 1387-1399	4
619	Advances in functional imaging of the human cerebellum. 2010 , 23, 382-7	49
618	Age differences in brain white matter microstructure in UK Biobank (N = 3,513).	2
617	Association of polygenic risk for major psychiatric illness with subcortical volumes and white matter integrity in UK Biobank.	1
616	Reconstruction of the Cortical Maps of the Tasmanian Tiger and Comparison to the Tasmanian Devil.	1
615	Consistent local dynamics in the brain across sessions are revealed by whole brain modeling of resting state activity.	2
614	Sex differences in the adult human brain: Evidence from 5,216 UK Biobank participants.	9
613	Image Processing and Quality Control for the first 10,000 Brain Imaging Datasets from UK Biobank.	6
612	White Matter and Social Cognition.	1
611	Structural covariance of brain region volumes is associated with both structural connectivity and transcriptomic similarity.	2
610	Distance to white matter trajectories is associated with treatment response to internal capsule deep brain stimulation in treatment-resistant depression.	1
609	PSA and VIM DBS efficiency in essential tremor depends on distance to the dentatorubrothalamic tract.	2
608	Topographic organization of the human subcortex unveiled with functional connectivity gradients.	15

607	A comprehensive atlas of white matter tracts in the chimpanzee.	2
606	Diffusion MRI of the Unfolded Hippocampus.	1
605	Improving emotional-action control by targeting long-range phase-amplitude neuronal coupling.	2
604	Altered Thalamocortical Connectivity in Six-Week Old Infants at High Familial Risk for Autism Spectrum Disorder.	1
603	Direct structural connections between auditory and visual motion selective regions in humans.	0
602	An Age-Specific Atlas for Delineation of White Matter Pathways in Children Aged 6-8 Years.	O
601	A whole-cortex probabilistic diffusion tractography connectome.	3
600	Perturbations in dynamical models of whole-brain activity dissociate between the level and stability of consciousness.	4
599	Neurofeedback fMRI in the motor system elicits bi-directional changes in activity and white-matter structure in the healthy adult human brain.	1
598	On stability of Canonical Correlation Analysis and Partial Least Squares with application to brain-behavior associations.	9
597	Comparison of multiple tractography methods for reconstruction of the retinogeniculate visual pathway using diffusion MRI.	1
596	A Large-Scale Structural and Functional Connectome of Social Mentalizing.	O
595	Causal explanation of individual differences in human sensorimotor memory formation.	1
594	Pulvinar influences parietal delay activity and information transmission between dorsal and ventral visual cortex in macaques.	1
593	Stability and sensitivity of structural connectomes: effect of thresholding and filtering and demonstration in neurodegeneration.	4
592	Joint modelling of diffusion MRI and microscopy.	2
591	Mapping the human subcortical auditory system using histology, post mortem MRI and in vivo MRI at 7T.	5
590	Hierarchy of connectivity-function relationship of the human cortex revealed through predicting activity across functional domains.	1

589	Towards HCP-Style Macaque Connectomes: 24-Channel 3T Multi-Array Coil, MRI Sequences and Preprocessing.	2
588	Tractostorm: Rater reproducibility assessment in tractography dissection of the pyramidal tract.	1
587	Cross-species cortical alignment identifies different types of neuroanatomical reorganization in the temporal lobe of higher primates.	5
586	The effect of network thresholding and weighting on structural brain networks in the UK Biobank.	2
585	A data-driven approach to optimising the encoding for multi-shell diffusion MRI with application to neonatal imaging.	1
584	Early life maturation of human visual system white matter is altered by monocular enucleation.	1
583	Effects of Inaccurate Response Function Calibration on Characteristics of the Fiber Orientation Distribution in Diffusion MRI.	2
582	XTRACT - Standardised protocols for automated tractography in the human and macaque brain.	3
581	Awake surgery between art and science. Part I: clinical and operative settings. 2013, 28, 205-21	11
580	Using deep learning for a diffusion-based segmentation of the dentate nucleus and its benefits over atlas-based methods. 2019 , 6, 044007	3
579	A Structural Connectivity Approach to Validate a Model-based Technique for the Segmentation of the Pulvinar Complex. 2018 , 10578,	4
578	Prediction of Behavioral Traits via Anatomical Connectivity Fingerprint. 2019,	O
577	Clinical utility of structural connectomics in predicting memory in temporal lobe epilepsy. 2020 , 94, e2424-e2	4365
576	Fiber tractography based on diffusion tensor imaging compared with high-angular-resolution diffusion imaging with compressed sensing: initial experience. 2013 , 72 Suppl 1, 165-75	36
575	A comprehensive atlas of white matter tracts in the chimpanzee. 2020 , 18, e3000971	11
574	Bayesian Estimation of Conditional Independence Graphs Improves Functional Connectivity Estimates. 2015 , 11, e1004534	13
573	Functional Connectivity's Degenerate View of Brain Computation. 2016, 12, e1005031	22
572	Integrating functional and diffusion magnetic resonance imaging for analysis of structure-function relationship in the human language network. 2009 , 4, e6660	51

(2016-2010)

571	Chimpanzee (Pan troglodytes) precentral corticospinal system asymmetry and handedness: a diffusion magnetic resonance imaging study. 2010 , 5, e12886	33
570	Target identification for stereotactic thalamotomy using diffusion tractography. 2012 , 7, e29969	26
569	Hemispheric asymmetry in white matter connectivity of the temporoparietal junction with the insula and prefrontal cortex. 2012 , 7, e35589	60
568	White matter differences between healthy young ApoE4 carriers and non-carriers identified with tractography and support vector machines. 2012 , 7, e36024	17
567	Parametric representation of multiple white matter fascicles from cube and sphere diffusion MRI. 2012 , 7, e48232	52
566	A brain network processing the age of faces. 2012 , 7, e49451	10
565	Cortico-cortical white matter motor pathway microstructure is related to psychomotor retardation in major depressive disorder. 2012 , 7, e52238	61
564	White matter deficits in psychopathic offenders and correlation with factor structure. 2013 , 8, e72375	37
563	Functional reorganization of the locomotor network in Parkinson patients with freezing of gait. 2014 , 9, e100291	134
562	Autism and sensory processing disorders: shared white matter disruption in sensory pathways but divergent connectivity in social-emotional pathways. 2014 , 9, e103038	67
561	Fractional anisotropy in corpus callosum is associated with facilitation of motor representation during ipsilateral hand movements. 2014 , 9, e104218	11
560	Obesity Associated Cerebral Gray and White Matter Alterations Are Interrelated in the Female Brain. 2014 , 9, e114206	9
559	Probabilistic MRI tractography of the optic radiation using constrained spherical deconvolution: a feasibility study. 2015 , 10, e0118948	21
558	Adaptation of brain functional and structural networks in aging. 2015 , 10, e0123462	20
557	Spherical Deconvolution of Multichannel Diffusion MRI Data with Non-Gaussian Noise Models and Spatial Regularization. 2015 , 10, e0138910	21
556	D-BRAIN: Anatomically Accurate Simulated Diffusion MRI Brain Data. 2016 , 11, e0149778	10
555	Longitudinal Changes in White Matter Tract Integrity across the Adult Lifespan and Its Relation to Cortical Thinning. 2016 , 11, e0156770	31
554	Striatum-Centered Fiber Connectivity Is Associated with the Personality Trait of Cooperativeness. 2016 , 11, e0162160	2

553	Multimodal MR-imaging reveals large-scale structural and functional connectivity changes in profound early blindness. 2017 , 12, e0173064	27
552	Creating and parameterizing patient-specific deep brain stimulation pathway-activation models using the hyperdirect pathway as an example. 2017 , 12, e0176132	61
551	Free water: A marker of age-related modifications of the cingulum white matter and its association with cognitive decline. 2020 , 15, e0242696	4
550	A significant risk factor for poststroke depression: the depression-related subnetwork. 2015 , 40, 259-68	24
549	Mapping Language Networks Using the Structural and Dynamic Brain Connectomes. 2017, 4,	24
548	White-Matter Pathways for Statistical Learning of Temporal Structures. 2018, 5,	2
547	Tract-Specific White Matter Correlates of Age-Related Reward Devaluation Deficits in Macaque Monkeys. 2018 , 3, 13-26	7
546	Assessment of optic nerve and optic tract alterations in patients with orbital space-occupying lesions using probabilistic diffusion tractography. 2019 , 12, 1304-1310	4
545	Examining Microstructural White Matter in Active Duty Soldiers with a History of Mild Traumatic Brain Injury and Traumatic Stress. 2017 , 11, 46-57	12
544	Fiber tractography of the optic radiations: impact of diffusion model, voxel shape and orientation. 2021 , 65, 494-502	1
543	Divergent network properties that predict early surgical failure versus late recurrence in temporal lobe epilepsy. 2019 , 132, 1324-1333	12
542	Tractography and the connectome in neurosurgical treatment of gliomas: the premise, the progress, and the potential. 2020 , 48, E6	33
541	Structure and function of complex brain networks. 2013 , 15, 247-62	442
540	Amiloride, fluoxetine or riluzole to reduce brain volume loss in secondary progressive multiple sclerosis: the MS-SMART four-arm RCT. 2020 , 7, 1-72	6
539	A Bayesian Constraint Stochastic Framework for DT-MRI White Matter Fiber Tractography. 2010 , 32, 1786-1791	1
538	The physical and biological basis of quantitative parameters derived from diffusion MRI. 2012 , 2, 254-65	95
537	Strengths and limitations of tractography methods to identify the optic radiation for epilepsy surgery. 2015 , 5, 288-99	23
536	Perspectives on the neural connectivity of the fornix in the human brain. 2014 , 9, 1434-6	12

535	Recovery of multiply injured ascending reticular activating systems in a stroke patient. 2017 , 12, 671-672	3
534	Structural neural connectivity of the vestibular nuclei in the human brain: a diffusion tensor imagingS study. 2018 , 13, 727-730	6
533	Improvement of ataxia in a patient with cerebellar infarction by recovery of injured cortico-ponto-cerebellar tract and dentato-rubro-thalamic tract: a diffusion tensor tractography study. 2019 , 14, 1470-1472	1
532	Traumatic axonal injury of the cingulum in patients with mild traumatic brain injury: a diffusion tensor tractography study. 2019 , 14, 1556-1561	9
531	Probabilistic tractography of the posterior subthalamic area in Parkinson⊠ disease patients. 2013 , 06, 381-390	8
530	Diffusion Tensor Imaging and Its Application to Traumatic Brain Injury: Basic Principles and Recent Advances. 2012 , 02, 137-161	7
529	Serum Neurofilament Light Chain Levels Are Related to Small Vessel Disease Burden. 2018, 20, 228-238	54
528	[16. Brain Mapping of Common Marmoset Using Ultra-high Magnetic Field MRI-from Structure to Function]. 2019 , 75, 555-561	1
527	Rapid short-term reorganization in the language network. 2017 , 6,	29
526	Whole brain comparative anatomy using connectivity blueprints. 2018 , 7,	75
526 525	Whole brain comparative anatomy using connectivity blueprints. 2018 , 7, An afferent white matter pathway from the pulvinar to the amygdala facilitates fear recognition. 2019 , 8,	75 43
	An afferent white matter pathway from the pulvinar to the amygdala facilitates fear recognition.	
525	An afferent white matter pathway from the pulvinar to the amygdala facilitates fear recognition. 2019 , 8, Preserved extrastriate visual network in a monkey with substantial, naturally occurring damage to	43
525 524	An afferent white matter pathway from the pulvinar to the amygdala facilitates fear recognition. 2019, 8, Preserved extrastriate visual network in a monkey with substantial, naturally occurring damage to primary visual cortex. 2019, 8, A connectional hub in the rostral anterior cingulate cortex links areas of emotion and cognitive	43
525 524 523	An afferent white matter pathway from the pulvinar to the amygdala facilitates fear recognition. 2019, 8, Preserved extrastriate visual network in a monkey with substantial, naturally occurring damage to primary visual cortex. 2019, 8, A connectional hub in the rostral anterior cingulate cortex links areas of emotion and cognitive control. 2019, 8, Dichotomous organization of amygdala/temporal-prefrontal bundles in both humans and monkeys.	43 11 39
5 ² 55 5 ² 4 5 ² 3 5 ² 22	An afferent white matter pathway from the pulvinar to the amygdala facilitates fear recognition. 2019, 8, Preserved extrastriate visual network in a monkey with substantial, naturally occurring damage to primary visual cortex. 2019, 8, A connectional hub in the rostral anterior cingulate cortex links areas of emotion and cognitive control. 2019, 8, Dichotomous organization of amygdala/temporal-prefrontal bundles in both humans and monkeys. 2019, 8, Mapping the human subcortical auditory system using histology, postmortem MRI and in vivo MRI	43 11 39 31
525 524 523 522 521	An afferent white matter pathway from the pulvinar to the amygdala facilitates fear recognition. 2019, 8, Preserved extrastriate visual network in a monkey with substantial, naturally occurring damage to primary visual cortex. 2019, 8, A connectional hub in the rostral anterior cingulate cortex links areas of emotion and cognitive control. 2019, 8, Dichotomous organization of amygdala/temporal-prefrontal bundles in both humans and monkeys. 2019, 8, Mapping the human subcortical auditory system using histology, postmortem MRI and in vivo MRI at 7T. 2019, 8, Amyloid and tau accumulate across distinct spatial networks and are differentially associated with	43 11 39 31 29

517	Short-term modulation of the lesioned language network. 2020 , 9,	11
516	Improving emotional-action control by targeting long-range phase-amplitude neuronal coupling. 2020 , 9,	11
515	Parcellating connectivity in spatial maps. 2015 , 3, e784	37
514	Use of probabilistic tractography to provide reliable distinction of the motor and sensory thalamus for prospective targeting during asleep deep brain stimulation. 2021 , 1-10	2
513	Mechanisms of Network Changes in Cognitive Impairment in Multiple Sclerosis. 2021 , 97, e1886-e1897	3
512	neurolib: A Simulation Framework for Whole-Brain Neural Mass Modeling. 1	3
511	Personalizing deep brain stimulation using advanced imaging sequences.	0
510	Effects of Piano Training in Unilateral Cerebral Palsy Using Probabilistic and Deterministic Tractography: A Case Report. 2021 , 15, 622082	1
509	Combination of structural and functional connectivity explains unique variation in specific domains of cognitive function	О
508	fMRI neurofeedback in the motor system elicits bidirectional changes in activity and in white matter structure in the adult human brain. 2021 , 37, 109890	O
507	The Wernicke conundrum revisited: evidence from connectome-based lesion-symptom mapping in post-stroke aphasia.	
506	Clinical applications of magnetic resonance imaging based functional and structural connectivity. NeuroImage, 2021 , 244, 118649 7.9	1
505	Denoising Intra-voxel Axon Fiber Orientations by Means of ECQMMF Method. 2009, 303-312	
504	De Gruyter. 2009 , 15,	
503	Integration of Measures of Functional and Structural MRI. 2009 , 785-809	
502	Two-tensor tractography using a constrained filter. 2009 , 12, 894-902	6
501	Diffusion MRI Tractography of Crossing Fibers by Cone-Beam ODF Regularization. 2009 , 412-421	
500	DTI Connectivity by Segmentation. 2010 , 200-210	O

499	Processing and Visualization of Diffusion MRI. 2010 , 403-424	1
498	Diffusion-Tensor Imaging and Behavioral Medicine. 2011 , 49-66	
497	Evaluating volumetric brain registration performance using structural connectivity information. 2011 , 14, 524-31	1
496	Probabilistic tractography using Q-ball modeling and particle filtering. 2011 , 14, 209-16	4
495	From Diffusion MRI to Brain Connectomics. 2013 , 193-234	2
494	Estimating constrained multi-fiber diffusion MR volumes by orientation clustering. 2013 , 16, 82-9	5
493	Adaptive multi-modal particle filtering for probabilistic white matter tractography. 2013, 23, 594-606	1
492	DTI and Tractography in the Autistic Brain. 2013 , 267-279	
491	Normalisation of neonatal brain network measures using stochastic approaches. 2013, 16, 574-81	2
490	Adaptively constrained convex optimization for accurate fiber orientation estimation with high order spherical harmonics. 2013 , 16, 485-92	5
489	Quantifying Brain Morphology Using Diffusion Imaging. 2013 , 41-84	
488	Noise Model Selection for Multichannel Diffusion-Weighted MRI. 2014 , 149-153	
487	Groupwise Registration for Correcting Subject Motion and Eddy Current Distortions in Diffusion MRI Using a PCA Based Dissimilarity Metric. 2014 , 163-174	2
486	Kernel-Based Morphometry of Diffusion Tensor Images. 2014 , 229-247	
485	Bilateral Filtering of Multiple Fiber Orientations in Diffusion MRI. 2014 , 193-202	
484	A Bayesian Approach to Distinguishing Interdigitated Muscles in the Tongue from Limited Diffusion Weighted Imaging. 2014 , 8677, 13-24	4
483	Non-Conventional MRI Techniques as an Alternative Role to the Clinical Diagnosis in Alzheimer Disease. 2014 , 06, 2712-2723	
482	Riemann-Finsler Multi-valued Geodesic Tractography for HARDI. 2014 , 209-225	O

White matter microstructure predicts focal and broad functional brain dedifferentiation in normal 481 aging. Introduction. **2015**, 1-14 480 Quantifying Microstructure in Fiber Crossings with Diffusional Kurtosis. 2015, 150-157 479 2 478 A Continuous Flow-Maximisation Approach to Connectivity-Driven Cortical Parcellation. 2015, 165-172 Spherical Ridgelets for Multi-Diffusion Tensor Refinement. 2015, 437-442 477 Symmetric Wiener Processes for Probabilistic Tractography and Connectivity Estimation. 2015, 53-60 476 Graph-based clinical diagnosis and prediction using multi-modal neuroimaging data. 2, e8835 475 The visual white matter: The application of diffusion MRI and fiber tractography to vision science. 474 Single or Multi-Frequency generators in on-going brain activity: a mechanistic whole-brain model of \circ 473 empirical MEG data. Transcriptional signatures of connectomic subregions of the human striatum. 472 Improved Reference Tracts for Unsupervised Brain White Matter Tractography. 2017, 425-435 471 1 Multi-way Regression Reveals Backbone of Macaque Structural Brain Connectivity in Longitudinal 470 Datasets. 2017, 424-432 469 Repeated Tractography of a Single Subject: How High Is the Variance?. 2017, 331-354 O Nerve Pathways with MR Tractography. 2017, 89-111 468 Fiber tractography using machine learning. 467 1 466 Anatomical and functional organization of the human substantia nigra and its connections.

white matter pathway.

Bayesian Optimisation of Large-Scale Biophysical Networks.

Heritable cognitive and psychopathology factors in youth are predicted by brain fronto-temporal

465

464

463	The Impact of In-Scanner Head Motion on Structural Connectivity Derived from Diffusion Tensor Imaging.	1
462	Structural network maturation of the preterm human brain.	
461	Applications of community detection techniques to brain graphs: Algorithmic considerations and implications for neural function.	1
460	On the Impact of Interhemispheric White Matter: Age, Executive Functioning, and Dedifferentiation in the Frontal Lobes.	
459	Disrupted brain structural connectivity in Pediatric Bipolar Disorder with psychosis.	
458	Characterisation of the Corticospinal Tract Using Diffusion Magnetic Resonance Imaging in Unilateral and Bilateral Cerebral Palsy Patients. 2018 , 25, 68-78	2
457	Probabilistic Tractography for Complex Fiber Orientations with Automatic Model Selection. 2018 , 117-128	
456	Consistency in predicting functions from anatomical and functional connectivity profiles across the cortical cortex.	Ο
455	Whole brain comparative anatomy using connectivity blueprints.	1
454	No Evidence for Systematic White Matter Correlates of Dyslexia and Dyscalculia.	
453	The spatial correspondence and genetic influence of inter-hemispheric connectivity with white matter microstructure.	
452	Exploring the limits of network topology estimation using diffusion-based tractography and tracer studies in the macaque cortex.	
451	Using GPUs to accelerate computational diffusion MRI: From microstructure estimation to tractography and connectomes.	1
450	Hierarchical Complexity of the Adult Human Structural Connectome.	
449	On the interpretation of tractography-based parcellations.	
448	Optimization of Energy State Transition Trajectory Supports the Development of Executive Function During Youth.	1
447	Spatial Gradient of Microstructural Changes in Normal-Appearing White Matter in Tracts Affected by White Matter Hyperintensities in Older Age.	
446	Diffusion Acceleration with Gaussian process Estimated Reconstruction (DAGER).	

445	Intact extrastriate visual network without primary visual cortex in a Rhesus macaque with naturally occurring Blindsight.	2
444	The Brain-Derived Neurotrophic Factor Val66Met Genotype Does Not Influence the Grey or White Matter Structures Underlying Recognition Memory.	
443	3D Structural Connectivity in Healthy Adults: Detecting Structural Connections and Their Underlying Substrates for Olfactory Saccadic Pathway.	
442	Cognitive and white-matter compartment models revealed the contribution of microstructural variability along sensorimotor tracts to simple reaction time.	
441	Olfactory Spatial Attention: Neural Structural Connectivity Revealed.	
440	Treatment related DTI changes in the posterior thalamic radiation in survivors of childhood posterior fossa tumors. 2018 ,	
439	Shrinkage Estimation on the Manifold of Symmetric Positive-Definite Matrices with Applications to Neuroimaging. 2019 , 566-578	1
438	Introduction. 2019 , 1-16	
437	Partial Synchronization in 2-Community Networks. 2019 , 95-114	
436	Re-Discovering the Squid Brain.	
436	Re-Discovering the Squid Brain. Locally Linear Embedding of Anatomical Connectivity for Classification. 2019, 103-122	
435	Locally Linear Embedding of Anatomical Connectivity for Classification. 2019 , 103-122	
435	Locally Linear Embedding of Anatomical Connectivity for Classification. 2019 , 103-122 White matter changes in the perforant path in patients with amyotrophic lateral sclerosis. Quantitative assessment of dMRI-based dentate-rubro-thalamic tractography in squirrel monkey.	1
435 434 433	Locally Linear Embedding of Anatomical Connectivity for Classification. 2019, 103-122 White matter changes in the perforant path in patients with amyotrophic lateral sclerosis. Quantitative assessment of dMRI-based dentate-rubro-thalamic tractography in squirrel monkey. 2019,	1 3
435 434 433 432	Locally Linear Embedding of Anatomical Connectivity for Classification. 2019, 103-122 White matter changes in the perforant path in patients with amyotrophic lateral sclerosis. Quantitative assessment of dMRI-based dentate-rubro-thalamic tractography in squirrel monkey. 2019, Two fiber pathways connecting amygdala and prefrontal cortex in humans and monkeys.	
435 434 433 432 431	Locally Linear Embedding of Anatomical Connectivity for Classification. 2019, 103-122 White matter changes in the perforant path in patients with amyotrophic lateral sclerosis. Quantitative assessment of dMRI-based dentate-rubro-thalamic tractography in squirrel monkey. 2019, Two fiber pathways connecting amygdala and prefrontal cortex in humans and monkeys. Human lateral Frontal Pole contributes to control over social-emotional action.	

Myelin development in visual scene-network tracts beyond late childhood: A multimethod 427 neuroimaging study. Skill acquisition increases myelination and strengthens functional connectivity in the sensorimotor 426 circuit of the adult rat. Stratifying major depressive disorder by polygenic risk for schizophrenia in relation to structural 425 brain measures. Comparison of CPU and GPU Bayesian Estimates of Fibre Orientations from Diffusion MRI. 424 Reduced frontal white matter microstructure in healthy older adults with low tactile recognition 423 performance. White matter microstructure in attention-deficit/hyperactivity disorder: a systematic tractography study in 654 individuals. Spatial versus angular resolution for tractography-assisted planning of deep brain stimulation. 421 420 Diffusion MRI free water is a sensitive marker of age-related changes in the cingulum. A causal role for pulvinar in coordinating task independent cortico-cortical interactions. 419 Functional and diffusion MRI reveal the functional and structural basis of infants[hoxious-evoked 418 brain activity. Microstructural integrity of the major nuclei of the thalamus in Parkinson disease. 417 MESMERISED: Super-accelerating T1 relaxometry and diffusion MRI with STEAM at 7 T for 416 quantitative multi-contrast and diffusion imaging. Structural alterations in the macaque frontoparietal white matter network after recovery from 415 prefrontal cortex lesions. Stick Stippling for Joint 3D Visualization of Diffusion MRI Fiber Orientations and Density. 414 Topological Aberrance of Structural Brain Network Provides Quantitative Markers of post-TBI 413 Attention Deficits in Children. A collaborative resource platform for non-human primate neuroimaging. 412 NOise Reduction with Distribution Corrected (NORDIC) PCA in dMRI with complex-valued 411 O parameter-free locally low-rank processing. An MRI protocol for anatomical and functional evaluation of the California sea lion brain. 410

409	Generalizing effects of frontostriatal structural connectivity on self-esteem using predictive modeling. 2021 , 146, 66-73	О
408	Altered thalamocortical structural connectivity in persons with schizophrenia and healthy siblings.	
407	Notes on Techniques. 2020 , 127-167	
406	Relating Response Inhibition, Brain Connectivity, and Freezing of Gait in People with Parkinson's Disease. 2021 , 27, 733-743	
405	Neuropredictome: a data-driven predictome for cognitive, psychiatric, medical, and lifestyle factors on the brain.	
404	Injury of Corticostriatal Tract between the Striatum and the Premotor Area in a Patient with Traumatic Brain Injury. 2020 , 32, 391-393	
403	Anatomically informed multi-level fiber tractography.	1
402	Network-Based Imaging and Connectomics. 2020, 73-91	
401	Missing the forest because of the trees: Slower alternations during binocular rivalry are associated with lower levels of visual detail during ongoing thought.	
400	An Examination of Psychomotor Disturbance in Current and Remitted MDD: An RDoC Study. 2020 , 5,	5
399	Intrinsic Connectivity Changes Mediate the Beneficial Effect of Cardiovascular Exercise on Sustained Visual Attention. 2020 , 1, tgaa075	1
398	A Deep-Generative Hybrid Model to Integrate Multimodal and Dynamic Connectivity for Predicting Spectrum-Level Deficits in Autism. 2020 , 437-447	1
397	Physical and Physiological Principles of Diffusion. 2020 , 457-476	0
396	Diffusion MRI Fiber Tractography by Flow Field Formation with Extended Physarum Solver: A Pilot Study with 2D Phantoms. 2020 , 183-192	
395	Frontostriatal Structural Connectivity and Striatal Glutamatergic Levels in Treatment-Resistant Schizophrenia: An Integrative Analysis of DTI and 1H-MRS. 2020 , 1,	2
394	Data augmentation based on dynamical systems for the classification of brain states.	o
393	Modeling Fiber Orientations Using Diffusion MRI. 2020 , 1, 509-532	
392	Diffusion MRI Fiber Tractography. 2020 , 1, 533-569	1

391	Novel Cost Function Definition for Minimum-Cost Tractography in MR Diffusion Tensor Imaging. 2020 , 1194, 135-150	
390	Enhanced Bidirectional Connectivity of the Subthalamo-pallidal Pathway in 6-OHDA-mouse Model of Parkinson's Disease Revealed by Probabilistic Tractography of Diffusion-weighted MRI at 9.4T. 2020 , 29, 80-92	1
389	Functional and resting-state characterizations of a periventricular heterotopic nodule associated with epileptogenic activity. 2020 , 48, E10	1
388	Structural connectomics: Where we are and where we should be?. 2021 , 41-63	
387	Non-Negative Data-Driven Mapping of Structural Connections in the Neonatal Brain.	
386	Brain mechanisms of pain and dysautonomia in diabetic neuropathy: connectivity changes in thalamus and hypothalamus. 2021 ,	O
385	Serum neurofilament light chain correlates with myelin and axonal magnetic resonance imaging markers in multiple sclerosis 2022 , 57, 103366	О
384	Life after mild traumatic brain injury: Widespread structural brain changes associated with psychological distress revealed with multimodal magnetic resonance imaging.	O
383	Brain-behavior investigation of potential cognitive markers of Alzheimer's disease in middle age: a multi-modal imaging study. 2021 , 1	О
382	Modelling white matter in gyral blades as a continuous vector field.	
381	Divergence-based framework for diffusion tensor clustering, interpolation, and regularization. 2007 , 20, 507-18	1
380	Differential effects of emotional valence on mnemonic performance with greater hippocampal maturity.	
379	Diffusion MRI Changes in the Healthy Aging Canine Brain.	
378	In vivo human whole-brain Connectom diffusion MRI dataset at 760 fh isotropic resolution.	O
377	Local and Distant responses to single pulse electrical stimulation reflect different forms of connectivity.	
376	A Pig White Matter Atlas and Common Connectivity Space Provide a Roadmap for the Introduction of a New Animal Model in Translational Neuroscience.	1
375	Multimodal imaging brain markers in early adolescence are linked with a physically active lifestyle.	
374	Two cortical representations of voice control are differentially involved in speech fluency.	

373	Frontal cortical regions associated with attention connect more strongly to central than peripheral V1.	
372	Dorsal-to-ventral imbalance in the superior longitudinal fasciculus mediates methylphenidate⊠ effect on beta oscillations in ADHD.	
371	DIffusion-Prepared Phase Imaging (DIPPI): quantifying myelin in crossing fibres.	О
370	Concurrent anatomical, physiological and network changes in cognitively impaired multiple sclerosis patients.	1
369	Empty sella syndrome as a window into the neuroprotective effects of prolactin.	
368	DTI Tractography Metrics. 2020 , 109-116	
367	Reproducibility of connectivity based parcellation: primary visual cortex. 2013, 2089	1
366	White matter structure assessment from reduced HARDI data using low-rank polynomial approximations. 2012 , 15, 186-197	1
365	Diffusion tensor imaging fiber tracking with reliable tracking orientation and flexible step size. 2013 , 8, 1481-90	1
364	Improvement of white matter and functional connectivity abnormalities by repetitive transcranial magnetic stimulation in crossed aphasia in dextral. 2014 , 7, 3659-68	4
363	Deconvolution of High Dimensional Mixtures via Boosting, with Application to Diffusion-Weighted MRI of Human Brain. 2014 , 27, 2699-2707	1
362	Comparative Evaluation for Brain Structural Connectivity Approaches: Towards Integrative Neuroinformatics Tool for Epilepsy Clinical Research. 2016 , 2016, 446-54	1
361	Disrupted Eye Gaze Perception as a Biobehavioral Marker of Social Dysfunction: An RDoC Investigation. 2020 , 5,	1
3 60	Early life factors and white matter microstructure in children with overweight and obesity: The ActiveBrains project. 2021 , 41, 40-48	O
359	The human raphe-hippocampal tract and affective sensitivity: a probabilistic tractography study. 2021 , 1	
358	Structural brain connectivity predicts acute pain after mild traumatic brain injury.	
357	CHIASM, the human brain albinism and achiasma MRI dataset. 2021 , 8, 308	1
356	mrHARDIflow: A pipeline tailored for the preprocessing and analysis of Multi-Resolution High Angular diffusion MRI and its application to a variability study of the PRIME-DE database.	

355	Multi-band- and in-plane-accelerated diffusion MRI enabled by model-based deep learning in q-space and its extension to learning in the spherical harmonic domain. 2021 ,		О
354	Widespread effects of dMRI data quality on diffusion measures in children. 2021,		3
353	Opposing white matter microstructure abnormalities in 22q11.2 deletion and duplication carriers. 2021 , 11, 580		О
352	An MRI Method for Parcellating the Human Striatum into Matrix and Striosome Compartments In Vivo. <i>NeuroImage</i> , 2021 , 118714	7.9	1
351	Relationship between Dizziness and the Core Vestibular Projection Injury in Patients with Mild Traumatic Brain Injury. 2021 , 11,		2
350	Subiculum IBNST Structural Connectivity in Humans and Macaques.		
349	The effect of external stimulation on functional networks in the aging healthy human brain.		О
348	Functional Topography of the Human Subthalamic Nucleus: Relevance for Subthalamotomy in Parkinson's Disease. 2021 ,		3
347	Structural connectivity-based segmentation of the human entorhinal cortex. <i>NeuroImage</i> , 2021 , 245, 118723	'.9	2
346	Differential structure-function network coupling in the inattentive and combined types of attention deficit hyperactivity disorder. 2021 , 16, e0260295		О
345	A Taxonomy of the Brain's White Matter: Twenty-One Major Tracts for the 21st Century 2022,		3
344	The diffusion MRI connectome. 2021 , 4, 295-308		
343	Prolonged release of VEGF and Ang1 from intralesionally implanted hydrogel promotes perilesional vascularization and functional recovery after experimental ischemic stroke 2022 , 271678X2	1106	9927
342	General additive models address statistical issues in diffusion MRI: An example with clinically anxious adolescents 2022 , 33, 102937		O
341	Impact of white-matter mask selection on DTI histogram-based metrics as potential biomarkers in cerebral small vessel disease 2022 , 1		
340	White matter connectivity between structures of the basal ganglia using 3T and 7T 2021 , 483, 32-32		
339	Lesion correlates of auditory sentence comprehension deficits in post-stroke aphasia 2022, 2, None		О
338	The human mediodorsal thalamus: Organization, connectivity, and function <i>NeuroImage</i> , 2022 , 249, 118876	7.9	O

337	Using MRI to determine anatomic differences of the lateral geniculate nucleus in subjects with dyslexia. 2021 ,		
336	Potential Pitfalls of Using Fractional Anisotropy, Axial Diffusivity, and Radial Diffusivity as Biomarkers of Cerebral White Matter Microstructure 2021 , 15, 799576		1
335	Spatiotemporal Patterns of Adaptation-Induced Slow Oscillations in a Whole-Brain Model of Slow-Wave Sleep 2021 , 15, 800101		O
334	Maladaptive motor cortical excitability and connectivity in polyneuropathy with neuropathic pain 2022 ,		O
333	A Randomized Trial Directly Comparing Ventral Capsule and Anteromedial Subthalamic Nucleus Stimulation in Obsessive-Compulsive Disorder: Clinical and Imaging Evidence for Dissociable Effects. 2022 , 20, 160-169		0
332	Deciphering the Network Effects of Deep Brain Stimulation in Parkinson's Disease 2022 , 11, 265		O
331	White matter tract transcranial ultrasound stimulation, a computational study 2021, 140, 105094		O
330	Linking Multi-Modal MRI to Clinical Measures of Visual Field Loss After Stroke 2021 , 15, 737215		O
329	Cerebrospinal Fluid Biomarkers, Brain Structural and Cognitive Performances Between Normotensive and Hypertensive Controlled, Uncontrolled and Untreated 70-Year-Old Adults 2021 , 13, 777475		О
328	Hebbian activity-dependent plasticity in white matter.		
327	Blood-based epigenome-wide analyses of cognitive abilities 2022 , 23, 26		1
326	Prediction of Communication Impairment in Children With Bilateral Cerebral Palsy Using Multivariate Lesion- and Connectome-Based Approaches: Protocol for a Multicenter Prospective Cohort Study 2022 , 16, 788037		
325	Tai Chi Improves Brain Functional Connectivity and Plasma Lysophosphatidylcholines in Postmenopausal Women With Knee Osteoarthritis: An Exploratory Pilot Study 2021 , 8, 775344		O
324	Advances in Pediatric MRI. 2022 , 773-791		
323	Cortical development coupling between surface area and sulcal depth on macaque brains 2022 , 227, 1013		О
322	Resolution and b value dependent Structural Connectome in ex vivo Mouse Brain.		O
321	Cingulum bundle connectivity in treatment-refractory compared to treatment-responsive patients with bipolar disorder and healthy controls: a tractography and surgical targeting analysis 2022 , 1-13		
320	Quantitative mapping of the brain's structural connectivity using diffusion MRI tractography: a review <i>NeuroImage</i> , 2021 , 249, 118870	7.9	11

319	Mapping Frontostriatal White Matter Tracts and their Association with Reward-Related Ventral Striatum Activation in Adolescence 2022 , 1780, 147803	О
318	Evaluation of Structural Neural Connectivity Between the Primary Auditory Cortex and Cognition-Related Brain Areas Using Diffusion Tensor Tractography in 43 Normal Adults 2022 , 28, e936131	
317	The fornix supports episodic memory during childhood 2022,	2
316	White matter microstructure in children and adolescents with ADHD 2022 , 33, 102957	3
315	Deficits of Neurotransmitter Systems and Altered Brain Connectivity in Major Depression: A Translational Neuroscience Perspective. 2022 , 311-324	
314	The changes in white matter pathways that occur in acute sports-related mild Traumatic Brain Injury.	
313	Intrinsic Structural Connectivity of the Default Mode Network and Behavioral Correlates of Executive Function and Social Skills in Youth with Autism Spectrum Disorders 2022 , 1	О
312	Abnormal Anatomical and Functional Connectivity of the Thalamo-sensorimotor Circuit in Chronic Low Back Pain: Resting-state Functional Magnetic Resonance Imaging and Diffusion Tensor Imaging Study 2022 ,	О
311	Anatomical connectivity profile development constrains medial-lateral topography in the dorsal prefrontal cortex.	О
310	Structural connectivity associated with the sense of body ownership: a diffusion tensor imaging and disconnection study in patients with bodily awareness disorder 2022 , 4, fcac032	О
309	The structure of the superior and inferior parietal lobes predicts inter-individual suitability for virtual reality. 2021 , 11, 23688	1
308	A tractometry principal component analysis of white matter tract network structure and relationships with cognitive function in relapsing-remitting multiple sclerosis 2022 , 34, 102995	
307	Dorsal-to-ventral imbalance in the superior longitudinal fasciculus mediates methylphenidate's effect on beta oscillations in ADHD 2022 , e14008	2
306	A Review of Studies on the Role of Diffusion Tensor Magnetic Resonance Imaging Tractography in the Evaluation of the Fronto-Subcortical Circuit in Patients with Akinetic Mutism 2022 , 28, e936251	
305	Tract-specific statistics based on diffusion-weighted probabilistic tractography 2022, 5, 138	
304	Biophysical compartment models for single-shell diffusion MRI in the human brain: a model fitting comparison 2021 ,	
303	Constraining Functional Coactivation with a Cluster-based Structural Connectivity Network. 1-55	0
302	Differential Diagnosis of Akinetic Mutism and Disorder of Consciousness Using Diffusion Tensor Tractography: A Case Report 2022 , 16, 778347	

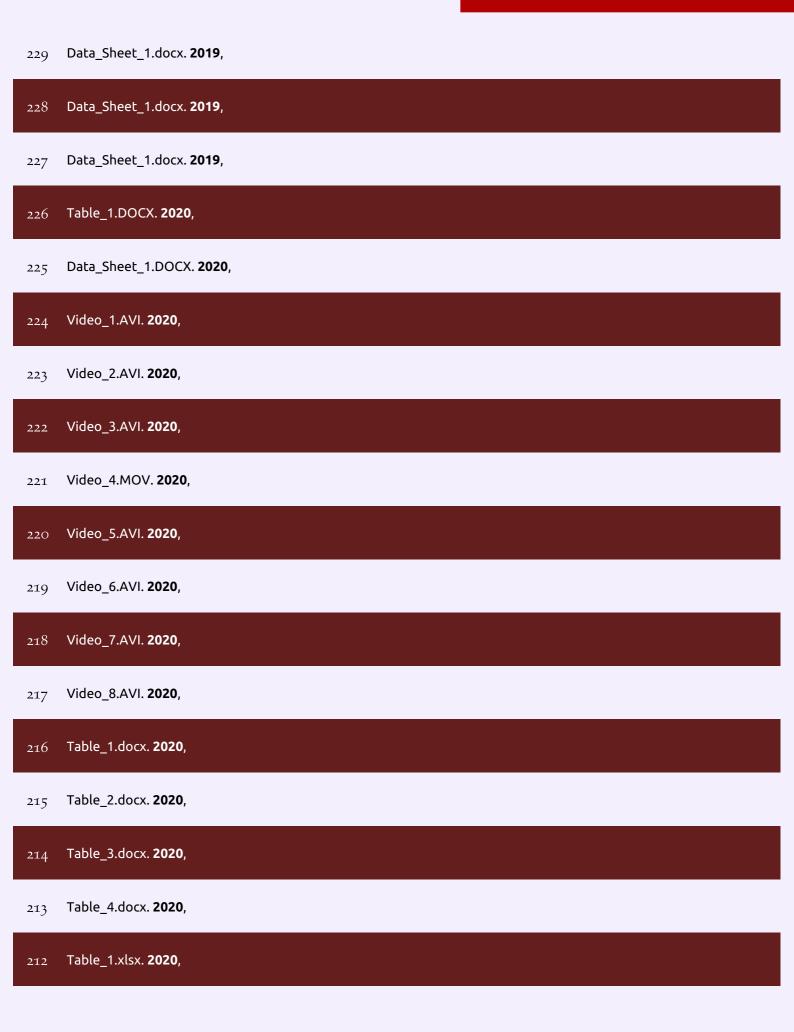
301	Multimodal Brain Connectomics-Based Prediction of Parkinson's Disease Using Graph Attention Networks 2021 , 15, 741489	1
300	Structural insight into the individual variability architecture of the functional brain connectome.	O
299	Flattened Structural Network Changes and Association of Hyperconnectivity With Symptom Severity in 2-7-Year-Old Children With Autism 2021 , 15, 757838	
298	Multimodal neuroimaging correlates of physical-cognitive covariation in Chilean adolescents. The Cogni-Action Project.	
297	The impact of levamisole and alcohol on white matter microstructure in adult chronic cocaine users 2022 , 27, e13149	O
296	The Digital Brain Bank, an open access platform for post-mortem datasets 2022, 11,	1
295	A novel method for estimating connectivity-based parcellation of the human brain from diffusion MRI: Application to an aging cohort 2022 ,	0
294	Concurrent mapping of brain ontogeny and phylogeny within a common connectivity space.	1
293	Inferring excitation-inhibition dynamics using a maximum entropy model unifying brain structure and function. 1-25	О
292	Life after mild traumatic brain injury: Widespread structural brain changes associated with psychological distress revealed with multimodal magnetic resonance imaging. 2022 ,	O
291	Uncovering Cortical Units of Processing From Multi-Layered Connectomes 2022 , 16, 836259	
290	Combining Regional and Connectivity Metrics of Functional Magnetic Resonance Imaging and Diffusion Tensor Imaging for Individualized Prediction of Pain Sensitivity 2022 , 15, 844146	
289	Integrated Diffusion Image Operator (iDIO): A tool for automated configuration and processing of diffusion MRI data.	
288	A novel male Japanese quail structural connectivity atlas using ultra-high field diffusion MRI at 11.7 T 2022, 1	O
287	Structural architecture and brain network efficiency links polygenic scores to intelligence.	О
286	Functional and structural brain network correlates of visual hallucinations in Lewy body dementia 2022 ,	O
285	Electrophysiological abnormalities as indicators of early-stage pathology in Primary Progressive Aphasia (PPA): A case study in semantic variant PPA 2022 , 1-13	
284	The effect of external stimulation on functional networks in the aging healthy human brain 2022,	O

283	Right fronto-parietal networks mediate the neurocognitive benefits of enriched environments 2022 , 4, fcac080		
282	Subjective cognitive decline predicts lower cingulo-opercular network functional connectivity in individuals with lower neurite density in the forceps minor.		
281	Deep brain stimulation of the "medial forebrain bundle": sustained efficacy of antidepressant effect over years 2022 ,		О
280	Mesolimbic Neurobehavioral Mechanisms of Reward Motivation in Anorexia Nervosa: A Multimodal Imaging Study 2022 , 13, 806327		1
279	Brain Network Connectivity and Executive Function in Children with Previous Infantile Hydrocephalus 2022 ,		О
278	Neuroplasticity in Motor Learning Under Variable and Constant Practice Conditions-Protocol of Randomized Controlled Trial 2022 , 16, 773730		O
277	Structural connectivity gradient associated with a dichotomy reveals the topographic organization of the macaque insular cortex.		О
276	Complex negative emotions induced by electrical stimulation of the human hypothalamus 2022,		O
275	Aberrant Inter-hemispheric Connectivity in Patients With Recurrent Major Depressive Disorder: A Multimodal MRI Study 2022 , 13, 852330		О
274	Directional DBS of the Fornix in Alzheimer's Disease Achieves Long-Term Benefits: A Case Report 2022 , 14, 809972		
273	Quantitative Structural Brain Magnetic Resonance Imaging Analyses: Methodological Overview and Application to Rett Syndrome 2022 , 16, 835964		О
272	Impaired brain network architecture as neuroimaging evidence of pain in diabetic neuropathy 2022 , 109833		О
271	Bilingual experience affects white matter integrity across the lifespan 2022, 169, 108191		О
270	Imaging versus electrographic connectivity in human mood-related fronto-temporal networks 2022 ,		О
269	Structure-function coupling within the reward network in preschool children predicts executive functioning in later childhood 2022 , 55, 101107		
268	The association between inadequate sleep and accelerated brain ageing 2022, 114, 1-14		О
267	Subiculum-BNST structural connectivity in humans and macaques NeuroImage, 2022, 253, 119096	7.9	
266	Soma and Neurite Density MRI (SANDI) of the in-vivo mouse brain and comparison with the Allen Brain Atlas <i>NeuroImage</i> , 2022 , 254, 119135	7.9	O

265	Accuracy and Reliability of Diffusion Imaging Models NeuroImage, 2022, 119138	7.9	О
264	A populational connection distribution map for the whole brain white matter reveals ordered cortical wiring in the space of white matter <i>NeuroImage</i> , 2022 , 119167	7.9	O
263	Fiber tracing and microstructural characterization among audiovisual integration brain regions in neonates compared with young adults <i>NeuroImage</i> , 2022 , 119141	7.9	О
262	Connectivity-based thalamus parcellation and surgical targeting of somatosensory subnuclei. 2021 , 1-8	:	
261	Investigating the Relationship between White Matter Connectivity and Motivational Circuits in Subjects with Deficit Schizophrenia: A Diffusion Tensor Imaging (DTI) Study 2021 , 11,		1
260	Deterministic Tractography Analysis of Rat Brain Using SIGMA Atlas in 9.4T MRI 2021 , 11,		O
259	Lesion Distribution and Early Changes of Right Hemisphere in Chinese Patients With Post-stroke Aphasia 2021 , 13, 632217		0
258	Disruption in structural-functional network repertoire and time-resolved subcortical-frontoparietal connectivity in disorders of consciousness.		1
257	White matter connectivity alterations in patients with MRI negative temporal lobe epilepsy using hippocampus specific tractography. 2021 ,		
256	Tracking the Corticospinal Tract in Patients With High-Grade Glioma: Clinical Evaluation of Multi-Level Fiber Tracking and Comparison to Conventional Deterministic Approaches 2021 , 11, 76110	59	3
255	A tractometry investigation of white matter tract network structure and relationships with cognitive function in relapsing-remitting multiple sclerosis.		
254	Differential Developmental Associations of Material Hardship Exposure and Adolescent Amygdala-Prefrontal Cortex White Matter Connectivity 2021 , 1-26		O
253	Prevalence of white matter pathways coming into a single white matter voxel orientation: The bottleneck issue in tractography 2021 ,		2
252	A large-scale diffusion imaging study of tinnitus and hearing loss. 2021 , 11, 23395		1
251	Lateral Prefrontal Cortex Is a Hub for Music Production from Structural Rules to Movements 2021,		О
250	Language recovery after brain injury: a structural network control theory study. 2021,		1
249	The "vestibular neuromatrix": A proposed, expanded vestibular network from graph theory in post-concussive vestibular dysfunction. 2021 ,		1
248	Using diffusion MRI data acquired with ultra-high gradient strength to improve tractography in routine-quality data. <i>Neurolmage</i> , 2021 , 245, 118706	7.9	2

(2018-)

247	Propofol disrupts alpha dynamics in distinct thalamocortical networks underlying sensory and cognitive function during loss of consciousness.	0
246	Aberrant dynamic structure-function relationship of rich-club organization in treatment-nalle newly diagnosed juvenile myoclonic epilepsy 2022 ,	Ο
245	Foundational number sense training gains are predicted by hippocampal-parietal circuits 2022,	1
244	The Structural and Functional Correlates of Frailty in Persons Living With HIV 2022,	O
243	Language and the cerebellum: structural connectivity to the eloquent brain.	
242	Neural mass modelling for the masses: Democratising access to whole-brain biophysical modelling with FastDMF.	Ο
241	Resolution and b value dependent Structural Connectome in ex vivo Mouse Brain <i>NeuroImage</i> , 7.9	0
240	Table_1.DOCX. 2019 ,	
239	Table_2.DOCX. 2019 ,	
238	Table_3.DOCX. 2019 ,	
237	Table_1.docx. 2017 ,	
236	Table_1.pdf. 2020 ,	
235	Image_1.TIFF. 2019 ,	
234	Presentation_1.pdf. 2019 ,	
233	Table_1.docx. 2019 ,	
232	Data_Sheet_1.pdf. 2018 ,	
231	Data_Sheet_1.pdf. 2020 ,	
230	Table_1.DOCX. 2018 ,	



(2020-2020)

Table_2.xlsx. 2020, 211 Data_Sheet_1.CSV. 2018, Data_Sheet_2.CSV. 2018, 209 Data_Sheet_3.CSV. 2018, 208 Data_Sheet_4.CSV. 2018, 207 Table_1.docx. **2020**, 206 205 Image_1.pdf. **2019**, Table_1.DOCX. **2019**, 204 Table_2.DOCX. 2019, 203 Image_1.TIF. 2019, 202 Table_1.DOCX. 2019, 201 Table_1.DOCX. 2018, 200 Data_Sheet_1.docx. 2019, 199 Table_1.xlsx. **2019**, 198 Image_1.JPEG. 2020, 197 196 Image_2.JPEG. **2020**, Table_1.docx. 2020, 195 Table_2.docx. 2020, 194

193	Table_3.docx. 2020 ,
192	Table_4.docx. 2020 ,
191	Image_1.tif. 2020 ,
190	Image_2.tif. 2020 ,
189	Comparison of CPU and GPU bayesian estimates of fibre orientations from diffusion MRI 2022 , 17, e0252736 $_{ m 1}$
188	A population-normalized tractographic fiber atlas of the anterior limb of the internal capsule: relevance to surgical neuromodulation 2022 , 1-11
187	Thalamic structural connectivity profiles in blepharospam/Meige's syndrome 2022 , 34, 103013
186	Reproducibility and Evolution of Diffusion Mri Measurements Within the Cervical Spinal Cord in Multiple Sclerosis. 2022 ,
185	Methodological evaluation of individual cognitive prediction based on the brain white matter structural connectome 2022 ,
184	Somatotopic Organization of Hyperdirect Pathway Projections From the Primary Motor Cortex in the Human Brain 2022 , 13, 791092
183	The Interhemispheric Auditory White Matter Tract is Associated with Impulsivity 2022, 113922
182	Pallidal Structural Changes Related to Levodopa-induced Dyskinesia in Parkinson's Disease. 2022 , 14,
181	Thalamo-hippocampal dysconnectivity is associated with serum cholesterol level in drug-naMe patients with first-episode schizophrenia. 2022 ,
180	Functional, but Minimal Microstructural Brain Changes Present in Aging Canadian Football League Players Years After Retirement. 2022 , 100036
179	Early structural connectivity within the sensorimotor network: deviations related to prematurity and association to neurodevelopmental outcome.
178	Meditation-induced effects on whole-brain structural and effective connectivity 2022, o
177	Associations between corpus callosum damage, clinical disability, and surface-based homologous inter-hemispheric connectivity in multiple sclerosis 2022 ,
176	Relationship between trunk function and corticoreticular pathway in stroke hemiplegic patients: analysis using probabilistic tractography. 2019 , 10, 96-102

175	Observational Study of Neuroimaging Biomarkers of Severe Upper Limb Impairment After Stroke 2022 ,		О
174	Mapping brain-wide excitatory projectome of primate prefrontal cortex at submicron resolution and comparison with diffusion tractography 2022 , 11,		O
173	Aberrant cortico-striatal white matter connectivity and associated subregional microstructure of the striatum in obsessive-compulsive disorder.		
172	Automated optimization of deep brain stimulation parameters for modulating neuroimaging-based targets.		
171	Midbrain-Hippocampus Structural Integrity Selectively Predicts Motivated Memory Encoding.		
170	The expanding horizons of network neuroscience: From description to prediction and control. <i>NeuroImage</i> , 2022 , 119250	7.9	O
169	Visual Attention and Poor Sleep Quality. 2022 , 16,		
168	Multimodal Classification of Extremely Preterm and Term Adolescents Using the Fusiform Gyrus: A Machine Learning Approach. 2022 , 103078		O
167	Abnormal thalamocortical connectivity of preterm infants with elevated thyroid stimulating hormone identified with diffusion tensor imaging. 2022 , 12,		
166	Genetic architecture of the white matter connectome of the human brain.		O
165	White matter microstructure in autism. 2022 , 127-156		
164	Autologous cellular therapy for cerebral palsy: a randomized, crossover trial.		O
163	White Matter Correlates of Early-Onset Bipolar Illness and Predictors of One-Year Recurrence of Depression in Adults with Bipolar Disorder. 2022 , 11, 3432		
162	Mediation of Tremor Control by the Decussating and Nondecussating Part of the Dentato-Rubro-Thalamic Tract in Deep Brain Stimulation in Essential Tremor: Which Part Should Be Stimulated?. 2022 ,		
161	Dissociating the functional roles of arcuate fasciculus subtracts in speech production.		1
160	The structural brain network topology of episodic memory. 2022 , 17, e0270592		O
159	Structural insight into the individual variability architecture of the functional brain connectome. <i>NeuroImage</i> , 2022 , 119387	7.9	О
158	A new cortical parcellation based on systematic review of primate anatomical tracing studies on corticostriatal projections.		

157	Effects of White-Matter Tract Length in Sport-Related Concussion: A Tractography Study from the NCAA-DoD CARE Consortium.	
156	Magnetic resonance tractogtaphy: possibilities and limitations, modern approach to data processing.	
155	Hebbian activity-dependent plasticity in white matter. 2022 , 39, 110951	0
154	Aberrant impulse control circuitry in obesity.	O
153	The Wernicke conundrum revisited: evidence from connectome-based lesion-symptom mapping.	О
152	Deep Learning Guided Diffusion MRI Tractography in the Mouse Brain.	
151	The Impaired Subcortical Pathway From Superior Colliculus to the Amygdala in Boys With Autism Spectrum Disorder. 16,	O
150	Abnormal white-matter rich-club organization in obsessivedompulsive disorder.	О
149	Differential roles of delta and theta oscillations in understanding semantic gist during natural audiovisual speech perception: Functional and anatomical evidence.	
148	Transient, developmental functional and structural connectivity abnormalities in the thalamocortical motor network in Rolandic epilepsy. 2022 , 35, 103102	O
147	PhiPipe: a multi-modal MRI data processing pipeline with test-retest reliability and predicative validity assessments.	
146	Two Patterns of White Matter Connection in Multiple Gliomas: Evidence from Probabilistic Fiber Tracking. 2022 , 11, 3693	O
145	Towards PErsonalised PRognosis for children with traumatic brain injury: the PEPR study protocol. 2022 , 12, e058975	О
144	Comparing human and chimpanzee temporal lobe neuroanatomy reveals modifications to human language hubs beyond the frontotemporal arcuate fasciculus. 2022 , 119,	1
143	Microstructural alterations in association tracts and language abilities in schoolchildren born very preterm and with poor fetal growth.	0
142	Profiling morphologic MRI features of motor neuron disease caused by TARDBP mutations. 13,	O
141	A Hierarchical Graph Learning Model for Brain Network Regression Analysis. 16,	1
140	Widespread ripples synchronize human cortical activity during sleep, waking, and memory recall. 2022 , 119,	O

139	Automated optimization of deep brain stimulation parameters for modulating neuroimaging-based targets.	O
138	Determining the OPTIMAL DTI Analysis Method for Application in Cerebral Small Vessel Disease. 2022 , 103114	1
137	The Relationship Between Frontostriatal Connectivity and Striatal Dopamine Function in Schizophrenia: An 18F-DOPA PET and Diffusion Tensor Imaging Study in Treatment Responsive and Resistant Patients. 2022 , 19, 570-579	1
136	The connectional anatomy of the temporal lobe. 2022 , 3-16	
135	QuNex [An Integrative Platform for Reproducible Neuroimaging Analytics.	O
134	White matter abnormalities characterize the acute stage of sports-related mild traumatic brain injury. 2022 , 4,	
133	Fiber-Specific Structural Properties Relate to Reading Skills in Children.	
132	Distance-dependent distribution thresholding in probabilistic tractography.	
131	Native language leaves distinctive traces in brain connections.	1
130	A macroscopic link between interhemispheric tract myelination and cortico-cortical interactions during action reprogramming. 2022 , 13,	O
129	Brain Network Analysis: A Review on Multivariate Analytical Methods.	
128	Human brain structural connectivity matricesBeady for modelling. 2022, 9,	
127	Disruption in structuralfunctional network repertoire and time-resolved subcortical fronto-temporoparietal connectivity in disorders of consciousness. 11,	O
126	Brain metabolic changes and clinical response to superolateral medial forebrain bundle deep brain stimulation for treatment-resistant depression.	1
125	Freezing of gait in Parkinson disease is associated with the microstructural and functional changes of globus pallidus internus. 14,	0
124	Individual differences in white matter microstructure of the face processing brain network are more differentiated from global fibers with increasing ability. 2022 , 12,	
123	Remote cortical atrophy and language outcomes after chronic left subcortical stroke with aphasia. 16,	1
122	White matter pathways associated with empathy in females: A DTI investigation. 2022 , 162, 105902	

121	Combination of structural and functional connectivity explains unique variation in specific domains of cognitive function. 2022 , 262, 119531	0
120	Reproducible protocol to obtain and measure first-order relay human thalamic white-matter tracts. 2022 , 262, 119558	o
119	Structural connectivity of the ANT region based on human ex-vivo and HCP data. Relevance for DBS in ANT for epilepsy. 2022 , 262, 119551	0
118	Tractography indicates lateralized differences between trigeminal and olfactory pathways. 2022 , 261, 119518	
117	CTtrack: A CNN+Transformer-based framework for fiber orientation estimation & amp; tractography. 2022 , 2, 100099	
116	Age-dependent white matter microstructural disintegrity in autism spectrum disorder. 16,	1
115	Prolonged, Low-Level Exposure to the Marine Toxin, Domoic Acid, and Measures of Neurotoxicity in Nonhuman Primates. 2022 , 130,	2
114	Transformer-Based Framework for Fiber Orientation Estimation & amp; Tractography.	o
113	Voxelwise structural disconnection mapping: Methodological validation and recommendations. 2022 , 35, 103132	0
112	Preterm Birth Impact on White Matter Microstructure in In-Vivo Reconstructed Audiovisual Integration Fiber Bundles in the Neonatal Brain.	O
111	fMRI informed voxel-based lesion analysis to identify lesions associated with right-hemispheric activation in aphasia recovery. 2022 , 36, 103169	0
110	Cortical ripples during NREM sleep and waking in humans. JN-RM-0742-22	o
109	The BigMac dataset: an open resource combining multi-contrast MRI and microscopy in the macaque brain.	0
108	Volumetric and connectivity assessment of the caudate nucleus in California sea lions and coyotes.	1
107	Multi-band multi-shot diffusion MRI reconstruction with joint usage of structured low-rank constraints and explicit phase mapping.	0
106	Predicting the true extent of glioblastoma based on probabilistic tractography. 16,	O
105	Dissecting structural connectivity of the left and right inferior frontal cortex in children who stutter.	1
104	Neural network bases of thematic semantic processing in language production. 2022,	o

103	Social Health Is Associated With Tract-Specific Brain White Matter Microstructure In Community-Dwelling Older Adults. 2022 ,	Ο
102	On the performance of multi-compartment relaxometry for myelin water imaging Intra-subject and inter-protocol reproducibility.	O
101	Association Between the C4 Binding Protein Level and White Matter Integrity in Major Depressive Disorder. 2022 , 19, 703-711	0
100	Microsurgical anatomy of the auditory radiations: revealing the enigmatic acoustic pathway from a surgical viewpoint. 2022, 1-14	Ο
99	Low-dimensional organization of global brain states of reduced consciousness.	Ο
98	Indirect structural disconnection-symptom mapping.	O
97	Multi-compartment diffusion magnetic resonance imaging models link tract-related characteristics with working memory performance in healthy older adults. 14,	1
96	Structural connectome quantifies tumour invasion and predicts survival in glioblastoma patients.	2
95	White matter connectivity in brain networks supporting social and affective processing predicts real-world social network characteristics. 2022 , 5,	0
94	High cortical iron is associated with the disruption of white matter tracts supporting cognitive function in healthy older adults.	Ο
93	Subjective cognitive decline predicts lower cingulo-opercular network functional connectivity in individuals with lower neurite density in the forceps minor. 2022 , 263, 119662	Ο
92	Reduced basal ganglia tissue-iron concentration in school-age children with attention-deficit/hyperactivity disorder is localized to limbic circuitry.	Ο
91	Cholinergic white matter pathways along the Alzheimer's disease continuum.	О
90	Relationship between the consciousness level and the structural neural connectivity of the medial prefrontal cortex in hypoxic-ischemic brain injury: a pilot study. 2022 , 33, 750-755	O
89	Structural connectivity between the hippocampus and cortical/subcortical area relates to cognitive impairment in schizophrenia but not in mood disorders.	0
88	Morphological similarity of amygdala-ventral prefrontal pathways represents trait anxiety in younger and older adults. 2022 , 119,	O
87	Brain structural plasticity in rats subjected to early binocular enucleation characterized by high resolution anatomical magnetic resonance imaging and diffusion tensor imaging. 2022 ,	0
86	The relationship between motor pathway damage and flexion-extension patterns of muscle co-excitation during walking. 13,	1

85	Modulations of local synchrony over time lead to resting-state functional connectivity in a parsimonious large-scale brain model. 2022 , 17, e0275819	O
84	Mendelian randomization analyses support causal relationships between brain imaging-derived phenotypes and risk of psychiatric disorders. 2022 , 25, 1519-1527	O
83	Brainnetome atlas of preadolescent children based on anatomical connectivity profiles.	O
82	Topological reorganization of brain network might contribute to the resilience of cognitive functioning in mildly disabled relapsing remitting multiple sclerosis.	O
81	Identification of central amygdala and trigeminal motor nucleus connectivity in humans: An ultra-high field diffusion MRI study.	0
80	Concurrent mapping of brain ontogeny and phylogeny within a common space: Standardized tractography and applications. 2022 , 8,	O
79	White matter alterations associated with lifetime and current depression in adolescents: Evidence for cingulum disruptions.	О
78	BrainGB: A Benchmark for Brain Network Analysis with Graph Neural Networks. 2022 , 1-1	1
77	Structural brain connectivity predicts early acute pain after mild traumatic brain injury. 2022 , Publish Ahead of Print,	О
76	Using in vivo functional and structural connectivity to predict chronic stroke aphasia deficits.	O
75	Midbrain-Hippocampus Structural Connectivity Selectively Predicts Motivated Memory Encoding. JN-RM-094	15-@2
74	Signed graph representation learning for functional-to-structural brain network mapping. 2022 , 102674	O
73	Automated detection of axonal damage along white matter tracts in acute severe traumatic brain injury. 2023 , 37, 103294	0
72	Tractometric Coherence of Fiber Bundles in DTI. 2022, 137-148	O
71	Microstructural organization of the corpus callosum in young endurance athletes: A global tractography study. 16,	О
70	Early structural connectivity within the sensorimotor network: Deviations related to prematurity and association to neurodevelopmental outcome. 16,	O
69	Brain white matter microstructure abnormalities in children with optimal outcome from autism: a four-year follow-up study. 2022 , 12,	0
68	Altered development of structural MRI connectome hubs at near-term age in very and moderately preterm infants.	O

67	Turning and multitask gait unmask gait disturbance in mild-to-moderate multiple sclerosis: Underlying specific cortical thinning and connecting fibers damage.	1
66	Deep brain stimulation improves symptoms of spasmodic dysphonia through targeting of thalamic sensorimotor connectivity.	O
65	Classification accuracy of structural and functional connectomes across different depressive phenotypes.	0
64	Brain grey and white matter structural associations with future suicidal ideation and behaviors in adolescent and young adult females with mood disorders. 2022 , 2,	o
63	Association between real-time strategy video game learning outcomes and pre-training brain white matter structure: preliminary study. 2022 , 12,	O
62	A combined DTI-fMRI approach for optimizing the delineation of posteromedial vs. anterolateral entorhinal cortex.	o
61	Model Averaging and Bootstrap Consensus-based Uncertainty Reduction in Diffusion MRI Tractography.	O
60	Better characterization of attention and hyperactivity/impulsivity in children with ADHD: The key to understanding the underlying white matter microstructure. 2022 , 327, 111568	O
59	On the performance of multi-compartment relaxometry for myelin water imaging (MCR-MWI) [I] Test-retest repeatability and inter-protocol reproducibility. 2022 , 119824	0
58	Quantitative measures of topographic and divergent/convergent connectivity in diffusion MRI of the human cerebral cortex.	O
57	Imaging Modalities Used for Frameless and Fiducial-Less Deep Brain Stimulation: A Single Centre Exploratory Study among Parkinson Disease Cases. 2022 , 12, 3132	0
56	A structural connectivity atlas of limbic brainstem nuclei. 1,	O
55	Sampling strategies and integrated reconstruction for reducing distortion and boundary slice aliasing in high-resolution 3D diffusion MRI.	0
54	Brain plasticity of structural connectivity networks and topological properties in baseball players with different levels of expertise. 2023 , 166, 105943	O
53	Predicting insomnia severity using structure-function coupling in female chronic insomnia patients. 2023 , 441, 114283	0
52	A critical role of brain network architecture in a continuum model of autism spectrum disorders spanning from healthy individuals with genetic liability to individuals with ASD.	O
51	Fiber-specific structural properties relate to reading skills in children and adolescents. 11,	0
50	Applications of advanced diffusion MRI in early brain development: a comprehensive review.	Ο

49	Functional alteration due to structural damage is network dependent: insight from multiple sclerosis.	O
48	PhiPipe: A multi-modal MRI data processing pipeline with testEetest reliability and predicative validity assessments.	O
47	Applicability of automated tractography during acute care stroke rehabilitation. 2023, 35, 156-162	O
46	Fully Connected Multi-Kernel Convolutional Neural Network Based on Alzheimer Disease Diagnosis. 2023 , 1-20	O
45	White matter microstructure is associated with the precision of visual working memory.	O
44	Changes in Distributed Motor Network Connectivity Correlates With Functional Outcome After Surgical Resection of Brain Tumors. 2023 , 4,	O
43	Axonal and myelin changes and their inter-relationship in the optic radiations in people with multiple sclerosis. 2023 , 9, 205521732211476	O
42	White matter and gray matter changes related to cognition in community populations. 15,	O
41	Influence of mild cognitive impairment and body mass index on white matter integrity assessed by diffusion tensor imaging.	O
40	Structural architecture and brain network efficiency link polygenic scores to intelligence.	O
39	Using mesoscopic tract-tracing data to guide the estimation of fiber orientation distributions in the mouse brain from diffusion MRI. 2023 , 270, 119999	0
38	The anatomical networks based on probabilistic structurally connectivity in bipolar disorder across mania, depression, and euthymic states. 2023 , 329, 42-49	O
37	Current State of Diffusion-Weighted Imaging and Diffusion Tensor Imaging for Traumatic Brain Injury Prognostication. 2023 , 33, 279-297	0
36	Spatially regularized low-rank tensor approximation for accurate and fast tractography. 2023 , 271, 120004	O
35	Structural connectivity of an interoception network in schizophrenia. 2023, 331, 111636	O
34	Italian reference values and brain correlates of verbal fluency index I/s standard verbal fluency test I/o assess executive dysfunction in ALS. 1-9	O
33	A connectome-based deep learning approach for Early MCI and MCI detection using structural brain networks. 2023 , 3, 100118	0
32	Preterm birth and neonatal white matter microstructure in in-vivo reconstructed fiber tracts among audiovisual integration brain regions. 2023 , 60, 101202	O

31	Diffusion tensor tractography of the corticobulbar tract in a dysphagic patient with progressive supranuclear palsy: A case report. 2023 , 102, e32898	O
30	Evaluation of Kernel Low-Rank Compressed Sensing in preclinical Diffusion Magnetic Resonance Imaging.	O
29	Longitudinal associations between mother-child attachment security in toddlerhood and white matter microstructure in late childhood: a preliminary investigation. 2023 , 25, 291-310	0
28	Reconstruction of the Corticospinal Tract in Patients with Motor-Eloquent High-Grade Gliomas Using Multilevel Fiber Tractography Combined with Functional Motor Cortex Mapping. 2023 , 44, 283-290	O
27	Genetic architecture of the white matter connectome of the human brain. 2023, 9,	O
26	Neuroplasticity enables bio-cultural feedback in Paleolithic stone-tool making. 2023 , 13,	O
25	Brain network mapping and glioma pathophysiology. 2023 , 5,	О
24	Integrated diffusion image operator (iDIO): A pipeline for automated configuration and processing of diffusion MRI data. 2023 , 44, 2669-2683	O
23	Shared and unique effects of ApoEµ4 and pathogenic gene mutation on cognition and imaging in preclinical familial Alzheimer disease. 2023 , 15,	O
22	Prediction of post-stroke motor recovery benefits from measures of sub-acute widespread network damages. 2023 , 5,	O
21	Column-based cortical depth analysis of the diffusion anisotropy and radiality in submillimeter whole-brain diffusion tensor imaging of the human cortical gray matter in vivo. 2023 , 270, 119993	O
20	Neurophysiological and other features of working memory in older adults at risk for dementia.	O
19	Using graph theory as a common language to combine neural structure and function in models of healthy cognitive performance.	0
18	Localized White Matter Tract Integrity Measured by Diffusion Tensor Imaging Is Altered in People with Mild Cognitive Impairment and Associated with Dual-Task and Single-Task Gait Speed. 2023 , 92, 1367-1384	O
17	Differential effects of emotional valence on mnemonic performance with greater hippocampal maturity. 2023 , 30, 55-62	0
16	White Matter. 2013 , 205-244	O
15	Associations between dietary patterns and dementia-related neuroimaging markers.	0
14	Assessing the structure of the posterior visual pathway in bilateral macular degeneration. 2023, 13,	O

13	Subsets of cortico-cortical evoked potentials propagate as traveling waves.	O
12	White and Gray Matter Abnormality in Burning Mouth Syndrome Evaluated with Diffusion Tensor Imaging and Neurite Orientation Dispersion and Density Imaging. 2023 ,	O
11	Human habit neural circuitry may be perturbed in eating disorders. 2023 , 15,	О
10	Central Executive and Default Mode Networks: An Appraisal of Executive Function and Social Skill Brain-Behavior Correlates in Youth with Autism Spectrum Disorder.	O
9	White matter microstructure is associated with the precision of visual working memory. 2023 , 272, 120069	O
8	QuNexAn integrative platform for reproducible neuroimaging analytics. 17,	O
7	Automated three-dimensional major white matter bundle segmentation using diffusion magnetic resonance imaging.	О
6	Different aspects of hand grip performance associated with structural connectivity of distinct sensorimotor networks in chronic stroke. 2023 , 11,	O
5	Degeneration of nigrostriatal pathway in patients with middle cerebral infarct: A diffusion tensor imaging study. 2023 , 102, e33370	О
4	Early morning physical activity is associated with healthier white matter microstructure and happier children: the ActiveBrains project.	O
3	Life-course neighbourhood deprivation and brain structure in older adults: The Lothian Birth Cohort 1936.	О
2	Graph propagation network captures individual specificity of the relationship between functional and structural connectivity.	O
7	Fixel-Based Analysis Reveals Whole-Brain White Matter Ahnormalities in Cervical Dystonia	0